POLITECNICO DI TORINO

Collegio di Ingegneria Edile

Master of Science Course in Building Engineering

Master of Science Thesis

Integrated Digital Survey and H-BIM for Preservation and Planned Maintenance of Historical Architecture:

The Case Study of Santo Stefano Church at Candia Canavese.

Politecnico di Torino

Tutor/s
Prof. Marco Zerbinatti
Prof. Sara Fasana

Candidate
Juan Esteban Salazar Taborda

DECEMBER 2024

Table of Content

Abstract

The church of Santo Stefano in Candia Canavese is a historical structure that embodies the rich cultural heritage of the town and the surrounding region that host it. Despite its importance, the church lacks current digital documentation necessary for effective long-term conservation. This research addresses this need through a hybrid methodology that integrates traditional tools of architectural survey, like total stations and GPS alongside modern technologies, including terrestrial laser scanning (LiDAR) and drone-based aerial photogrammetry, as to produce a high-resolution point cloud that forms the basis for a precise three-dimensional model.

The final 3D model developed within a Heritage Building Information Modeling (H-BIM) framework is then exported to the 4main10ance web platform, where a planned maintenance strategy is created, enabling ongoing management and easy access for research and conservation activities.

The thesis highlights the benefits of combining traditional survey techniques with innovative digital tools to enhance documentation accuracy, data analysis, and interoperability across platforms. This work provides a practical reference for future applications by establishing a replicable framework for similar historical preservation projects, contributing to the broader effort to protect and maintain cultural heritage sites in an increasingly digital world.

Introduction

Italy is a country with a rich history and a distinctive cultural identity, particularly evident in its architectural heritage. Over time, considerable efforts have been made to preserve this heritage, including the designation of certain structures as World Heritage Sites. However, a considerable number of historically significant structures remain unrecognized, yet they continue to serve as tangible evidence of Italy's cultural and historical evolution. One such structure is the Church of Santo Stefano.

The selection of the Church of Santo Stefano as a case study for this thesis is rooted not only in its historical and cultural value but also in its relevance to previous research (in the form of a master’s thesis) conducted on the building. This prior research provided vital insights into the church's architectural and structural characteristics and the conservation needs of the building. The research focused on an exterior survey that produced an exterior point cloud file and comprehensive documentation of the church historical heritage.

The present study integrates modern and traditional tools in architectural surveying to enhance the analysis of the Church of Santo Stefano. This is achieved by generating an internal point cloud that complements the existing external one. The combination of these data sets allows for the creation of a highly detailed three-dimensional model, or "digital twin," developed within a BIM environment using a HBIM framework. This digital twin serves as a crucial foundation for the fulfillment of this thesis scope which is the association of data to the model and the development of a structured maintenance plan.

The final model is parameterized and exported to the 4main10ance platform, where the maintenance plan is developed. This plan forms the cornerstone for the conservation and management of the church. The methodology employed offers a replicable framework for future studies with similar objectives.

The thesis adopts a structured approach, beginning with an overview of the church’s geographical and historical context. This is followed by an explanation of the technologies utilized, such as LiDAR and photogrammetry, to generate the point cloud. Subsequently, the creation of the 3D model within a BIM environment using an HBIM framework is discussed, culminating in its export to the 4main10ance platform and the development of a structured maintenance plan.

1. The Church of Santo Stefano in Candia Canavese

Image 1 - Main entrance facade of the santo Stefano church at Candia Canavese.
source: www.ecomuseoami.it

The Church of Santo Stefano in Candia Canavese is the largest non-urban Romanesque church that still exists, is also a remarkable place of worship and a cultural beacon that has withstood the passage of time. Located on a gentle rise in the landscape, the church has served for centuries as a spiritual and communal anchor for the surrounding community. Its enduring presence represents the historical and religious heritage of the region and reflects the architectural values of an era.

The work on this thesis builds on previous research, using previous studies as a foundation for deeper exploration, particularly by documenting and developing work on the less explored interior spaces, as it will be explained further on.

Throughout this chapter, a geographical and historical overview will place the church in its broader context, followed by a thorough examination of its architectural and structural components in subsequent sections. Together, these elements illustrate the church's unique place within the architectural heritage of Candia Canavese and provide a basis for developing strategies for its conservation.

1.1. Geographical Overview

Image 2 - Aerial view of Candia Canavese.
Source: www. earth.google.com/web

In the Piedmont region, within the modern province of Turin, lies the historical area of the Canavese. In Roman times, its capital was known as Eporedia, now the city of Ivrea. This ancient territory extended over what is now the Ivrea morainic mountain range, the rivers Po and Stura di Lanzo, and the Graian Alps. Within this area is the municipality of Candia Canavese, located about 36 kilometers northeast of Turin, the capital of the Piedmont region, and 16 kilometers south of Ivrea. Candia Canavese is situated between the Candia Lake and Mount Santo Stefano, the latter being the last mountain range of the Ivrea morainic amphitheater in the lower Canavese area.

The subject of this thesis, the Church of Santo Stefano, is located inside the town, on the gentle rise of the Santo Stefano Mountain. Its position reflects the historical tradition of placing sacred buildings on higher ground. This elevation not only provides a commanding view of the surrounding landscape, but also emphasizes the church's role as a central landmark in the community. Its Romanesque architecture and historical significance make it a key feature of Candia Canavese, embodying the rich cultural and religious heritage of the region.

1.2. Historical Background and Architectural Evolution

The Church of Santo Stefano does not have a precise construction date; however, it is hypothesized to have been built in the 11th century[1], during which it served as a priory for the Benedictines. The first documented mention of the church appears in the papal bull issued by Pope Alexander III on June 18, 1177, where it read "ecclesiam Sancti Stephani de Monte cum decimis et aliis pertenentis suis"[2], meaning that this document granted the church to the canons of the Hospice of San Bernardo, who not only resided in and cared for the structure but also provided refuge to pilgrims traveling from Northern Europe to Rome.

Between the late 11th and 12th centuries, the church underwent significant reconstruction efforts. One of the most notable interventions was the collapse of the central apse, likely caused by foundation instability or the earthquake that struck the region in 1117. Additionally, during this period, the church's crypt was constructed and dedicated to the Virgin Mary. This space consists of three naves divided by two rows of columns, with three columns on each side. Notably, the columns on the right side lack uniformity in design; their shafts and capitals are in the style of the Early Middle Ages[3], suggesting that they were repurposed from other buildings within the town.

In December 1651, Monsignor Asinari visited the parish of Candia and documented the condition of the Church of Santo Stefano at the time. His report describes that the main and right naves were covered with tiled roofs, whereas the left nave was entirely roofless. The walls were left unfinished, retaining the rough and irregular appearance of their construction material. The church's floor was inconsistent, with some sections made of stone and others of bare earth. He also noted the presence of a chapel with three naves, featuring an altar with a statue of the Virgin Mary at the far end, illuminated by two windows and paved with small stones. Above this chapel was the church's choir, accessible via thirteen uneven steps. Finally, he described the western façade, where the entrance to the main nave featured a large door and the remnants of a bell tower in ruins, which at the time served as housing for a hermit responsible for maintaining the church.

---

[1] Ramella, P. (2006). *Canavese: 100 secoli: Archeologia, insediamenti, chiese, castelli, statuti, storia, personalità* (p. 69). Ivrea: Associazione Amici Museo del Canavese.

[2] BOBBIO C. (1910). *Le Chiese del Canavese* (p.20). Tipografia Ditta F.

[3] Cavallari Murat, A. (1976). *Tra Serra d'Ivrea Orco e Po* (p. 85). Torino: Istituto Bancario San Paolo.

It is believed that between the 16th and early 17th centuries, the interior of the church was decorated with mural paintings[4], some depicting scenes of Christ's Passion.

Allegedly[5] in the last quarter of the 17th century, the central apse was modified, its height reduced to the level of the crypt. The choir's depth was shortened by replacing its original concave structure with a flat wall. These changes also resulted in an extension of the crypt, adding an additional bay. Consequently, the main staircase leading to the choir was replaced by two lateral staircases.

In 1970, the Superintendency of Monuments of Piedmont initiated restoration efforts at the church. During these interventions, a vault constructed over the main nave was removed, revealing the wooden trusses that support the roof. Additionally, excavations were carried out at the base of the initial bell tower. In the same year, the original statue of the Virgin Mary, which had been housed in the crypt, was relocated and replaced with a wooden replica.

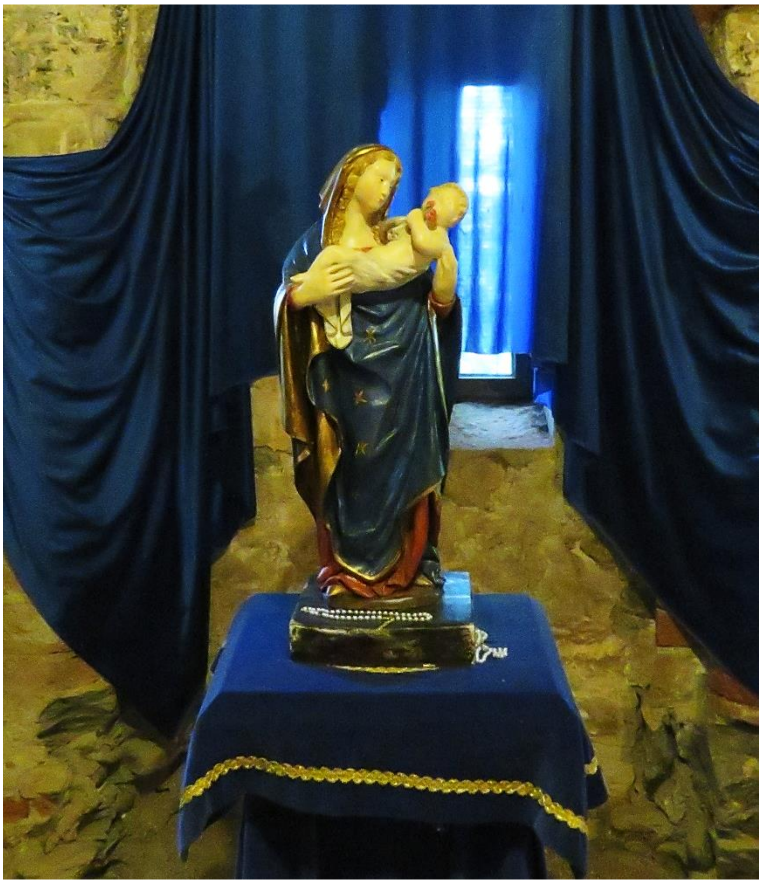

Image 3 - Replica of the statue of the Virgin Mary with Child in the crypt of the Church of Santo Stefano.

[4] Ramella, P. (2006). *Canavese: 100 secoli: Archeologia, insediamenti, chiese, castelli, statuti, storia, personalità* (p. 69). Ivrea: Associazione Amici Museo del Canavese.
[5] Forneris, G. (1999). *Candia Canavese: Due passi e cento Ricordi* (p.128). Comune Candia Canavese.

1.3. Description of the Current Architectural Structure

Once the Church of Santo Stefano has been contextualized in time and space, we return to the present to examine the architectural state of the structure as it stands today. This description will highlight the distinctive features of the building.

The Church of Santo Stefano is constructed with stone masonry. The exterior lacks elaborate ornamentation, instead emphasizing a simple geometric aesthetic. The main roof of the central nave is gabled, while the side naves are covered with single-pitched roofs.

The west façade, housing the main entrance, features a single, unadorned doorway crowned by a simple stone arch. Inside, there are elements such as a niche made of roman bricks as the handles in them suggest, the silhouette of the window of the original bell tower that used to be next to the entrance, and a mural depicting the Passion of Christ. The north façade is entirely blind, with no windows on either the lower or upper levels. A buttress supports the lower section of the wall, contributing to the structural stability of the façade. In contrast, the south façade is more dynamic, with five pointed-arch windows with brick archivolts along the lower level, along with a secondary doorway leading to the interior through the right nave. This façade is further reinforced by three buttresses. On the upper level, there are four windows, two of which are pointed-arch and two large rectangular openings. Both the upper and lower sections of this wall feature a row of hanging arches supported by corbels, that run the entire length of the façade.

The east façade has three semi-circular apses, along with a bell tower with a triangular base and a supporting arch that stabilizes the upper walls of the north and south façades. The lower section of the apses includes several windows: two on the left apse, three on the central apse, and one on the right apse. All of these windows are pointed-arch designs with brick archivolts, consistent with the aesthetic seen on the south façade.

Upon entering the church, the interior reveals a layout of three naves, as seen from the exterior. These naves are separated by rows of rectangular columns connected by semi-circular arches. Some of the columns are decorated with murals, adding subtle decorative elements to the otherwise austere interior. The central nave is the tallest and widest, with exposed wooden trusses supporting the roof. In contrast, the side naves are covered with groin vaults made of masonry and finished with plaster.

The left nave is continuous from the main entrance to the apse, with occasional level changes managed by simple two-step staircases. The central nave, on the other hand, has a more complex vertical organization, divided into three levels:

- The crypt, on the lowest level.
- The main floor, aligned with the western entrance.
- The presbytery, situated above the main floor, is accessible by two staircases that converge on a single landing above the crypt entrance.

The crypt consists of three small naves, defined by two rows of columns. The columns on the right side appear to have been repurposed, likely sourced from the town's earlier parish church, suggesting a history of adaptive reuse, as mentioned before.

Only accessible through the crypt a small chapel can be found at what would be the end of the right nave. This rectangular space has a domed vault, adorned with a painting depicting the Coronation of the Virgin Mary. At the corners of the chapel, four capitals support statues of the Four Evangelists.

Image 4 - Rectangular columns and semicircular arches in the right nave of Santo Stefano church.

Image 5 – Mural paintings on the interior columns of the Santo Stefano church.

Image 6 – Mural painting on the interior face of the entrance wall of the Santo Stefano church.

Image 7 - Groin vault in the side nave of the Santo Stefano church: Masonry structure with plaster finishes.

Image 8 - Wooden trusses supporting the central nave roof of Santo Stefano Church.

Image 9 – Access to the presbytery.

Image 10 – Columns in the crypt of the church.

Image 11 - Details of the capitals of the columns in the crypt of the church.

Image 12 - Interior view of the crypt: Columns and vault of the church of Santo Stefano.

Image 13 - Mural depicting the Coronation of the Virgin in the side chapel dome.

2. Techniques and Methodologies of 3D Surveying Applied to Architectural Heritage

Over time, significant advancements have occurred across various fields of modern society. However, all contemporary developments are fundamentally based on previous practices and work that have evolved to the state of the art we see today. This is particularly true for engineering and architecture, where understanding, studying, and preserving the architectural heritage in historical buildings has been crucial.

Architectural heritage refers to the historical legacy that enriches both the present and future architectural landscapes. Its conservation, protection, and maintenance are essential because these buildings provide historical context and cultural identity to the sites that host them. They serve as invaluable educational resources, offering physical examples of architectural styles, construction techniques, and design philosophies from different historical periods. Moreover, these buildings hold significant aesthetic and artistic value, exemplify sustainable practices through their reuse or repurpose, and generate economic and social benefits by attracting visitors and researchers.

In a country like Italy, the importance of architectural heritage conservation cannot be overstated. Italy, home to the highest number of UNESCO World Heritage sites[6] , places great emphasis on preserving its cultural heritage, a priority shared by numerous organizations and professionals.

Modern technologies and methodologies offer highly detailed and precise results that traditional methods alone cannot achieve. These advancements facilitate superior data analysis and visualization, predominantly in digital formats, thus enhancing study and research capabilities. Key modern tools include 3D scanning, photogrammetry, Building Information Modeling (BIM), and virtual and augmented reality.

For this thesis, traditional methods were supplemented with modern technologies. Traditional tools included the total station, which measures distances, angles, and local coordinates relative to a reference point, and GPS for converting these into global coordinates. Modern

[6] According to the UNESCO table with the number of world heritage properties in each state party, in which Italy has 59 properties inscribed.

technologies employed include 3D laser scanning (LiDAR), which captures high-resolution three-dimensional data representing the geometry and characteristics of surfaces, known as point clouds. Photogrammetry, which uses high-resolution images to generate point clouds or 3D models, and BIM, a process that utilizes a modeling software to create digital representations of the study subject which then gets integrated with relevant information of the building.

In conclusion, the combination of traditional tools with advanced technologies ensures the accurate, georeferenced, three-dimensional representation of buildings with significant architectural heritage. This approach not only enhances the precision of the documentation but also establishes a solid foundation for further academic research and practical applications in the fields of architecture and engineering. Examples of such applications include the preservation and conservation of architectural heritage.

2.1. Topographic Survey

A topographic survey can be defined as a specialized type of land survey that focuses on the accurate measurement and mapping of the natural and man-made features of a specific area of land. The primary objective of a topographic survey is to create a detailed representation of the area's terrain, elevation changes, and key features, such as hills, valleys, bodies of water, trees, buildings, roads, and other structures. This survey provides a comprehensive and scaled representation of the land's surface, allowing for a better understanding of its physical characteristics and providing essential data for a wide range of applications.[7]

To achieve this precise and comprehensive representation, a series of operations or steps must be performed, starting with the planning of the topographic survey. This includes defining its scope, understanding the purpose of its execution, and determining the required level of detail. Once the work is planned, the fieldwork is conducted, during which all necessary information is collected to achieve the set objective. In this thesis, this step was carried out using multiple instruments, including a total station for measuring distances, angles, and elevations to reference points, and a GPS that provided precise location data using satellite signals to accurately georeference the network of reference points. After gathering the field data, firstly it's processed and cleaned to eliminate errors and inconsistencies, and then various data groups are integrated, as in this case, where local coordinates from the total

[7] Datumate. (n.d.). *Topographic Survey.* Retrieved July 13, 2024, from www.datumate.com/glossary/topographic-survey/

station and reference points from the GPS were combined. Finally, the analyzed information is created and compiled into a report to provide a starting point for subsequent planning or decision-making.

There are various methods for conducting a topographic survey, each tailored to the specific type of measurement required, whether horizontal or vertical. For vertical measurements, only the elevations of points on the terrain are considered, where "elevations of points or differences in elevation are determined."[8] Contrariwise, when the focus is solely on the horizontal positions of points projected onto a reference surface, a planimetric survey is employed. This type of survey can be executed using traversing or triangulation methods. Traversing involves "a series of consecutive lines whose ends have been marked in the field and whose lengths and directions have been determined from observations."[9] This method is particularly useful for defining boundaries and creating detailed maps of an area. On the other hand, triangulation, "which is a method for determining positions of points from which horizontal distances can be computed,"[10] is ideal for surveying areas with fewer observations, as it relies on a network of triangles to determine the positions of points.

In the context of this thesis, a planimetric survey using triangulation was selected. This method involved establishing fixed stations within the study area, strategically placed to provide a comprehensive view of the various detailed points to be captured.

2.2. LiDAR Technology

LiDAR, which stands for Light Detection and Ranging, is a technology that "uses electromagnetic (EM) waves in the optical and infrared wavelengths. It is an active sensor that sends out an EM wave and receives the reflected signal back."[11] The primary purpose of LiDAR is to measure a parameter of the reflected signal to calculate the distance between two points, thus creating a detailed map of the target surface. In our case, LiDAR is utilized to map the interior of the case study building accurately.

All LiDAR devices are fundamentally composed of a laser that emits pulses of light towards the target. The word laser is an acronym for the phrase "Light Amplification by the Stimulated

[8] Ghilani, C. D., & Wolf, P. R. (2012). *Elementary Surveying: An Introduction to Geomatics* (13th ed., p. 73). Pearson.
[9] Ibidem, p. 231
[10] Ibidem, p. 132
[11] McManamon, P. F. (2019). *LiDAR technologies and systems*. Society of Photo-Optical Instrumentation Engineers.

Emission of Radiation."[12] Additionally, there is a receiver that detects the reflected signal, which is then processed to calculate the distance between the equipment and the surface. Finally, apertures or optics are included to direct the laser beam toward the target and collect the reflected light.

There are many ways to classify LiDAR devices; however, generally, they can be categorized based on their mobility. These devices can be stationary or mobile. Mobile LiDAR systems collect data while mounted on vehicles, airplanes, drones, etc. This type of LiDAR is ideal for covering large areas and is commonly used in urban and natural terrains. For stationary equipment, they can be further subdivided based on how they measure the distance of the reflected laser. This can be done through Time-of-Flight (ToF), phase shift, or triangulation methods.

For this thesis work, the equipment used operated by measuring distances using ToF technology. This method works by measuring the time it takes for a laser pulse to travel to a target and return. This information is then complemented with the inclination angles of the laser used, thus allowing the calculation of the 3D coordinates of the captured points.

The distance is calculated as follows:

$$d = \frac{\Delta t * c}{2}$$

Where,

d is the distance

Δt is the time of flight

C is the speed of light

2.3. Photogrammetry

Photogrammetry is a sophisticated method utilized in contemporary practices to extract spatial or three-dimensional information from frames or photographs. Essentially, it “may be defined as the science, art, and technology of obtaining reliable information from photographs."[13] This technique is indispensable in fields such as geography, architecture,

[12] National Institute of Standards and Technology. (n.d.). *What is a laser?*. Retrieved July 13, 2024, from www.nist.gov/director/pao/nists-role-laser-measurements-and-applications/what-laser

[13] Ghilani, C. D., & Wolf, P. R. (2012). *Elementary Surveying: An Introduction to Geomatics* (13th ed., p. 799). Pearson.

engineering, and archaeology due to its ability to produce accurate and detailed models of various environments and structures.

Photogrammetry can be broadly classified into aerial and terrestrial categories based on how the images are captured for interpretation. Aerial photogrammetry involves taking photographs from the sky with aircrafts or drones. This approach is particularly useful for mapping large areas, topographic surveys, and environmental monitoring. On the other hand, terrestrial photogrammetry involves capturing images from ground level, such as cameras mounted on tripods or handheld devices, making it ideal for detailed surveys of buildings, monuments, and other structures.[14]

The core methodology for data extraction in photogrammetry remains consistent regardless of the type. It starts with the acquisition of a series of photographs with sufficient overlap (typically 60-85%). Specialized software then processes these images, identifying common points (or tie points) in the overlapping areas, it also extracts features that can be matched across different frames, as well as the position and angle of the camera and its focal length. Through a process called triangulation, the software calculates and assigns precise coordinates to these points, creating a detailed three-dimensional model. [15]

Photogrammetry is a highly valuable and versatile tool in numerous fields of application, offering significant benefits such as high precision in measurements obtained from records. In many cases, conducting a topographic survey using photogrammetry is more cost-effective and faster than traditional methods. Additionally, due to its wide range of terrestrial and aerial capabilities, it can be employed across various industries and on different scales of work.

However, there are certain limitations to consider when using this tool in some projects. Aerial photogrammetry is heavily constrained by unfavorable weather conditions, as precise flights cannot be conducted under such circumstances, or flights may be entirely impossible. Additionally, it is limited by the physical condition of the site being measured. For terrestrial photogrammetry, executing large-scale projects can be challenging. In the case of aerial photogrammetry, urban or natural environments may impose height restrictions on flights necessary for capturing images. Another notable limitation is that the process relies on software to identify tie points for 3D model reconstruction. Homogeneous surfaces over large

[14] Coursera. (n.d.). *What is photogrammetry?* Retrieved July 13, 2024, from www.coursera.org/articles/what-is-photogrammetry

[15] 3DSourced. (n.d.). *Photogrammetry guide.* Retrieved July 13, 2024, from www.3dsourced.com/guides/photogrammetry-guide/

areas pose a challenge for the software, making it difficult to assign correlation points between images.[16]

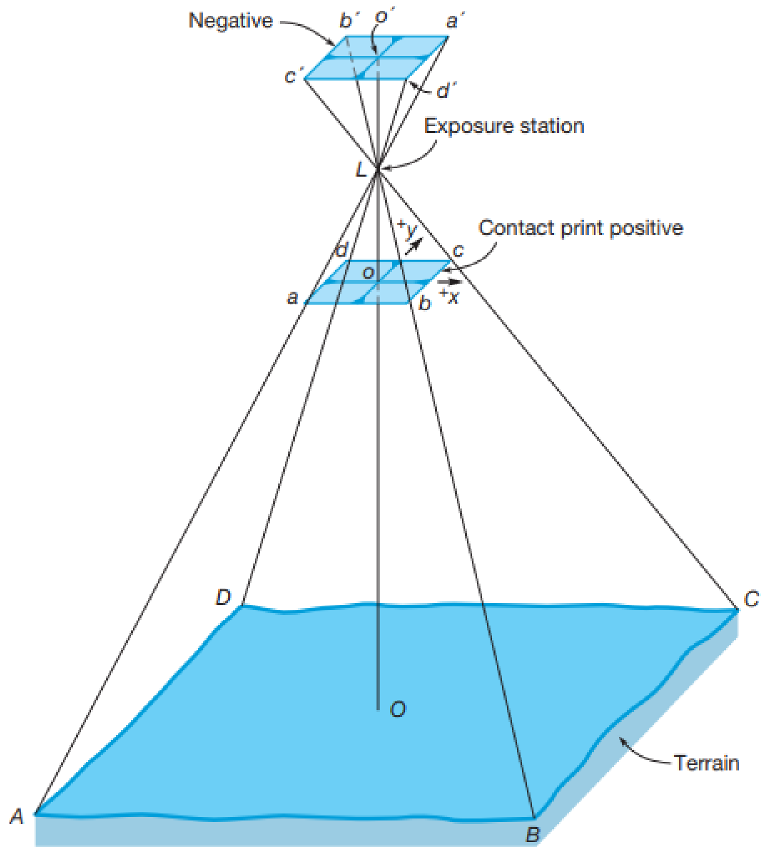

Image 13 - Geometry of a vertical aerial photograph.
source: Ghilani, C. D., & Wolf, P. R. (2012). Elementary Surveying: An Introduction to Geomatics (13th ed., p. 806). Pearson.

Where,

A,B,C,D are where the fiducial marks are on the terrain

a,b,c,d are where the fiducial marks are on the image

x,y are the axis for measuring coordinates

O, o are the principal point of the terrain and image

The distance between L and o is the focal length

[16] Ibidem

2.3.1. UAV Aerial Photogrammetry

Aerial photogrammetry involves the use of unmanned aerial vehicles (UAVs), also known as drones, equipped with high-definition cameras to capture detailed images from the air. UAVs have been utilized throughout history for various purposes, including defense, environmental monitoring, and civil applications.

These aircraft are remotely controlled, meaning that they operate without a human pilot onboard, allowing for significant advancements in their design and technology. This remote operation enables UAVs to be built in a variety of types, these can be based on different criteria's such as, the way the land, their aerodynamics or if it's a multi rotor type, as seen below.

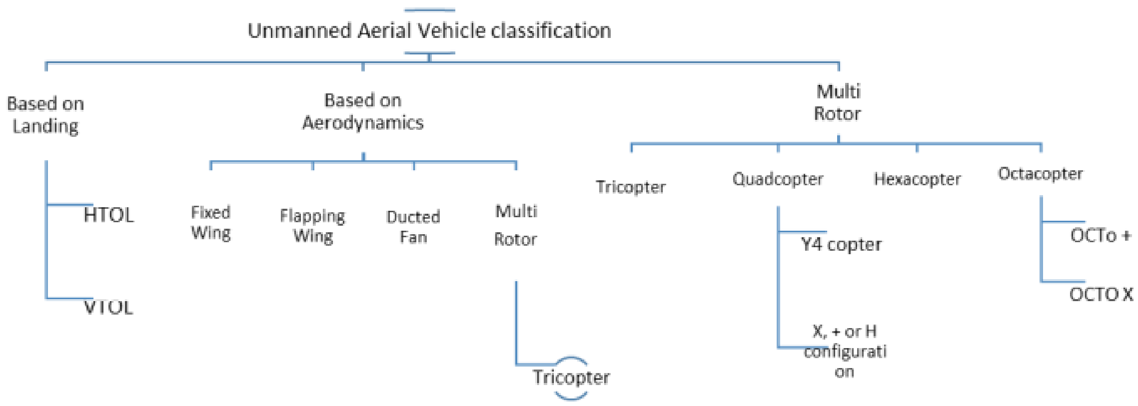

Image 14 - Classification of UAV based on Landing, Aerodynamics and weight
source: Singhal, G., Bansod, B., & Mathew, L. (2018). *Unmanned aerial vehicle classification, applications, and challenges: A review*.

Image 15 - Fixed wing (left) and Quadcopter (right) drone
Source: JOUAV. (2024, June 26). *Different types of drones and uses (2024 full guide).* JOUAV. https://www.jouav.com/blog/drone-types.html

The focus in this thesis work is on the civil use of UAVs, specifically in the fields of engineering and architecture.

In the context of the case study which involves interior flight, the most suitable types of drones for performing the required job are micro and mini, according to the Unmanned Aerial Vehicle Systems Association [17] classification. These lightweight drones are particularly effective for aerial photogrammetry due to their ability to maneuver easily and capture detailed images of the architectural elements and structures. These classifications are based on their size, weight, and capabilities.

UAV Categories	Acronym	Range (km)	Climb rate (m)	Endurance (hours)	Mass (kg)
Micro	μ (Micro)	< 10	250	1	< 5
Mini	Mini	< 10	150-300	< 2	150
Close Range	CR	10-30	3000	2-4	150
Short Range	SR	30-70	3000	3-6	200
Medium Range	MR	70-200	5000	6-10	1250
Medium Range Endurance	MRE	> 500	8000	10-18	1250
Low Altitude Deep Penetration	LADP	> 250	50-9000	0,5-1	350
Low Altitude Long Endurance	LALE	> 500	3000	> 24	< 30
Medium Altitude Long Endurance	MALE	> 500	14000	24-48	1500

Table 1: Classification of UAV's according to Unmanned Aerial Vehicle Systems Association
source: Gašparović, M., & Gajski, D. (2016, May). *Unmanned Aerial Photogrammetric Systems in the Service of Engineering Geodesy.* Conference paper presented at SIG 2016 - International Symposium on Engineering Geodesy, Varaždin, Croatia, page 4.

[17] Gašparović, M., & Gajski, D. (2016, May). *Unmanned Aerial Photogrammetric Systems in the Service of Engineering Geodesy.* Conference paper presented at SIG 2016 - International Symposium on Engineering Geodesy, Varaždin, Croatia, page 4.

3. Acquisition of Survey Data

The data gathering process for the case study began in June 2023, with a series of operations conducted directly at the Church of Santo Stefano, situated on the mount in Candia Canavese. These operations combined traditional surveying instruments, such as a total station, with advanced technologies, including terrestrial laser scanning and aerial drone photography. Additionally, a variety of software tools were utilized to process and integrate the data, resulting in a three-dimensional representation of the church's internal surfaces. When combined with previous surveys conducted at the same site, this data enables the creation of a georeferenced three-dimensional digital model.

The primary objective of this thesis is to develop a planned maintenance program that supports the conservation and preservation of this historic structure by using the resulting model as a foundational resource.

3.1. The Survey Campaign

At the beginning of the survey, the total station was positioned on coded marks that were intended to form the basis of a network or grid. These marks were selected with the objective of encompassing the entire interior of the building. While this was performed, multiple markers were positioned on the different vertical surfaces that form the structure. With the assistance of an eidotype, a relative position and a unique code were assigned to each marker, thus facilitating their identification. The markers were then saved with coordinates in the topographic survey conducted with the total station and were subsequently utilized as supplementary information in other processes.

In total, 27 scans were conducted, the majority of which were internal, with three exceptions. These were carried out to assist in matching the current work with the existing exterior survey of the building. In instances where areas were challenging to capture or inaccessible to the LiDAR instrument, a drone flight was employed.

3.2. The Control and Detail Network

The control network was established by positioning triangulation points in strategic locations that covered the different areas of the structure, allowing an unobstructed view of the targets or points that made up the detail network. These points were placed in the main nave, the corridor leading to the crypt, and within the crypt itself. Additionally, two external points were captured using GNSS (Global Navigation Satellite System) to later transform local coordinates into global ones, ensuring the georeferencing of all captured points.

Image 16 - Example of Target Positioning in the Building for survey (left) and positioning of Total Station and Survey Points: Eidotype Diagram (right).

Each vertex was marked on the ground to indicate the instrument's position, and it was then transferred to another triangulation point using a prism mounted on a tripod. All relevant information for each triangulation point, such as the coordinate system used, the instrument height, and the local coordinates, was recorded in a monograph, which can be found in the appendices of this document.

For the detail network, chessboard-type markers were used and placed on various vertical surfaces within the church, as seen on the left part of image 16. Each marker's position was stored in the instrument's memory along with a code identifying the control network triangulation point used for the measurement. This system ensured clear identification and easy data assignment, facilitating the organization and accuracy of the survey.

Image 17 - Total station setup at a vertex of the control network with chessboard target or point of the detail network inside the church's crypt.

STATION	COORDINATE	
11000	East (m)	412476,881
	North (m)	5020530,802
	Height (m)	420,19477
12000	East (m)	412486,455
	North (m)	5020533,365
	Height (m)	419,49214
13000	East (m)	412487,4175
	North (m)	5020529,502
	Height (m)	419,343

Table 2 - Some of the coordinates of the control network point in a local reference system.

3.3. Acquisition of Scans Through Laser Scanner

The instrument used for laser scanning was a LEICA RTC360 which is mounted on a tripod and activated at different positions of interest within the case study, it then rotates on two orthogonal axes to scan its surroundings, capturing a point cloud that provides a three-dimensional representation of the space. The workflow of this modern equipment allows for a somewhat more intuitive operation without much planning on the part of the user, as each scan or take that is performed, the equipment connects and syncs with a tablet that allows the control and verification of the results obtained at the end of each scanning session.

Scans were performed at 27 different points in the church, which were encoded and made up the complete point cloud of the case study. A significant part of the creation of the unique point cloud was carried out automatically by the same software used by the equipment, significantly reducing the manual intervention that would have been necessary with less modern equipment.

However, as previously mentioned, manual intervention in the processing of data when merging the clouds is not entirely ruled out. It turns out that the presence of targets in individual takes is of utmost importance as they assist in the possible overlapping of clouds and subsequently in their georeferencing, with the help of data from the total station.

Image 18 - Positioning of the laser scanner Leica RTC360 inside the churchs crypt (left), representation of laser scanner Leica RTC360 (right).

Source: www.leica-geosystems.com

GENERAL	
3D laser scanner	High-speed 3D laser scanner with integrated HDR spherical imaging system
PERFORMANCE	
Data acquisition	‹3 mins for complete full dome scan and spherical HDR image at 6mm @ 10 m resolution
Double scan	Automatic removal of moving objects
Check & Adjust	Field procedure for targetless checking of angular parameters
SCANNING	
Distance measurement	High-speed, high dynamic time of flight enhanced by Waveform Digitising (WFD) technology
Laser class	1 (in accordance with IEC 60825-1:2014), 1550 nm (invisible)
Field of view	360° (horizontal) / 300° (vertical)
Range	Min. 0.5 - up to 130 m
Speed	Up to 1,000,000 pts / sec
Resolution	3 user selectable settings (3/6/12 mm @ 10 m)
Accuracy*	Angular accuracy 18" Range accuracy 1.0 mm + 10 ppm 3D point accuracy 1.9 mm @ 10 m 2.9 mm @ 20 m 5.3 mm @ 40 m
Range noise* **	0.4 mm @ 10 m, 0.5 mm @ 20 m
IMAGING	
Camera	36 MP 3-camera system captures 432 MPx raw data for calibrated 360° x 300° spherical image
Speed	1 minute for full spherical HDR image at any light condition
HDR	Automatic, 5 brackets
NAVIGATION SENSORS	
Tilt	IMU based, Accuracy: 18" (for upright and upside down setups with +/- 5° inclination)
Additional sensors	Altimeter, Compass, GNSS

OPERATION	
On scanner	Touch-screen control with finger touch, full colour WVGA graphic display 480 x 800 pixels
Mobile devices	Leica Cyclone FIELD 360 app for iOS and Android tablet computers and smartphones including: - Remote control of scan functions - 2D & 3D data viewing - Tagging - Visual alignment of scans
Wireless	Integrated wireless LAN (802.11 b/g/n)
Data storage	Leica MS256, 256 GB exchangeable USB 3.0 flash drive
DESIGN & PHYSICAL	
Housing	Aluminium frame and sidecovers
Dimensions	120 mm x 240 mm x 230 mm / 4.7" x 9.4" x 9.1"
Weight	5.2 kg / 11.5 lbs, nominal (without batteries)
Mounting mechanism	Quick mounting on 5/8" stub on lightweight tripod / optional tribrach adapter / survey tribrach adapter available
POWER	
Internal battery	2 x Leica GEB361 internal, rechargeable Li-Ion batteries. Duration: Typically up to 4 hours Weight: 340 g per battery
External	Leica GEV282 AC adapter
ENVIRONMENTAL	
Operating temperature	-5° to +40°C
Storage temperature	-40° to +70°C
Operating low temperatures****	-10° to +40°C
Dust/Humidity***	Solid particle/liquid ingress protection IP54 (IEC 60529)

Leica RTC360

Leica Cyclone FIELD 360

Leica Cyclone REGISTER 360

Image 19 - Extract from the technical sheet of the laser scanner Leica RTC360

Source: www.leica-geosystems.com

3.4. Acquisition of Frames Via UAV

TThe laser scanner alone is insufficient for obtaining a point cloud with sufficient detail of the interior of the church. Therefore, it was necessary to create a point cloud using photographs captured by a drone from areas not visible to ground-based equipment.

These areas of interest include the upper windows on the south wall of the church and the trusses supporting its roof. To obtain these details, a DJI Mini 3 Pro aircraft was utilized, as illustrated in Image 20. The device executed the same route on two occasions, with a distinct target selected for each flight.

The flight was conducted by a technician with the necessary qualifications, who took photographs at a fixed height (that of the center of the window) and along a path that the drone would follow, stopping at regular intervals to capture a picture. These were subsequently employed and processed to construct a point cloud utilizing photogrammetry, as will be explained in greater detail later in this paper.

Up next it is shown the relevant technical specifications of the aircraft and photography equipment that make up the drone used:

TECHNICAL SPECIFICATIONS			
AIRCRAFT DJI MINI 3 PRO		**Camera FC3582**	
TAKEOFF WEIGHT	<249gr	Model	FC 3582
MAX ASCENT SPEED	5 m/s	Number of pixels	12 MP
MAX DESCENT SPEED	5 m/s	Image Sensor	1/1.3” CMOS
MAX HORIZONTAL SPEED	16 m/s	Lens	24 mm
MAX FLIGHT TIME	34 min	Max Image Size	4032x3024 pi
GNSS	GPS + BEIDOU + GALILEO	ISO	ISO-160

Table 3: Technical specifications of the UAV used.

Image 20 - Drone DJI Mini 3 Pro.

Source: www.dji.com

4. Processing of Survey Data

Once all the necessary on-site data has been collected, the next step is to process and refine it for subsequent phases. For each type of data, the appropriate software was used: for points acquired through topographic equipment, Star*Net was employed; for the drone-captured images, Agisoft Metashape (Photoscan); and for the laser scans, Cyclone Register 360 Plus, a software developed from the same company as the equipment used.

This entire process aimed at producing a single output that best represents the geometric and material information of the building. The workflow is summarized as follows:

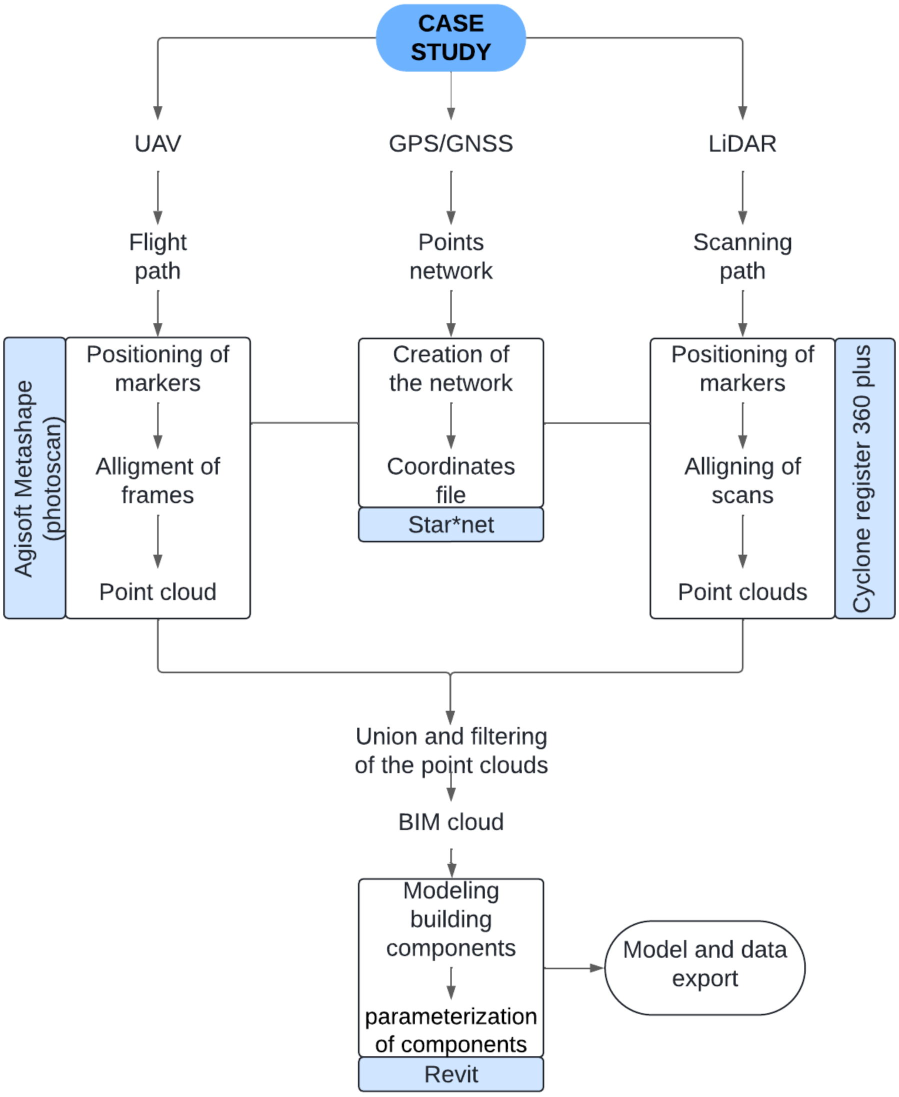

Image 21 - Workflow diagram for processing a point cloud to be used in a BIM environment.

4.1. Creating the Coordinates File

The starting point for creating the final coordinate document is the file obtained from the total station and GPS, which contains all the local coordinates X,Y,Z taken from various objectives or points.

Using Star*Net, a corrected topographic point network was generated by configuring parameters such as the type of network to compensate, the coordinate system (in this case, WGS 84 / UTM Zone 32), and the instrument precision. The purpose of these settings ensures optimal results.

The final output results in a file containing a graphical representation of the network with the corresponding dispersion ellipses of the individual collimated points, and the coordinates, which are exported in .txt file that later will be uploaded or imported in a different program for spatial localization, i.e., georeferencing the point cloud.

Below is a portion of the software's calculations and the representation of the topographic network obtained from the software.

Station	**H (m)**	**Collimated point**			
12000	1.655	12100	DN 12100 4.6199	V 12000-12100 96.809 1.655/0	D 12000-12100 14.8505 1.655/0
12000	1.655	12101	DN 12101 7.4649	V 12000-12101 97.62 1.655/0	D 12000-12101 18.6419 1.655/0
12000	1.655	12102	DN 12102 12.1051	V 12000-12102 93.0113 1.655/0	D 12000-12102 15.1902 1.655/0
12000	1.655	12103	DN 12103 13.2627	V 12000-12103 94.8437 1.655/0	D 12000-12103 11.9206 1.655/0
12000	1.655	12104	DN 12104 12.7987	V 12000-12104 101.9909 1.655/0	D 12000-12104 11.8744 1.655/0
12000	1.655	12105	DN 12105 194.5671	V 12000-12105 92.9472 1.655/0	D 12000-12105 2.6178 1.655/0
12000	1.655	12106	DN 12106 302.9718	V 12000-12106 89.154 1.655/0	D 12000-12106 1.6229 1.655/0
12000	1.655	12107	DN 12107 303.6613	V 12000-12107 112.2535 1.655/0	D 12000-12107 6.1017 1.655/0
12000	1.655	12108	DN 12108 319.2387	V 12000-12108 111.3682 1.655/0	D 12000-12108 4.7003 1.655/0

Table 4 – Fragment of the data obtained from Star*Net.

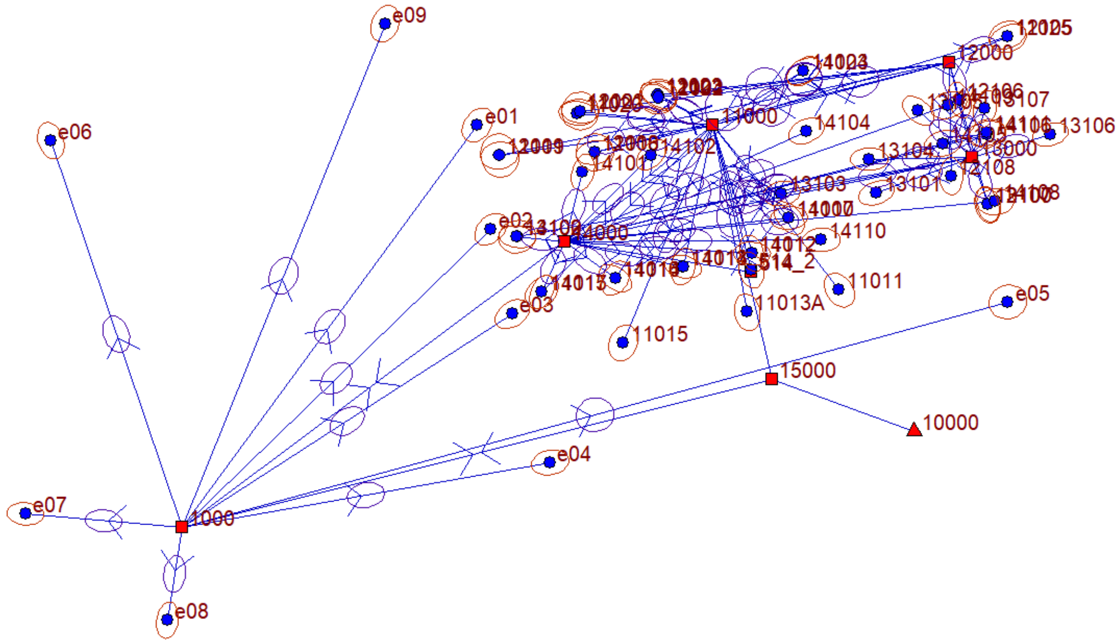

Image 22 - Result of the compensated network obtained from the STAR*NET software.

4.2. Processing of Data Acquired with Terrestrial Laser Scanner

In the present case study, laser scanner instruments were employed because they facilitate the rapid acquisition of comprehensive geometric information and surface characteristics of the building, offering a significant time-saving advantage over more traditional methods. Subsequently, the data is employed for analytical and modeling purposes. The simplicity of the equipment's handling and operation facilitated the execution of numerous scans conducted in various locations within the building, including the exterior, the central nave, the crypt, and the presbytery of the church. This resulted in a total of 27 scans. The reference below image (Image 23) illustrates the floor plan view of the church, indicating the location of the scans.

The 3D laser scanner's capture capability, when paired with the software Cyclone Register 360 Plus, a product of the same suite of Leica software, ensures that all necessary operations can be conducted smoothly, with minimal or no manual intervention and no need for revisiting the work site. This approach not only saves time but also ensures the data's completeness and accuracy. Cyclone Register 360 Plus facilitated the setting of specific parameters during the data acquisition phase and the management of data during the processing phase. This meticulous process guarantees the collection of precise and efficient data, thus providing the basis for detailed analysis and modeling in subsequent stages.

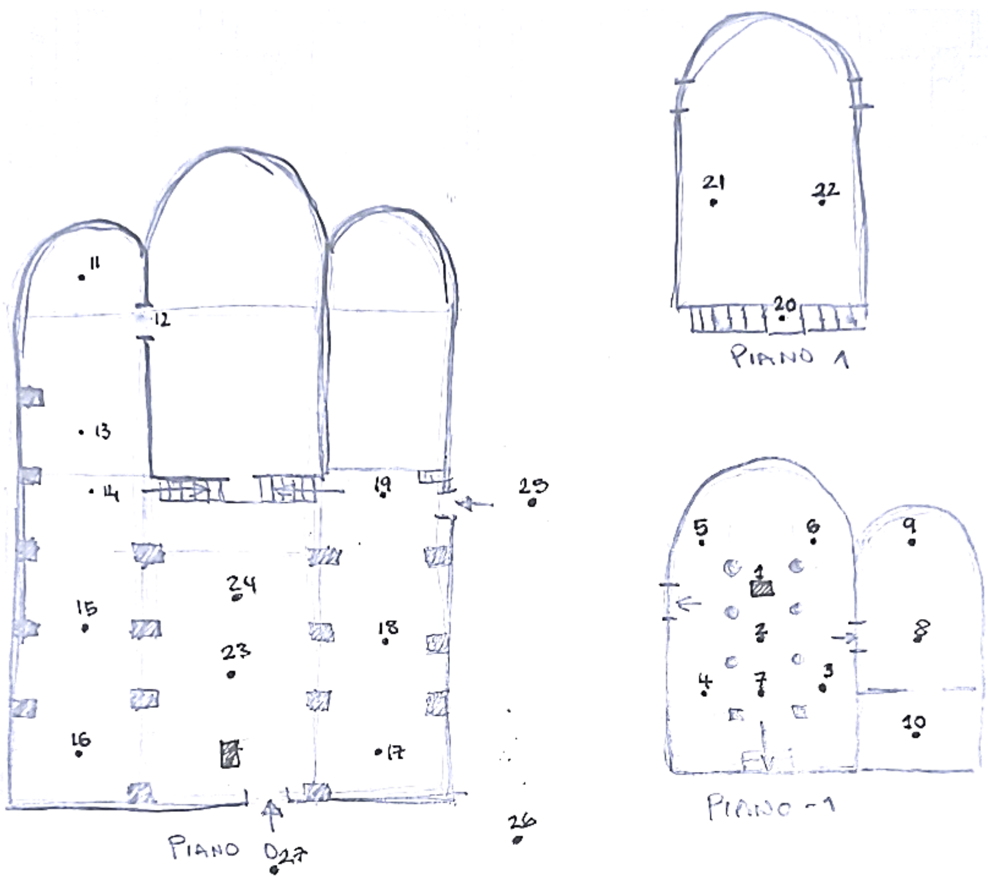

Image 23 - Positioning of the laser scan: Eidotype Diagram

4.2.1. Cyclone Register 360 Plus

Cyclone Register by Leica Geosystems is a sophisticated software module with a robust algorithm that efficiently aligns and merge individual laser scans into a singular, accurate and cohesive three-dimensional representation of the scanned environment.

Its improvement with respect to outdated similar programs come from some features that are automatic like the 'Cloud-to-Cloud' registration technique that uses geometry within the point clouds themselves, promoting a more seamless and targetless alignment process, proving advantageous in environments where placing targets is impractical or when scans have been conducted without them. In addition to this, a user interaction feature or ‘Visual Registration’ is still available and provides a manual alignment, supplementing the automatic registration process allowing for a hybrid approach combining both registration methods.

Some advanced error analysis tools within the software allows the assessment of the quality of the registration in real-time, providing immediate feedback on potential misalignments and suggesting the necessary adjustments to achieve the best possible results.

As a result, a fully merged and aligned scans produce a unique point cloud that is then georeferenced by linking markers within the point cloud and coordinates points taken from the topographic survey.

4.2.2. Loading and Alignment of Scans

The loading and aligning scans in Cyclone Register begin with the importation of the raw point cloud data, which consists of multiple individual scans that have been previously connected or linked.

The software automatically separates the scan data into groups, categorized based on their geographic and spatial characteristics. By leveraging the visual alignment feature of the software, the adjustment and overlaying of different scan groups was performed to unify them into a single aligned point cloud.

Initially when the scans were created an initial number of links were obtained that behaved in a sequential manner as observed on the left side of image 24, showing the first upload of raw data, later these links were increased to create a denser and more accurately aligned point cloud, as observed on the right side of image 24. This process involved controlling the overlap percentage and the mean error estimated by the program. For scans like 25, 26 and 27, visual alignment was utilized to merge them into a single set of connected points, as depicted later in the chapter.

For a favorable outcome in the alignment, notable overlapping points were selected to precisely associate both scans. As a reference or point of overlap, a clearly marked corner of an external wall façade was used on both scans, as seen on the left side of image 25, these scans were moved in a vertical and horizontal manner until a viable result was achieved, thus fixing the link between them.

The same procedure was applied to scans 27 and 23, aiming to align overlapping surfaces to create a linkage between the exterior and interior (right side of image 25). This process ensured that the internal and external scans were connected correctly, forming a comprehensive point cloud of the structure (Image 26).

Finally, by optimizing the complete set accounting for both the internal consistency of scans and their collective alignment, a single unified cluster was obtained, resulting in a cohesive and accurately aligned point cloud that fulfills the minimums thresholds expected, leaving a ready to work with cloud for further processing or analysis.

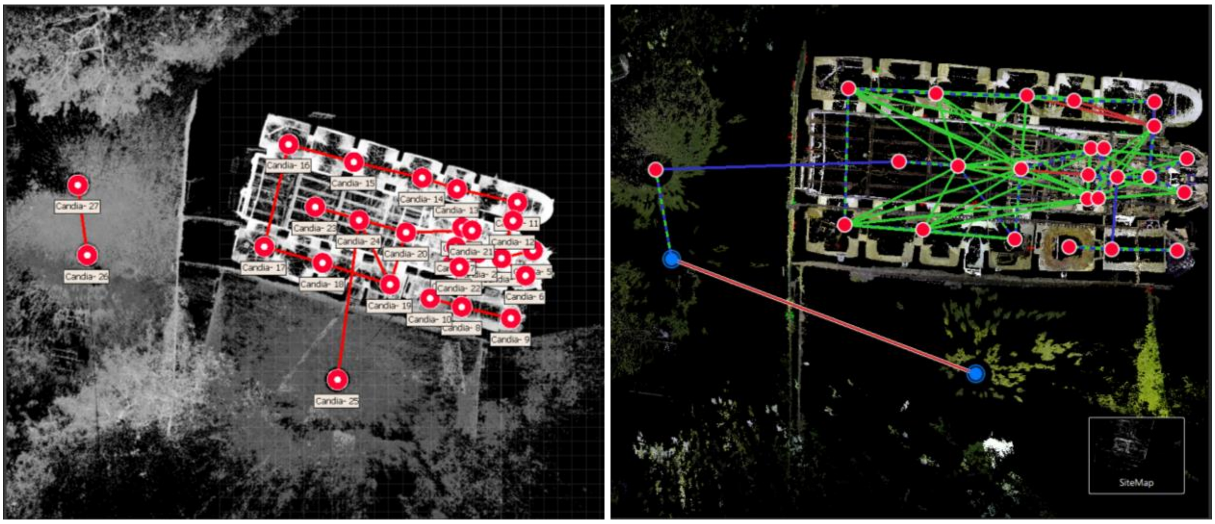

Image 24 - Upload of the laser scans to the Cyclone REGISTER 360 PLUS software (left) and Linkage of the laser scans (right).

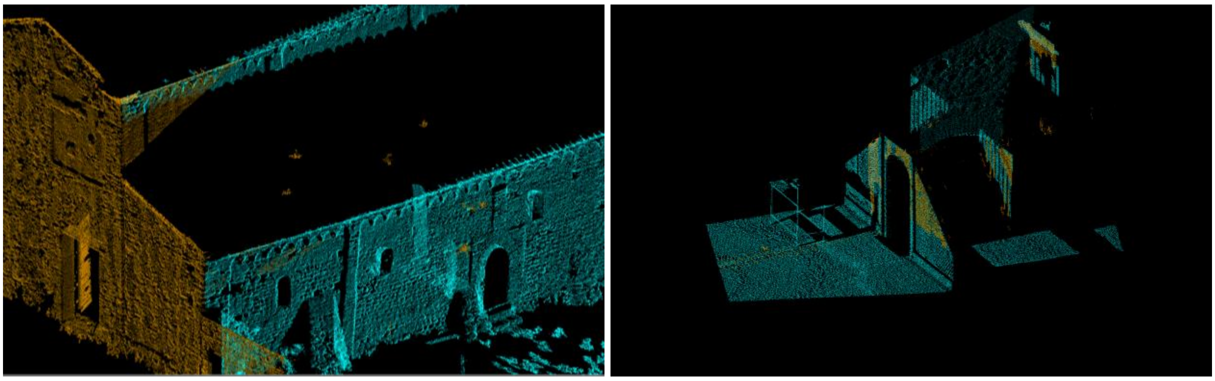

Image 25 - Manual overlaying of exterior (left) and interior scans (right).

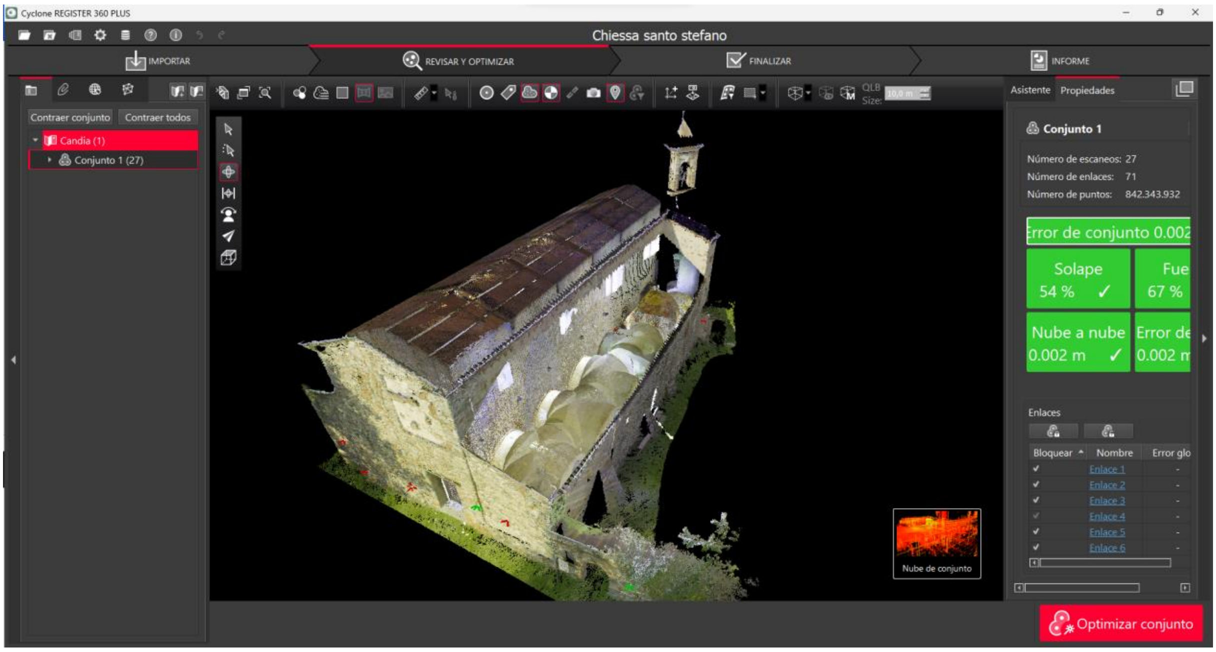

Image 26 - Aligned point cloud with acceptable threshold.

4.2.3. Setting the Reference System and Positioning of Markers

Once the scans have been aligned and organized, the next stage is to apply a global georeference to them in order to position them correctly, as they are automatically saved in local coordinates created by the equipment. This is accomplished with the assistance of the marked points that have been captured and stored in the total station.

The procedure begins with the importation of all captured coordinate points into the program. These points correspond to a defined target that was captured and codified by the topography equipment, as illustrated in the left side of Image 27. Subsequently, all scans exhibiting a discernible image of one of these targets are subjected to a review process, during which a virtual marker is created and associated with each one of them. The objective is to establish a connection between the visible targets in all the scans. The right side of Image 27 illustrates this assignment process.

Upon completion of the assignment process, a georeferenced point cloud is generated, which can then be utilized in subsequent steps.

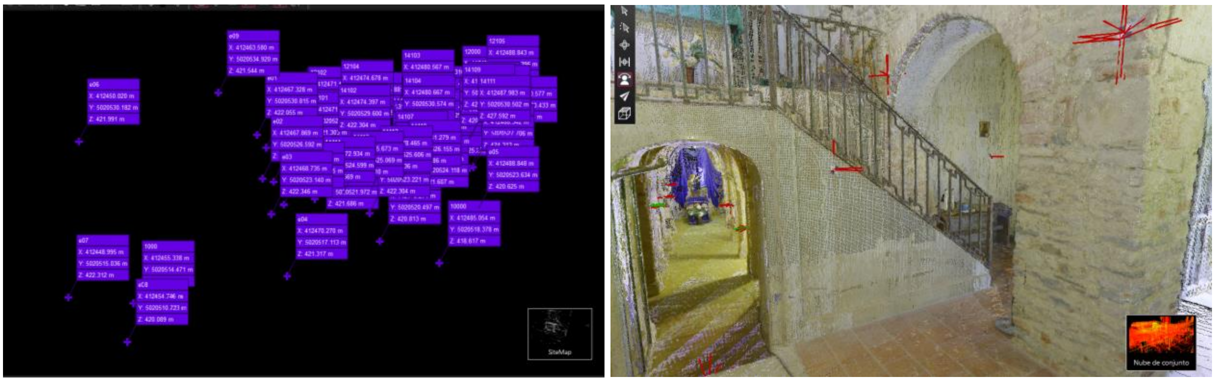

Image 27 - Upload of the survey marker coordinates (left) and positioning of them (right) to the Cyclone REGISTER 360 PLUS software.

4.2.4. Export of the Point Cloud and Final Report Obtain

As the concluding phase of this stage of the procedure, the point cloud must be exported in a format that is compatible with the other software programs that will be utilized. Cyclone Register 360 Plus enables the export of the file in a variety of formats that are easily readable by other programs with similar functionality. In accordance with the considerations applied in the preceding work conducted on the same case study, the .E57 format was chosen as it is compatible with the programs to be utilized in the subsequent sections.

Given that the complete point cloud comprises 27 scans, the export can be conducted either as a single unified file or as 27 separate files, with each file corresponding to a single scan. The distinction between these newly generated files and the original ones lies in the fact that they are now georeferenced and aligned. For the purposes of this work, exporting each scan individually is an appropriate decision, as processing smaller files is more efficient than dealing with a larger, more complex single file.

Upon completion of this phase, the software generates and stores a comprehensive report detailing the overlay of the scans, their degree of linkage, and the mean error value. This information can be found in the appendices of the present thesis.

4.3. Processing of Data Acquired with Aerial Photogrammetry from UAVs

The photogrammetry process was performed on the interior south wall of the church, a decision that was driven by the limitations of captured details inherent to the ground-level laser scanning performed.

This is especially true for out of reach areas such as the windows jambs and sills, which require a vantage point that is on the same level of the windows itself, to ensure accurate representation.

Therefore, aerial photogrammetry was employed to capture the required data. The UAV was able to fly at the height of the windows, providing a unique perspective that allowed the necessary angles and level of detail needed for a high-resolution imagery of the element used in its analysis and reconstruction.

4.3.1. Agisoft Metashape (Photoscan)

Agisoft Metashape, previously known as PhotoScan, is an advanced photogrammetry software that enables users to process digital images to generate high-quality 3D spatial data. This process is conducted through the reconstruction of the geometry of captured images from various angles, using computer vision algorithms to identify and match common points across the images. From these points, the program can calculate the position and orientation from which each photo was taken, allowing for the three-dimensional reconstruction of the photographed object or scene.

The workflow in Metashape is generally sequential and includes several key stages: uploading images, aligning them to create a sparse 3D point model, optimizing the model to enhance accuracy, generating a dense point model, and finally, constructing a textured 3D model or an orthomosaic and elevation models, depending on the project's goal. Throughout the process, users can adjust parameters and use tools to improve the quality of the model, such as selecting and positioning markers for geometric calibration and defining a reference system.

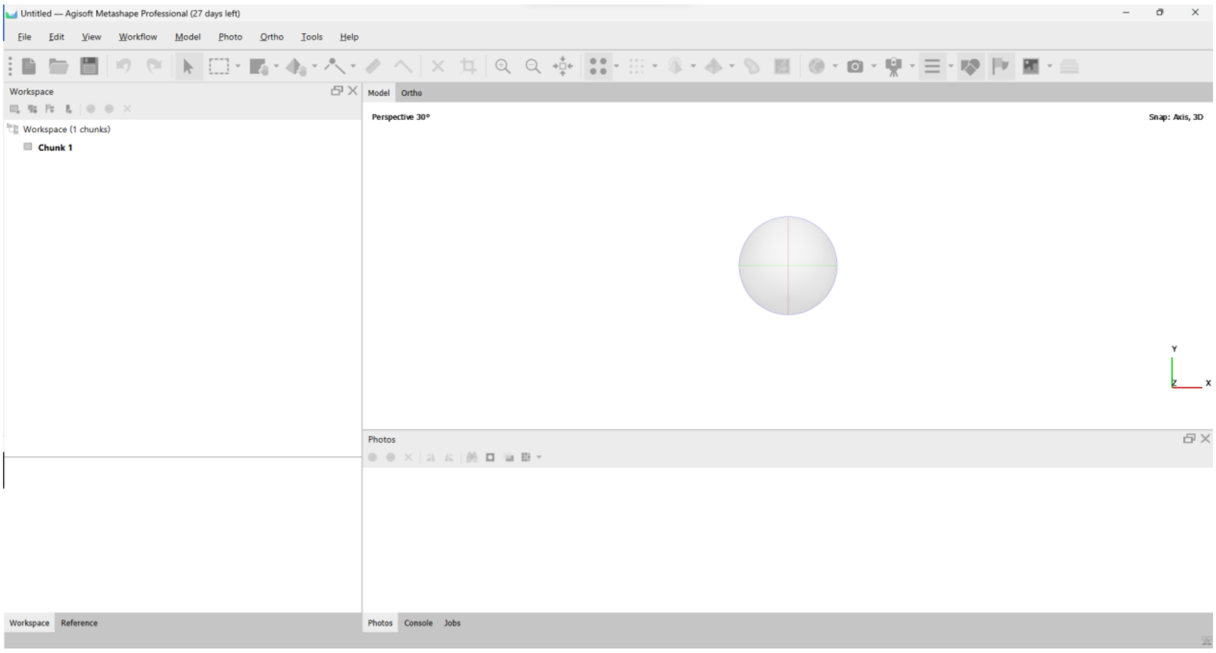

Image 28 - Agisoft Metashape initial interface.

4.3.2. Selection, Loading and Alignment of Frames

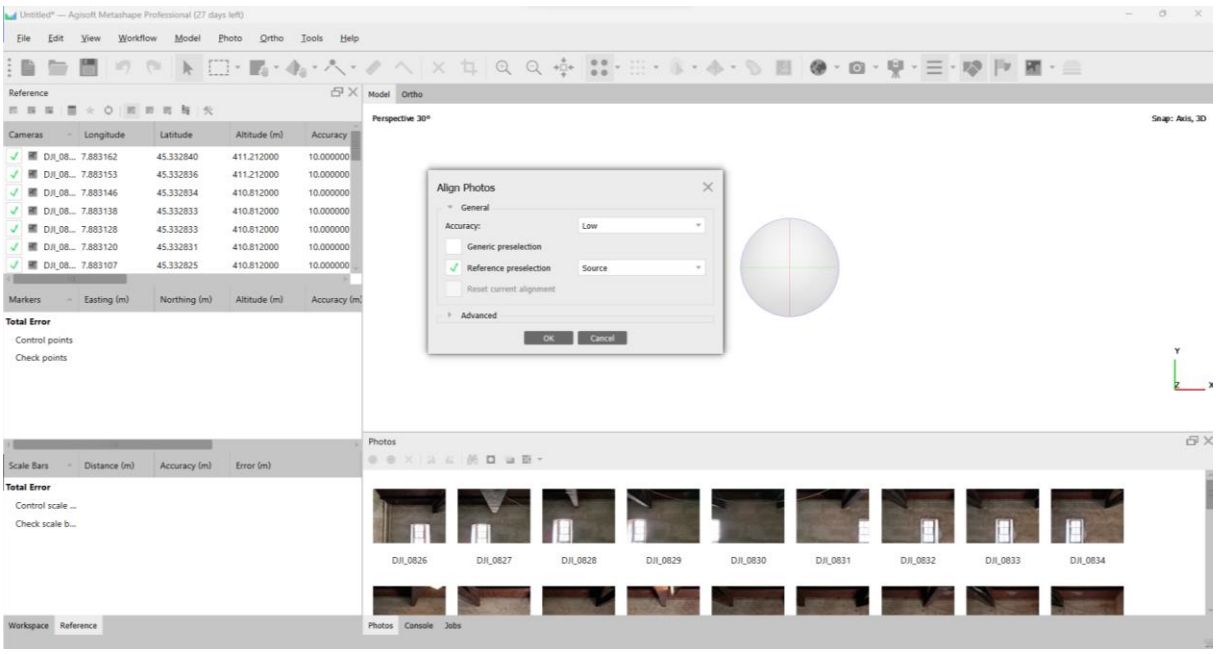

Image 29 - Upload and Alignment of the photographs.

The first task was the selection and loading of imagery. The chosen images were those captured via drone, selected for their overlap and coverage of the study area, ensuring comprehensive data input for the creation of the point cloud. These images were then loaded into the Metashape project workspace. Care was taken to ensure that the images were of high quality, with good lighting and clarity to facilitate precise alignment.

The alignment process began with the selection of the alignment settings within the program. The software provides options to adjust the accuracy level, ranging from lowest to highest, allowing the user to make a choice based on the desired quality. For the initial alignment, a low-resolution setting was used to quickly generate a sparse cloud and to identify any gross misalignments or errors in the dataset.

Subsequently, the 'Align Photos' function was executed, which initiated the matching of common points between the frames using Metashape's algorithms. This process involves detecting and matching thousands of keypoints across the images to establish their relative positions. Once the photos were aligned, a sparse point cloud was generated, providing a preliminary 3D visualization of the surveyed area. This allowed for an assessment of the alignment quality and the detection of any potential issues that might require re-alignment or the exclusion of any problematic frames.

During this process, the software utilized its photogrammetric capabilities to triangulate the position of each camera shot, effectively reconstructing the scene in three dimensions, as seen below.

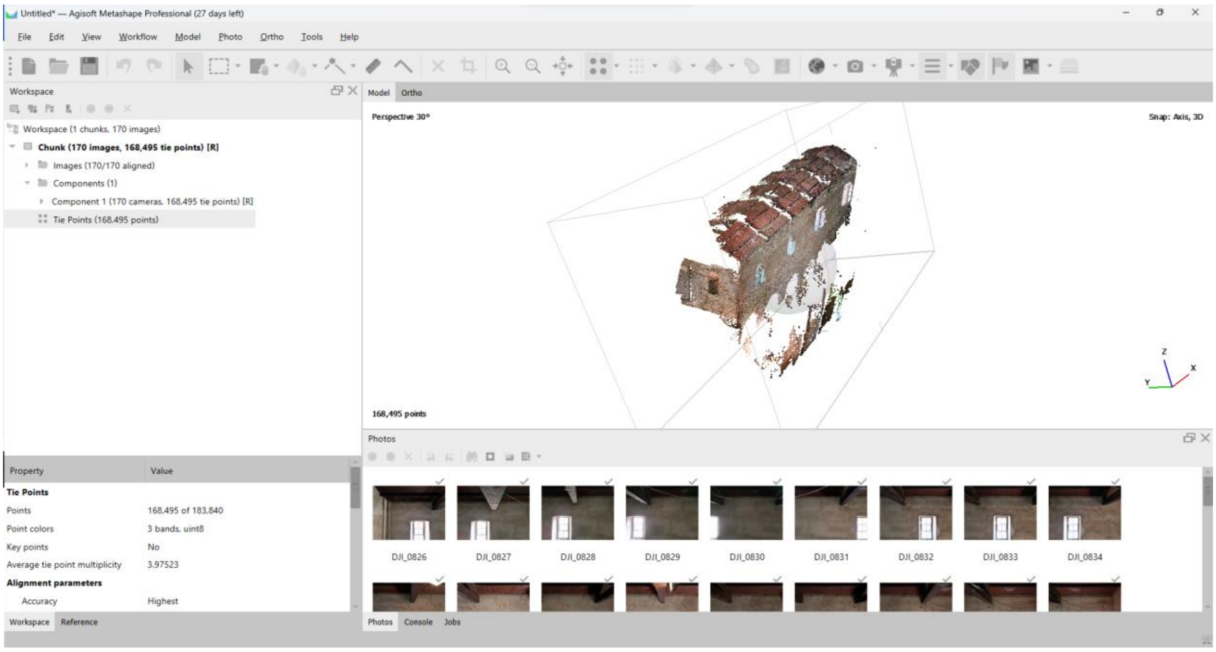

Image 30 - Three-dimensional reconstruction of the aligned photos.

4.3.3. Setting the Reference System and Positioning of Markers

After the successful alignment of images and creation of a preliminary point cloud, the next crucial step was to georeference the data within a chosen coordinate system. In Agisoft Metashape, this was achieved by setting a reference system to ensure that the spatial data corresponds to real-world coordinates. The software provides a range of coordinate systems, from local to global datums, allowing for the selection of a system that best fits the project requirements.

For this project, the World Geodetic System 1984 (WGS 84) was selected due to its compatibility with GPS data. To set this coordinate system within Metashape, I accessed the 'Reference Settings' panel where I could specify the desired system. This established the framework for the subsequent georeferencing of the point cloud.

Markers, or ground control points (GCPs), are crucial for accurate georeferencing. These markers had been previously placed in the field and recorded using a total station, providing precise local coordinates. The task then was to input these local coordinates into Metashape and transform them into the global WGS 84 system. This transformation imbued the point cloud with accurate location data.

Using the 'Markers' panel, each GCP was matched to its corresponding marker within the point cloud. The software interface displayed thumbnail images below the point cloud visualization, here it can be visually identified and the markers placed on the exact location of each GCP. By selecting a marker and its corresponding location across multiple images, Metashape triangulated its position in three dimensions, integrating the marker into the point cloud with high precision.

The accuracy of marker placement was of utmost importance. Metashape provided tools to assess and adjust the accuracy of each marker's position. Adjustments were made until the error was within acceptable limits, ensuring the highest level of accuracy for the georeferenced point cloud.

Image 31 - Upload (left) and positioning (right) of the survey marker coordinates to Agisoft Metashape software.

Markers	Easting (m)	Northing (m)	Altitude (m)	Accuracy (m)	Error (m)	Projections	Error (pix)
516A	412485.848820	5020527.134980	425.295450	**0.005000**	0.027656	19	1.480
515A	412480.406200	5020526.063790	425.369460	**0.005000**	0.020431	20	4.542
11011	412482.009000	5020524.118000	421.607220	0.005000	0.017048	4	0.992
14110	412481.278800	5020526.155000	422.686090	0.005000	0.015431	9	0.686
11012	412478.462900	5020525.608000	422.424820	0.005000	0.012597	9	1.100
11017	412469.940200	5020524.040000	422.693120	0.005000	0.012482	4	1.324
14108	412488.341600	5020527.706000	424.312920	0.005000	0.012246	7	2.307

Image 32 - Precision check of some of the survey markers coordinates in the point cloud.

4.3.4. Export of the Point Cloud and Final Report Obtain

Once the alignment and georeferencing work is completed, the next step is to export the point cloud. By Clicking on the “workflow” tab and selecting the option “build point cloud” a window opens that allows to adjust the quality and depth filtering. Due to the nature of the case study, the options "medium" and "moderate" respectively are sufficient to achieve the desired results.

The chosen export file type was .E57, the same as in the previous step. Similarly, the program generates a report where data related to the images, the camera used for capturing the frames, and the relative errors in the positioning of the markers can be reviewed. All this information can be checked and verified in the appendices of this document.

5. Processing Point Clouds

Once the terrestrial laser scanning and the aerial photogrammetry georeferenced point clouds have been created, a framework is obtained for the merging into a unified, lightweight cloud. This foundational cloud serves as the basis for the subsequent three-dimensional model.

The process is aimed at producing a singular and complete point cloud that incorporates the detailed attributes of both the terrestrial and aerial data for their further refinement, which includes cleaning, comparing, and ultimately merging the two datasets. Even though these tasks can be performed within the same software used to generate the original clouds, the project benefited in this specific case from exporting the data to a third-party program. This allowed for more sophisticated operations such as enhanced comparison and verification of results, facilitating a deeper analysis of the cloud's characteristics.

The goal of this meticulous procedure is not only to achieve a high-quality merged point cloud but also to enhance the interoperability between different software platforms. This interoperability testing is crucial for evaluating how well the data can be integrated and manipulated across various applications, ensuring a robust, accurate, and visually compelling three-dimensional model suitable for further analysis and application.

5.1. Refinement and Optimization of the Point Cloud

The point clouds obtained are characterized by having a high number of points due to areas captured outside the main building and the high-density capture capability of the scanning equipment. While this level of detail is advantageous for certain applications, it reduces the manageability and operability of the file for this case study. To address this, the point cloud must be cleaned and subsampled, focusing specifically on the space surrounding the Church of Santo Stefano (for the exterior scans) and removing redundant areas captured more than once (for the interior scans). This process involves deleting elements like plants, trees, and all elements that are outside the scope of the current work. By refining the point cloud, the data becomes more efficient and useful for subsequent analysis steps.

5.1.1. The Software Cloudcompare

CloudCompare is an open-source software that supports a wide range of commands for processing, managing, and modifying large point clouds originating from any type of instruments, including those used in our case study which are terrestrial laser scanners and UAV photogrammetry. The point clouds obtained before were exported individually, totaling 28 files in .E57 format, 27 from the laser scanner plus one from the photogrammetry.

CloudCompare facilitates the handling of these files without limits on formats and sizes, enabling users to easily import, clean, reduce noise, and merge or separate the imported clouds. The software includes advanced algorithms that allow for the extraction of mutual distances between dense point clouds, evaluation of geometric characteristics, and execution of numerous statistical calculations. One of its distinctive features is the "Scalar fields", where the program generates an RGB color scale directly associated with the distance between points in the compared clouds.

The interface of CloudCompare is simple and intuitive, allowing users to optimize the results based on quality, geometric characteristics, and user objectives. The results can be exported in various formats. Utilizing CloudCompare has significantly enhanced the cleanliness and manageability of the point clouds, achieving high-quality results in a timely manner.

5.1.2. Export, Subsample and Cleanup of the Point Clouds

The initial step involves opening the georeferenced point clouds produced in the previous software. A significant part of the workflow is dedicated to lightening these point clouds to enhance manageability for subsequent modeling steps. This is achieved by creating subsamples of the original files and then cleaning these subsamples to remove redundant portions, distant acquisitions relative to the scanning equipment, or elements outside the designated study structure.

Initially in some scans, the number of points amounted to approximately 41 million, which were then reduced to about 2 million points for a more effective management (basically 1/20 of points reduction), even before additional cleaning is applied.

Further details are incorporated into the model through UAV photogrammetry as explained before, by being able to capture elements like window details, which were inaccessible to ground-based scanning due to physical limitations.

Once all the scans are thoroughly cleaned, a lighter and cleaner subsampled point cloud is produced.

Image 33 - Before (left) and after (right) comparison of a subsampled point cloud on the CloudCompare software.

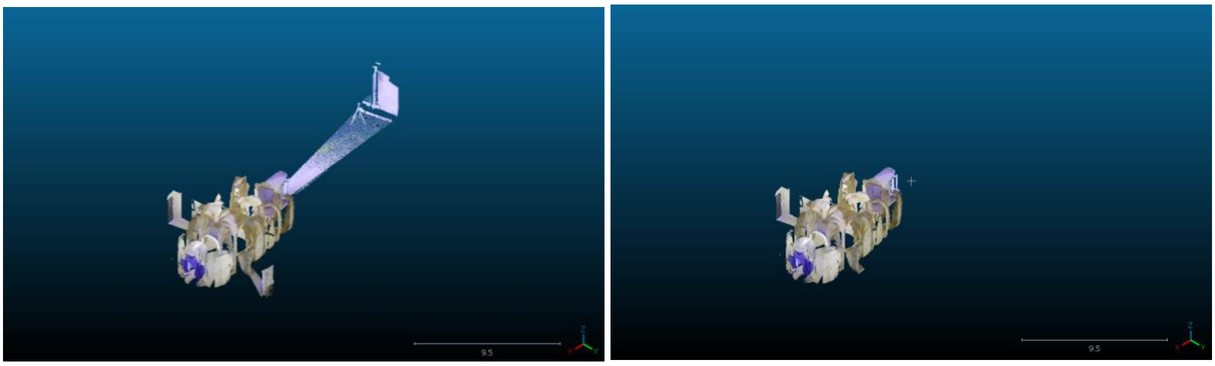

Image 34 - Before (left) and after (right) of the cleaning of a point cloud on the CloudCompare software.

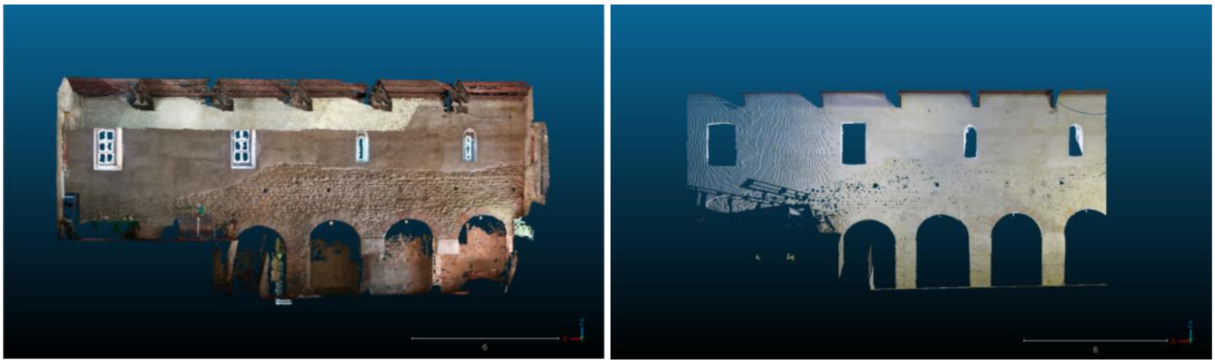

Image 35 - Comparison between the photogrammetry (left) and laser scanner (right) point clouds.

Image 36 - Enhanced laser scan point cloud with photogrammetry details (left) and final unified, subsampled, cleaned and Enhanced point cloud (right).

5.1.3. Clouds Comparison and Union

The next phase involves a meticulous review of the overlap between the processed internal cloud and the existing external one received from the university data base, focusing particularly on matching architectural details by carefully sectioning and verifying the cloud's superimposition. Visual modification tools present on the program allows a better graphical representation and distinction between the internal and external cloud points, these are seen in the plant view showing matching corners and consistent wall thickness, alongside aligned doors and other exterior details, displaying the expected results.

Even though the scope of this works focuses on the interior of the case study building, some exterior scans were performed and used as an auxiliary external point cloud, enhancing the building's linkage and referencing. Some distance measurements between this auxiliary scan and the main external cloud were also conducted to ensure accuracy with the overlaying. Most points showed in the scalar field a variance in the distance between the set of clouds below the 5cm mark, confirming the precision of these scans.

The analysis shown on image 38 produced some small green areas which are points that represent elements like foliage and decorative features on the tower that were not present in the original external cloud. This comprehensive process in CloudCompare ensures detailed and accurate architectural and structural analysis, leveraging advanced tools for optimal point cloud management and analysis.

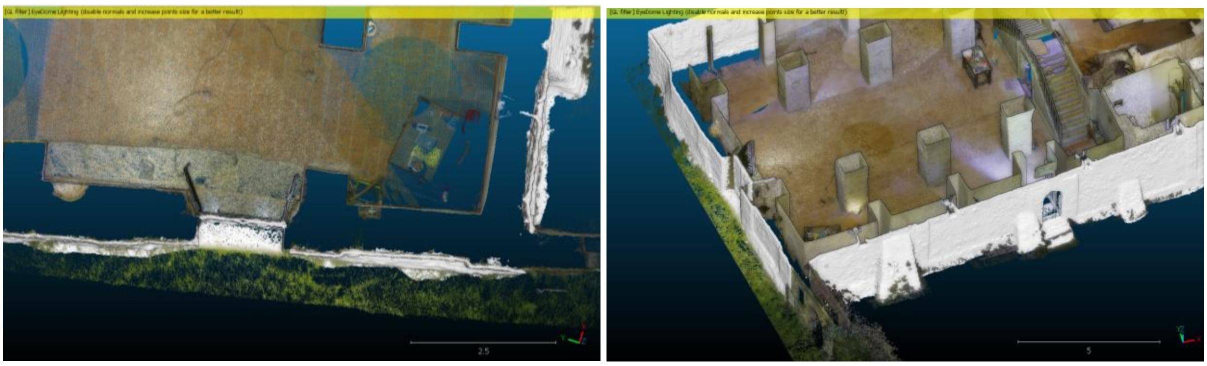

Image 37 - Inspection of the overlaying between the internal and external point clouds.

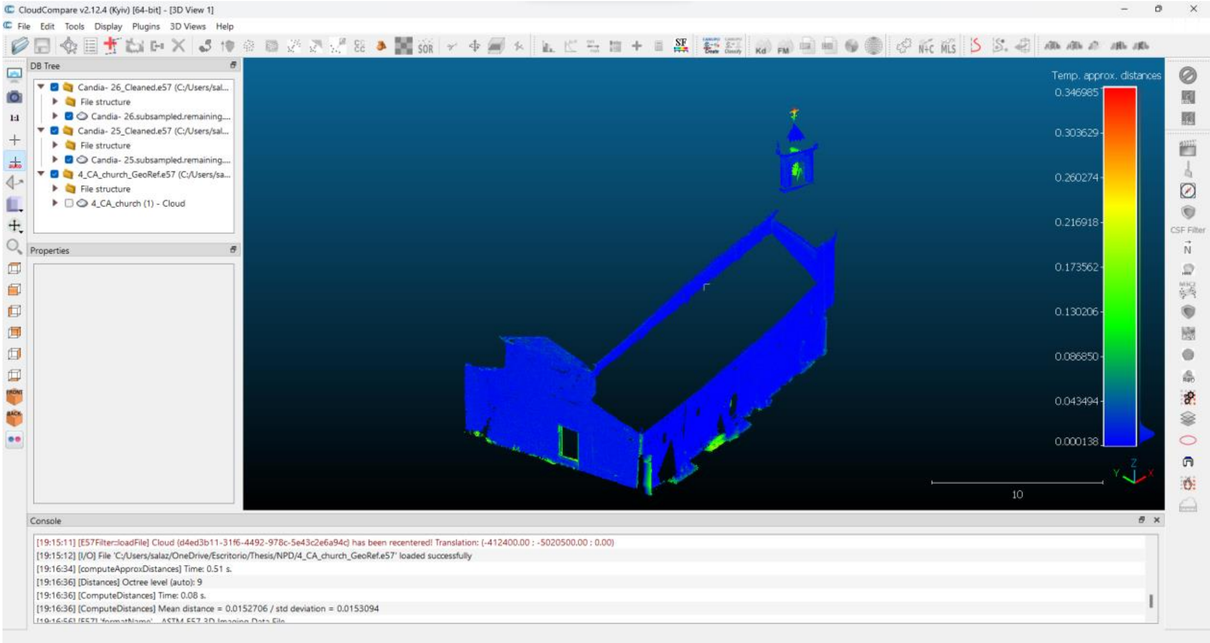

Image 38 - Accuracy check of the overlaying between the internal and external point clouds.

5.2. Preparation of the Point Clouds

The final, usable point clouds obtained from the integration of the two 3D metric survey techniques were exported in the .las format. This file format is a standard for the storage of airborne LiDAR data, including 3D point data and related attributes such as color and intensity. Despite its robustness for managing lidar data, this format is not directly compatible with Autodesk Revit, a software commonly used for building information modeling (BIM).

To overcome this compatibility issue, an additional program was utilized to facilitate the reading of the .las extension and its conversion into a format that Revit can interpret and utilize. This conversion process is crucial for integrating the detailed 3D data into subsequent phases of the workflow, which entail more sophisticated modeling and analysis in Revit. This step guarantees the preservation of the valuable geometric and spatial data captured in the survey, ensuring its full utilization in the BIM environment. This enhances the project's overall accuracy and utility in architectural planning and analysis.

5.2.1. The Software RECAP

ReCap360 is particularly effective because it is designed for seamless integration into Building Information Modeling (BIM) workflows. It was chosen specifically for its specialized capability to manage and export point clouds, as in this case, into another Autodesk software such as

Revit. This ensures better interoperability and minimizes issues related to format compatibility and data handling.

5.2.2. Point Cloud Export

The point cloud was exported from ReCap360 software in .rcp format, a format readable in Revit that also retained intrinsic information related to spatial and RGB coordinates. Within a new project in ReCap, the external and internal point clouds of the church were loaded. Subsequently, distinctions were made between these clouds (a region was created for each point cloud) to ensure that when exported to Revit, they appeared as two separate elements and not a single point cloud. However, despite Revit retaining the color distinctions of the point clouds, it did not allow them to be handled as two separate and individual elements. Therefore, each point cloud was exported individually.

This approach was preferred for the work being done, as having two different elements within the model allowed for them to be visualized or isolated individually, which facilitated the modeling of the church's components.

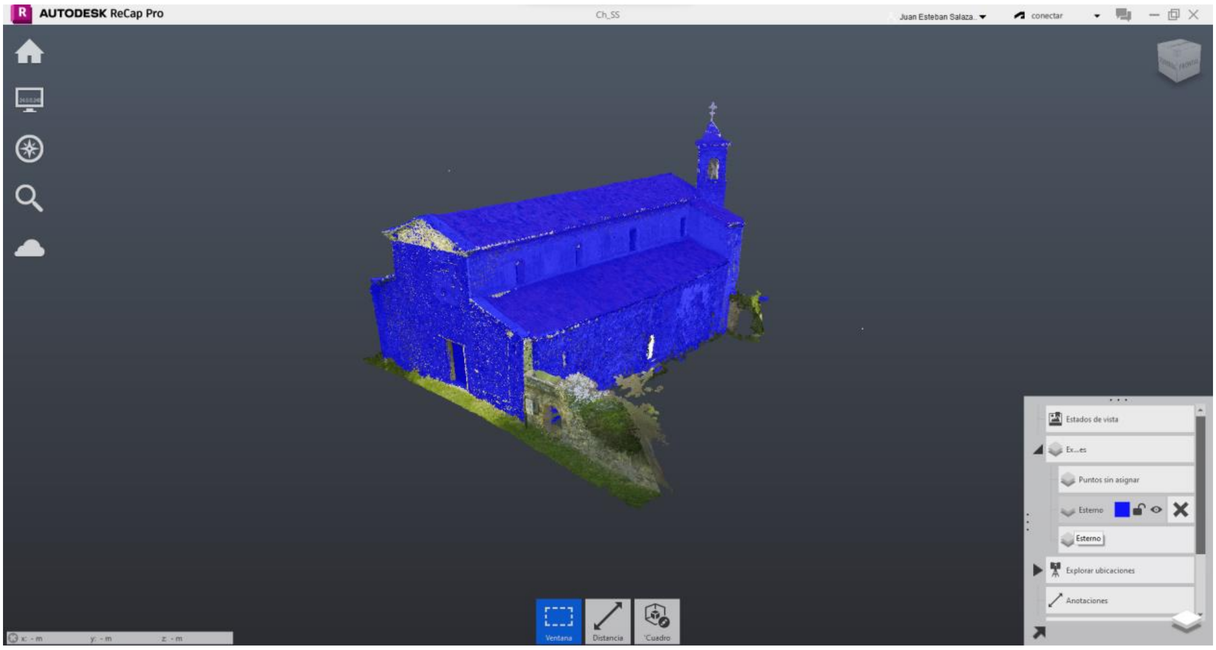

Image 39 - Creation of a region using Recap software.

6. Utilizing Point Cloud Data for Tridimensional Modelling

Once the point clouds have been processed and exported into a workable file, the next phase begins: the creation of an architectural 3D model of the Church of Santo Stefano. While the point cloud provides a highly detailed and accurate geometric representation, capturing even the most intricate details of the building's surface, it is inherently raw and unstructured. This unrefined nature makes it challenging to use directly for practical applications such as maintenance and restoration planning. The creation of a 3D model bridges this gap, transforming raw data into a structured, accessible, and visually coherent representation that facilitates planning and decision-making. A well-constructed model not only visualizes the building's geometry but also encapsulates its structural and design elements, making it an invaluable tool for future interventions.

In subsequent sections of this chapter, the software environment and key framework employed in the development of this 3D representation are explained in detail. While the model plays a crucial role in this work, it remains a tool serving a broader objective: the creation of a planned maintenance program. This plan links specific activities to elements within the model, enabling efficient and targeted conservation efforts.

6.1. BIM Methodology

The civil construction environment is one of the most demanding sectors regarding documentation creation and management, relying heavily on the comprehensive participation of multiple disciplines to successfully develop any project. In fact, is expected at the commencement of any engineering project some form of documentation that works as a guide or referment for the development of any given phase. Typically, a collection of documents and 2D representations, such as construction or architecture plans, technical specifications, project budget, schedules for operation and maintenance, among others, are indispensable. These documents are interdependent, requiring constant comparison and referencing throughout the project to verify correctness and progress, adding complexity to the construction process.

It's precisely the extensive array of interrelated information the cornerstone that created the necessity of a methodology to facilitate the efficient management and interpretation of project documentation.

The Building Information Modeling (BIM) methodology translates bidimensional information into a tridimensional digital model, integrating all construction and design data. This approach prevents information duplication, ensures consistency, and enhances coordination, thereby avoiding conflicting data. All information incorporated into a digital model becomes interactive, allowing for automatic updates and corrections in response to any modifications. In summary, "*BIM is a process that relies on a computerized virtual 3D model of the built object that is capable of reacting to changes in the 'virtual' world in the same way that the physical built object would react when actually constructed".*[18]

BIM encourages the collaboration of working and design by allowing all the various consultants to work on the same model, improves visualization with detailed 3D models, and increases cost saving and time efficiency by identifying potential issues in an early manner, proving its implementation to have numerous advantages in multiples aspects of the construction cycle. However, BIM also has disadvantages, such as high initial costs for software and training, complexity requiring skilled professionals, and interoperability issues between different software platforms.

A graphical representation of this is the MacLeamy curve as shown next, which presents the difference between traditional and preferred design process in terms of variation in effort and cost through different project phases.

[18] Barnes, P. (2019). *BIM in principle and in practice* (3rd ed., p. 7). ICE Publishing.

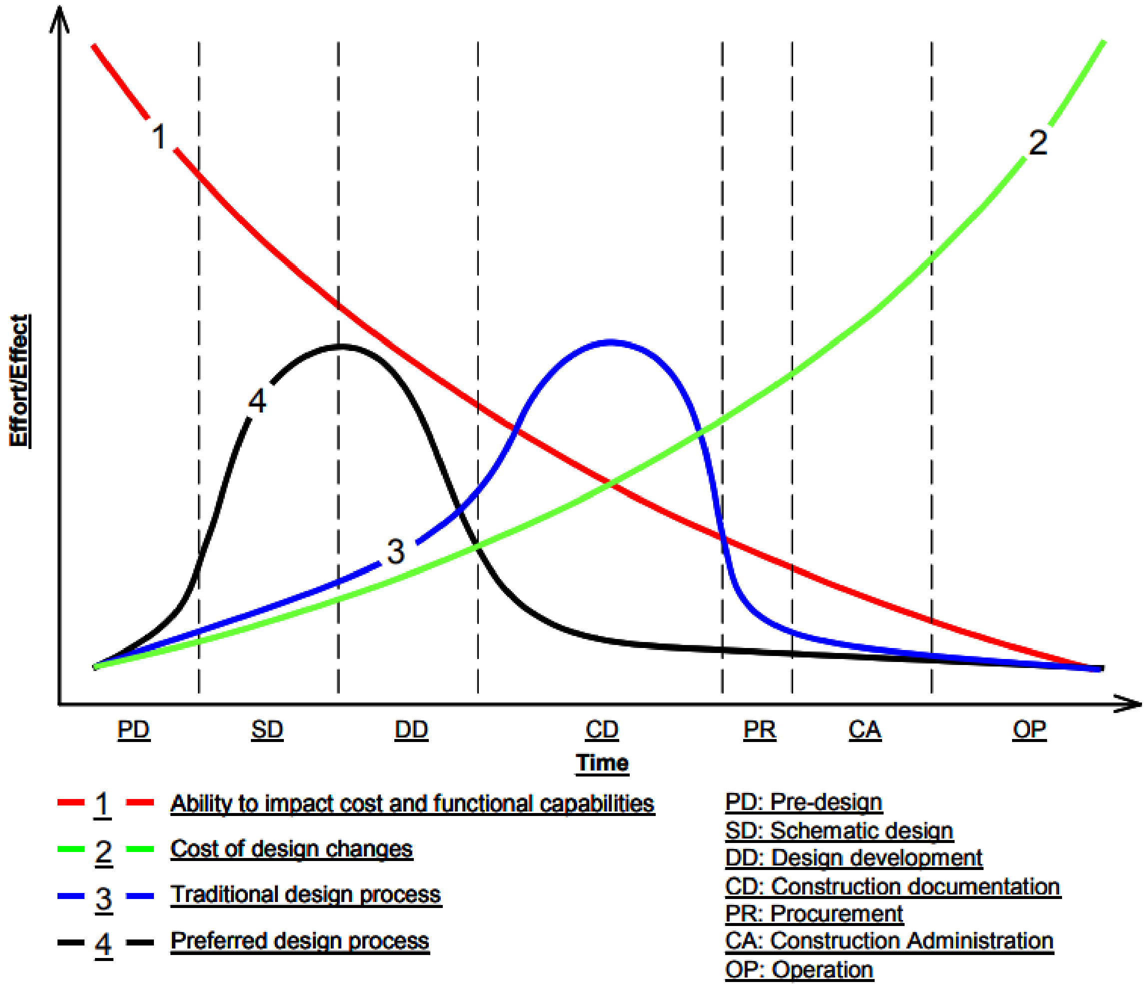

Image 40 - The MacLeamy curve effort vs stage in design build cycle.
source: The Construction Users Roundtable (CURT). (2004). *Collaboration, integrated information, and the project lifecycle in building design, construction, and operation (WP-1202).* The Construction Users Roundtable.

According to the type of document or information to be developed, the BIM methodology assigns a specific classification or subdivision for these, which are commonly referred to as dimensions, and they are: 3D BIM, which represents the three-dimensional physical model; 4D BIM, which incorporates time-related information for scheduling; 5D BIM, which adds cost estimation; 6D BIM, which includes sustainability and energy analysis; and 7D BIM, which focuses on facility management.

6.2. HBIM Methodology

For the present thesis, although BIM tools are used, the workflow differs from the traditional one described earlier. Typically, BIM starts from 2D documentation to create a 3D model of a structure to be built. However, the case study here is an existing building, requiring reverse engineering. This involves digitally reconstructing the building to generate detailed 2D representations, such as sections, elevations, and floor plans.

This reverse engineering approach, often applied to historical buildings where construction data may be limited or outdated, is referred to as Historic Building Information Modeling (HBIM), a term coined by Professor Maurice Murphy in 2009. In the present work the base for the reconstruction is a point cloud obtained from high-definition technologies such as digital photogrammetry and laser scanning.

One notable challenge with this methodology is the complexity of modeling an existing building, particularly when architectural elements are highly irregular or unique. These complexities extend the modeling process, as many BIM tools are designed for regular, new buildings. In this case, custom parametric libraries and families must be created for irregular or unique elements. Additionally, the current state of the building's conservation is often considered in the model, leading to the subdivision of elements into subcomponents. For example, the crypt column in the studied church was divided into the capital, shaft, and base in the digital model.

As exposed before it’s clear that this methodology presents clear distinctions from traditional BIM. The following chapters will expand in detail the considerations, strategies, and methods employed in modeling this case study.

6.2.1. Revit

The scope of this work includes the development of a three-dimensional model. Despite many options in the market, Autodesk Revit was selected due to it being the most common and recognized modelling software.

Revit is specifically designed to function within the BIM environment, enabling multi-disciplinary collaboration by integrating architectural, structural, and MEP[19] designs into a unified digital model. This allows users to view, modify, and manage the entire project within a single space.

One of the key advantages of using Revit is its ability to create and utilize parametric components, referred to as "families." These components can be adapted to meet the specific design needs of any project. The use of parametric families makes the model dynamic, as any changes to related elements are automatically reflected throughout the project, ensuring consistency and reducing the risk of errors.

[19] MEP stands for: mechanical, electrical and plumbing.

Revit classifies families into three main types. The most common are system families, which include essential building elements such as walls, roofs, floors, and ceilings. These components are created and stored directly within the project environment, meaning they are integral to the project and cannot be edited outside of it.

Loadable families, by contrast, are created in a separate family editor environment. These families allow for greater customization and are loaded into the project as needed. They are often used for complex or highly specific elements. These families offer the flexibility to modify parameters and adapt components to specific project needs.

Lastly, in-place families are custom elements that are created and modified directly within the project. These are typically unique, non-reusable components that are specific to the design or structure being modeled.

However, despite its strengths, Revit does have some limitations. First, its effective use requires a significant level of training and familiarity with the platform's tools, presenting a steep learning curve for new users. Additionally, the software demands high-performance hardware, as standard computers may struggle with its resource requirements. Revit files are also not backward compatible, which means that older versions of the software can quickly become obsolete with each new release. Finally, as models grow in complexity, the software may experience slowdowns, making it challenging to work with large files due to performance issues.

Revit, as shown in the following chapters proves to be an excellent tool that enhances, facilitates, and deepens the understanding of the entire case study.

6.2.2. Import of Point Clouds and Workset Creation

The modeling process begins with the import of the point clouds, on the *manage project* tool of the *manage* tab. Files in format .rcp can be added only to the project environment. The first georeferenced point cloud gets added and its positioning is set to *by shared coordinates*, meaning that its spatial values correspond to those set before, for the second and last file the positioning corresponds to *origin to last place*, to ensure correct overlaying. As explained previously, this import of two files corresponds to a modelling decision set for this project as it is also the creation of multiple worksets that will be used for each type of architectural element that composes the model. These include the external and internal clouds, columns, pavements, vaults, arches, roofs, walls, among others.

The decision to create these multiple and specific worksets is based on the ability to group elements with similar characteristics, allowing them to be hidden or isolated when necessary. This prevents screen clutter and speeds up the interpretation of the church's structure.

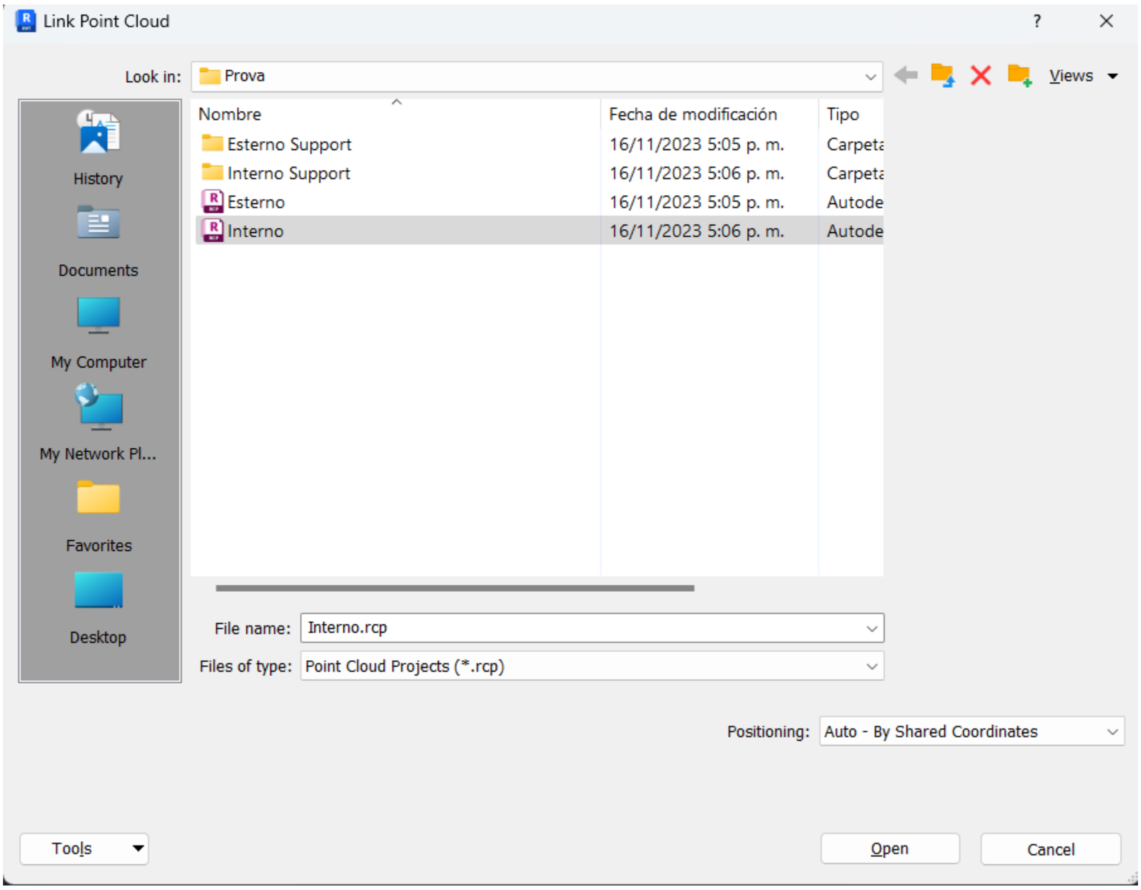

Image 41 - Import of the internal and external point clouds in the Revit software.

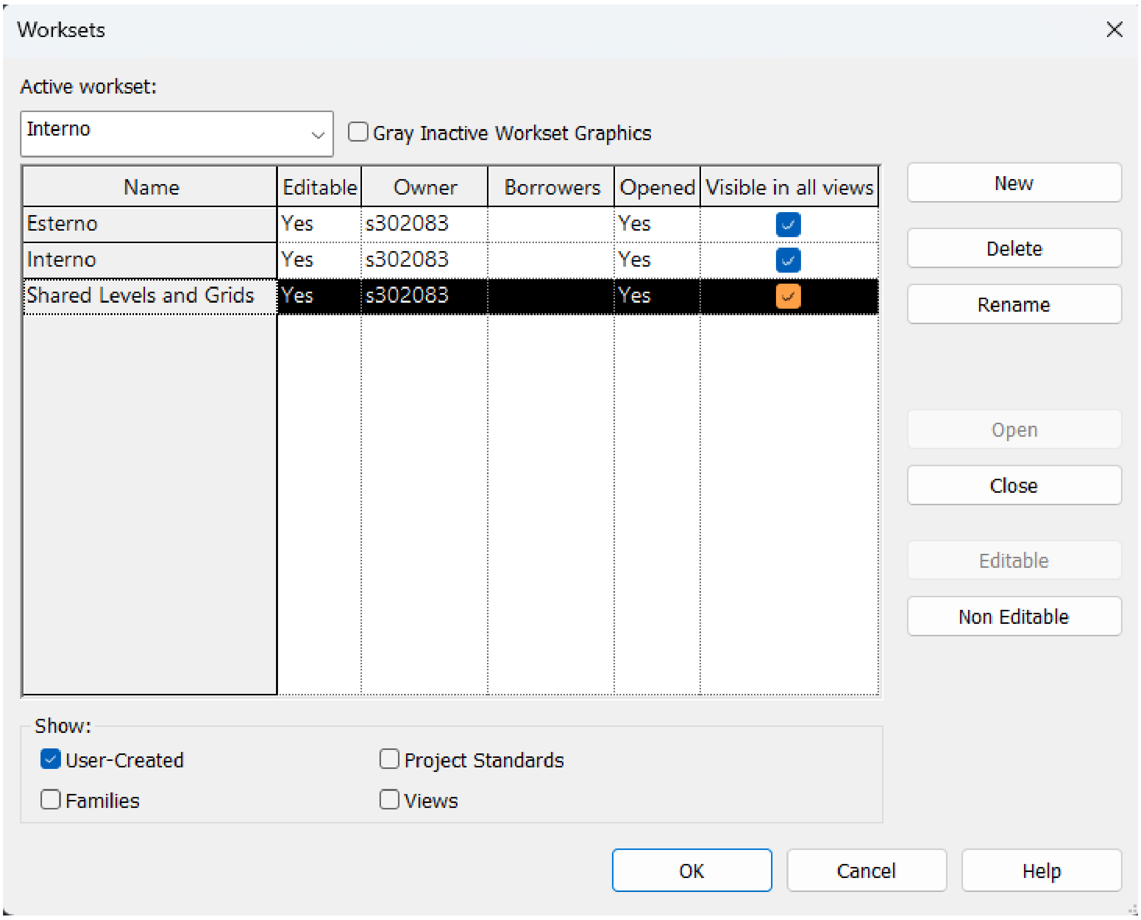

Image 42 - Creation of worksets in the Revit software.

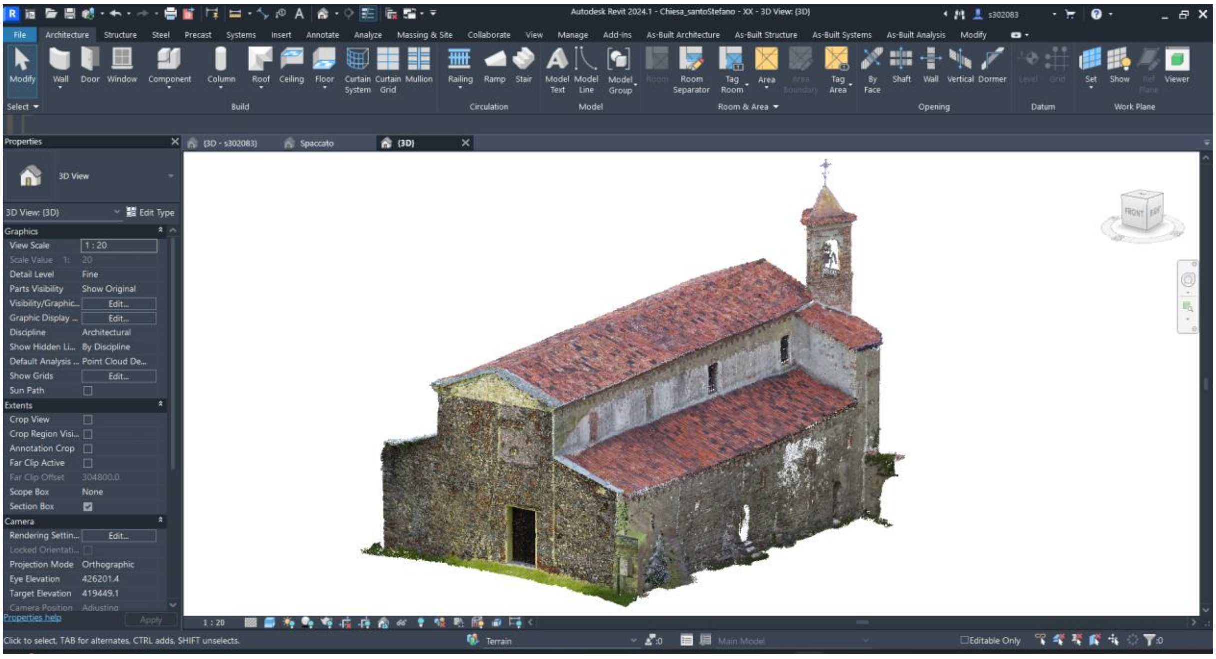

Image 43 - Autodesk Revit Interface with Imported Point Clouds.

6.2.3. Modeling System Families

Image 44 - Plan View (left) and Section (right) of the point clouds.

To correctly individualize and position the elements that make up the church's structure, sections or slices of the point clouds were made. This was done to establish, by inspection, the internal spaces left by the overlapping clouds and where it is clearly explainable that there is an architectural or structural element.

An example of this is the empty spaces observed in the floor plan view of the church (left side of image 44), specifically those rectangles that divide the nave of the aisles in the building. These correspond to the columns that support the inner walls of the construction. Similarly, it is possible to assume that the perimeter spaces that surround the entire building are the walls.

By sectioning and isolating elements, as mentioned before, it is possible to trace or extrapolate dimensions and measurements of the elements that constitute the structure. With this information, the modeling of elements with predominantly regular geometry begins by inserting system families into the project environment, such as all the building's walls, floors, roofs, and stairs.

For the walls, "basic wall" elements were used with different thicknesses and heights corresponding to those extrapolated from the point clouds. The floors belong to the "floor" family, their perimeter is linked to the walls, and their slope is defined according to the differences in levels obtained from the point cloud. The height assigned corresponds to that of a typical value since the actual height is unknown. The church roofs are "basic roof" elements and follow the same logic as the floors.

All the stairs are from the "cast in place stair" family, as they closely resemble those found in the church. Their location, start, end, and all geometric information are based on the point cloud data. As a particular note, at the entrance of the church's interior, there is a single step, which was modeled as a floor at a higher level.

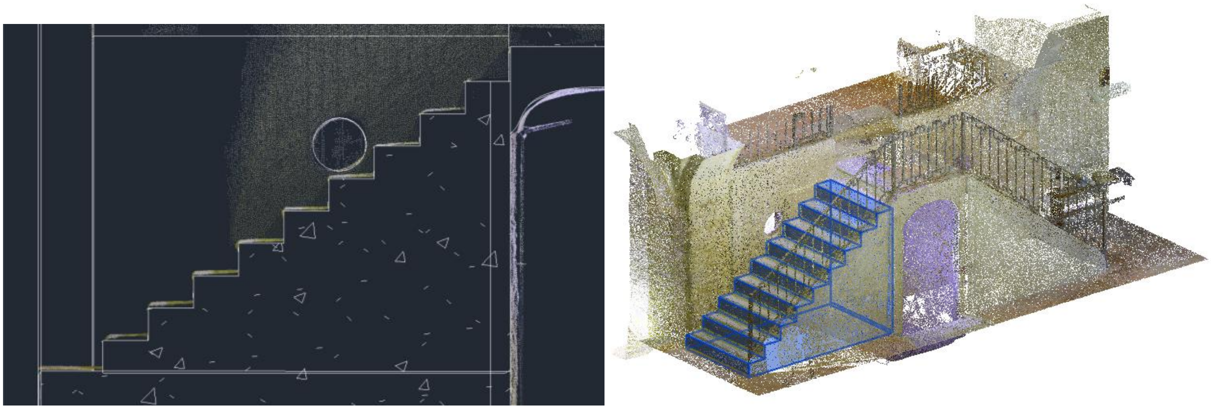

Image 45 - section (left) and isometric view (right) of stairs leading to the presbytery.

6.2.4. Modeling In-Place Families

Image 46 - Arch on the nave wall in the church (left) and its virtual representation on the model done with in-situ tool (right).

Once all the elements with regular geometry were inserted, the next step was to identify and model those components with more complex shapes, limited repetition in the structure, or those that are essential to achieve the objectives of this thesis.

These elements include the exterior buttresses, the bell tower, the arches of the nave walls, the internal niche in the entrance wall, and all the vaults found in the church, such as those in the corridors, crypt, and auxiliary rooms.

The main goal in the development of the model is to create representations with proportions and dimensions similar to the case study. One of the key advantages of creating these in-place elements directly in the project environment is the ability to trace the point cloud from the sections created, using them as a base or guide.

To model all these pieces, the architecture tab was used, specifically the model in-place tool, then an appropriate family category is assigned to the element. For example, the arches in the nave of the church were categorized as ceilings, and their modeling was done by creating an extrusion whose perimeter followed the surface generated by the point cloud.

For the buttresses the assigned family category was that of wall, then positioned according to the point cloud. To give it the diagonal support shape for the external walls of the church a blend tool is used.

For more detailed elements, in addition to the preliminary extrusion, void volumes were created to cut the solid, adding a higher level of detail to the model. A clear example of this process is the bell tower, which was classified as a wall element, then by extruding the perimeter generated from a horizontal section of the point cloud the solid block was created. Finally, a void volume was generated to cut out the space where the bell is located, as seen on image 48.

For the church vaults, it was decided to model each one individually due to their handcrafted construction, which imparts a high degree of irregularity to their form. These vaults were classified under the ceiling category. The modeling approach starts with the extrusion of a solid block representing the overall volume of the vault, then longitudinal and transverse sections were created based on the point cloud data. These sections provided the necessary profiles for defining the exact geometry of the void volumes. The void volumes were then used to subtract from the initial solid block, carving out the surfaces of the vaults, as seen on image 49.

It is also important to mention the modeling of the niche found in the entrance wall of the church, as it contains bricks of historical significance to the case study. These bricks feature handles that were used for manipulation and transportation, an important characteristic of bricks from the Roman period. This detail gives some historical context to the structure, on image 50 a side-to-side comparison between the real object and the modelled one is shown.

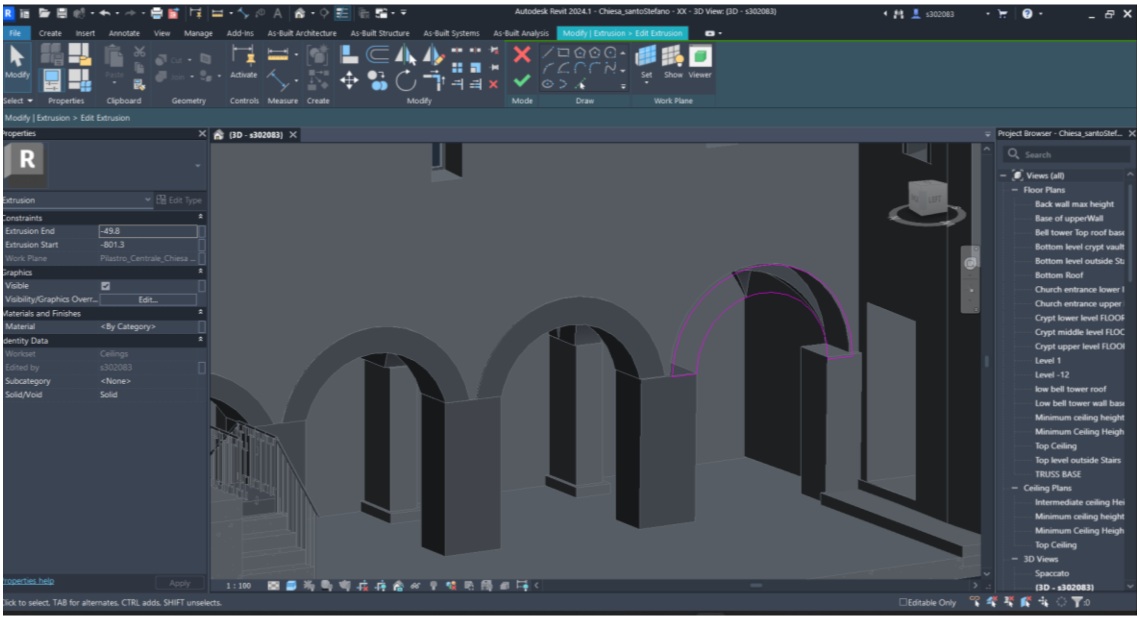

Image 47 - Extrusion silhouette of nave wall arch.

Image 48 - Santo Stefano's modelled belfry.

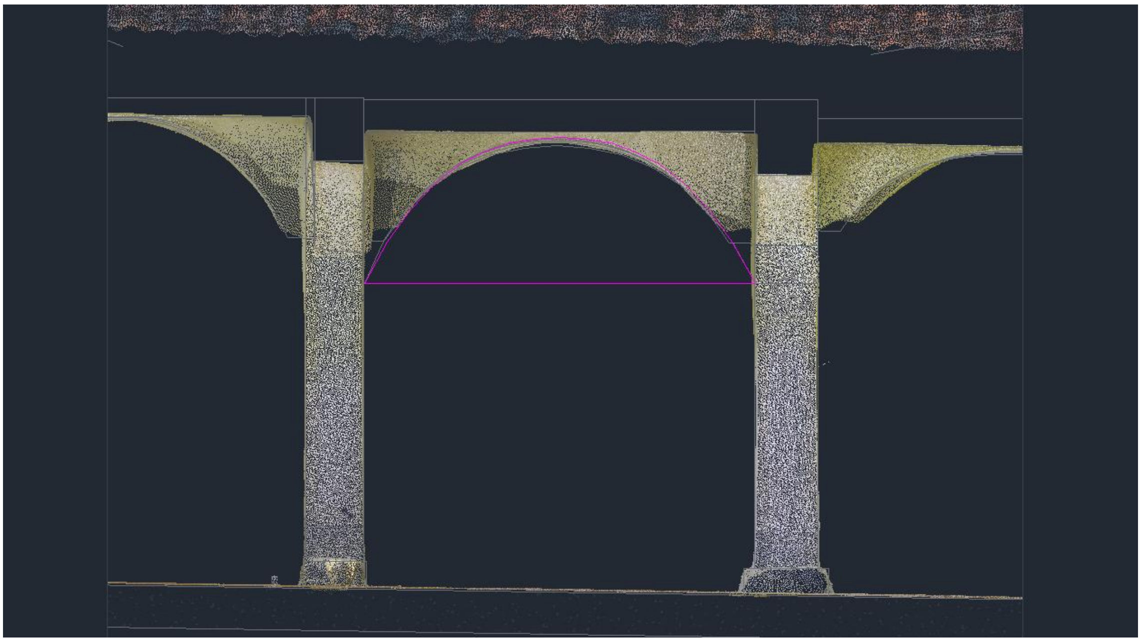

Image 49 - Longitudinal section of typical church vault with void volume silhouette based on point cloud data.

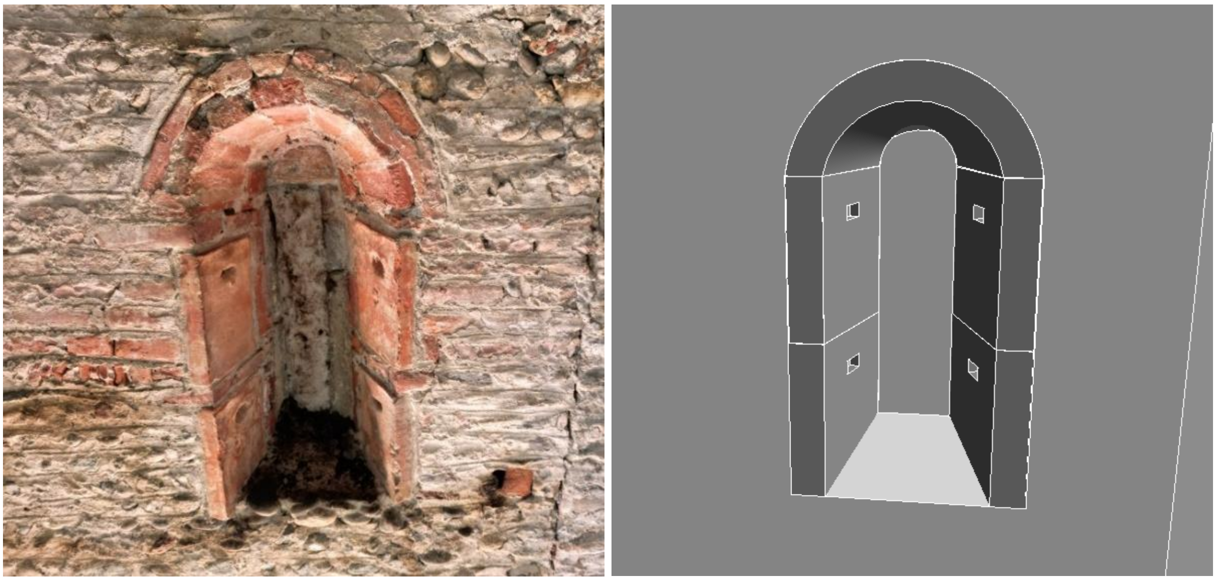

Image 50 - Niche on the entrance wall in the church (left) and its virtual representation on the model done with in-situ tool (right).

6.2.5. Modeling Loadable Families

For the remaining elements to be modeled, loadable families were used. Although they possess complex geometries, much like in-place families, they tend to be replicated across various components of the structure.

Among the elements modeled using loadable families are the doors, windows, trusses, and all the columns in the crypt. To create any of these components, the process begins with a completely new family file. In other words, the modeling starts in a family environment, where the specific element is created and later loaded into the project environment, where it will be integrated into the overall model in development.

Unlike in-place families, where the point cloud can be directly used as a reference to create sections and guide the modeling process, loadable families do not allow the point cloud to be viewed in the family environment. However, these components offer the advantage of creating geometric parameters that control the element's proportions. This flexibility means that, once the loadable families are inserted into the project environment, their parameters can be easily adjusted to fit the shapes and dimensions derived from the point cloud. This method provides a way to fine-tune the elements to match the real-world structure without losing the benefits of family-based design.

For the modeling of the five trusses that support the church’s roof, a generic family was created, using measurements taken directly from the point cloud. Subsequently, the truss model was loaded into the project and replicated as many times as necessary according to the building’s layout. Similarly, the roof purlins were modeled, adjusting their length according to the data obtained from the point cloud.

The doors were modeled using reference photographs, and their proportions were parametrized to fit correctly within the model once inserted into the project. The same process was followed for the two types of windows in the church: one square-shaped and the other with an arched top. The parameters created for these windows included height, width, length, and the slope of the sills. This allowed for the creation of a base window family with multiple variations, where the differences were only in the parameter values assigned.

A particular case in the modeling process involved crypt columns. All of them share a similar morphology, consisting of capital, shaft, and base, but present significant variations in design. Some columns have cylindrical shafts, while others are parallelepiped. The capitals vary in design and dimensions, and the bases do not repeat exactly. To model them, columns with significant similarities were grouped, resulting in four main types of columns or families, each with several copies within themselves. The dimensions of these columns were parametrized, with the column width serving as the main parameter for other dimensions, such as height or base. These dimensions were automatically adjusted through formulas to maintain correct proportions. Once created, they were inserted into the project, where their dimensions were further adjusted to match the forms derived from the point cloud, resulting in a model that reflects the real dimensions of the objects.

Finally, an additional consideration in the modeling process was the individualization of the subcomponents of each column. Instead of placing a complete column as a single element, the capital, shaft, and base were modeled separately. This decision was made with future work in mind, specifically the creation of a maintenance plan for the building. By individualizing each subcomponent, the interrogability of the model is significantly improved, allowing for a greater degree of control and flexibility in the planning of interventions and repairs, thus ensuring more effective conservation of the building in the long term.

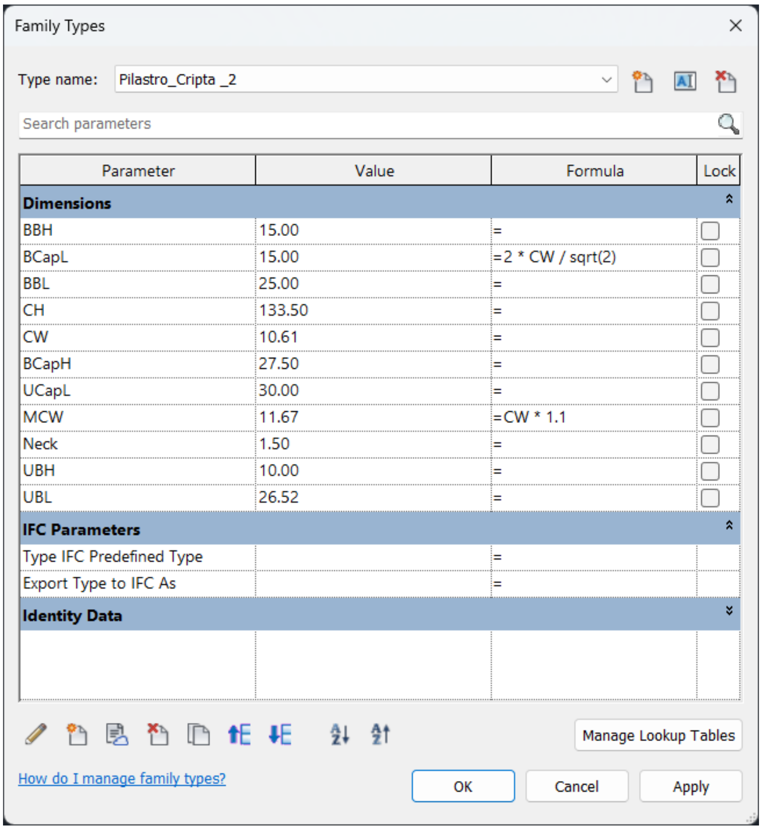

Image 51 - Parameterized Family Type Settings for Crypt Column in Revit.

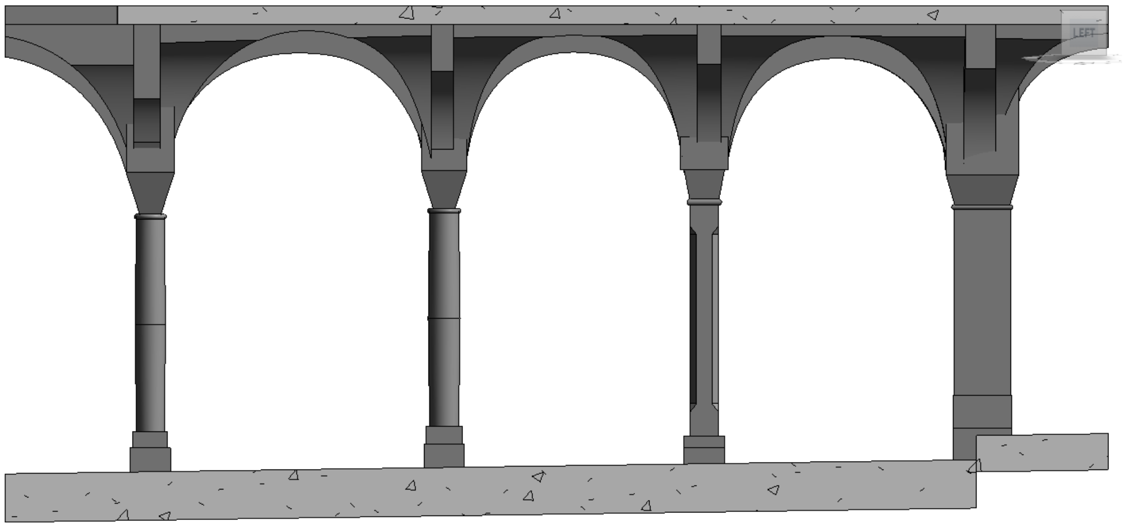

Image 52 - Visualization of the Different Column Types in the church's Crypt.

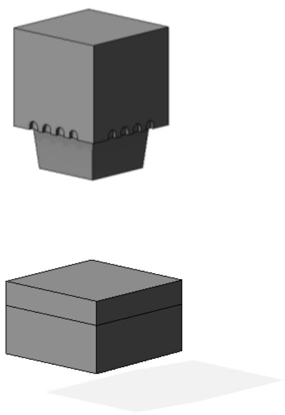

Image 53 - Individual Components of a crypt column: Capital (top left), Base (bottom left), and Shaft (right).

Image 54 - Side-by-Side comparison of point clouds (left) and Revit model (right).

6.2.6. Terrain Creation

Although the insertion of the terrain corresponding to the building in the case study is not essential to meet the objectives of this work, the methodology used will be presented as a practical reference for future projects where this aspect may be relevant.

For this, a GIS application was used to extract the contour lines of the area where the church is located. These contour lines were exported in a CAD file, which includes the corresponding spatial coordinates of the site. The CAD file was then linked or imported into Revit. Next, from the Massing and Site tab, the Toposolid > Create from Import tool was used, and the loaded file was selected.

This method can be applied in similar cases for the generation of detailed topographic models, useful in infrastructure planning or analyzing the interaction between the building and the surrounding terrain. It can also be used to assess geotechnical risks, such as soil stability, or in landscaping projects, optimizing water drainage or planning access and levels in areas with complex topographies.

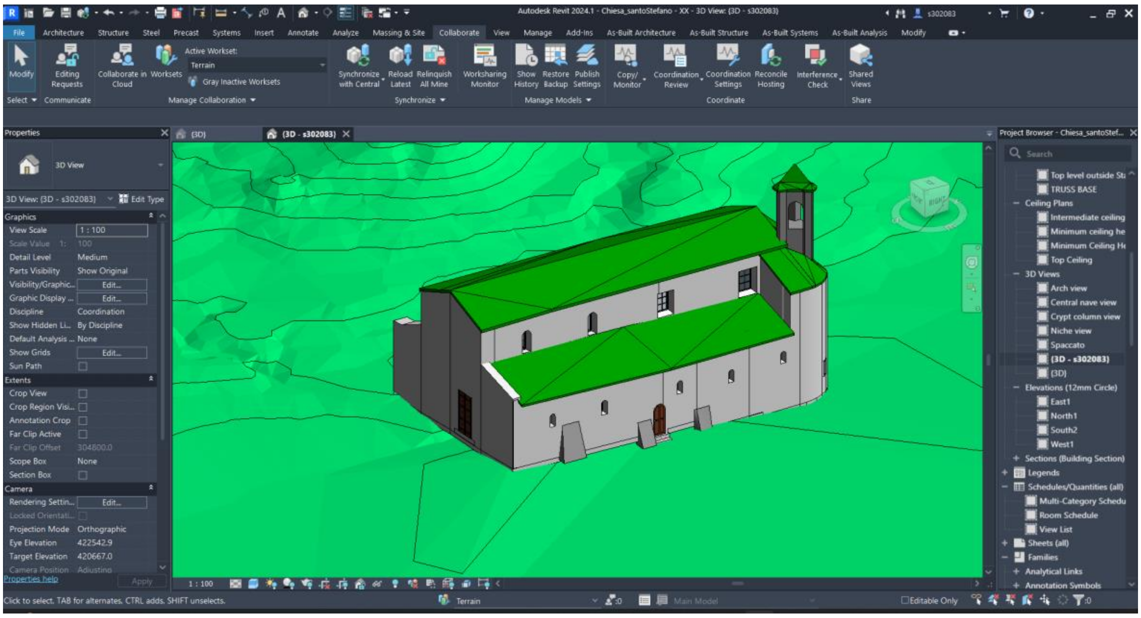

Image 55 - 3D Model of Case Study Building with Topography in Revit.

6.2.7. Model Offset from the Point Cloud

Once all the elements composing the church were modeled and positioned, a check for the offset or distance between the components created and the point cloud surface was carried out. The purpose of this analysis was to measure and verify the geometric accuracy and correct positioning of the elements within the project.

Verifying the precision of the generated model is essential for conservation or maintenance of buildings, such as the case study. To perform this analysis, the FARO As-Built for Autodesk Revit plug-in was used, allowing for a point-by-point comparison between the digital model's geometry and the surfaces generated by the point cloud. The results of the software are visualized through a color map applied to the analyzed surface, which facilitates the identification of the offset distances between the digital model and reality. The following image illustrates a scheme for determining the deviation values between the model and the point cloud.

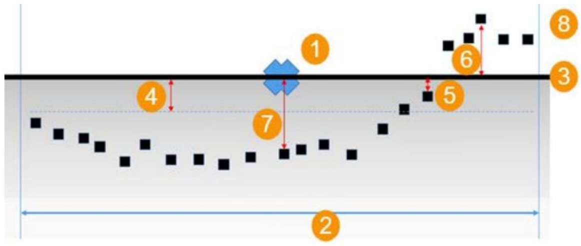

Image 56 - Scheme for Determining Deviation Values of the Model with Respect to the Point Cloud. (1) Center of grid cell, (2) Cell width, (3) Surface cut, (4) Average Value, (5) Minimum Value, (6) Maximum Value, (7) Nearest Value, (8) Point cloud points.
Source: FARO Technologies, Inc. (2024). As-Built for Autodesk Revit user manual. FARO Technologies, Inc.

To generate the color map, the default colors from the program's initial configuration were used. Blue indicates areas of the model that are below the actual surface, green represents areas with little or no deviation, and red highlights areas that are above the actual surface. In the plug-in's analysis settings, only the threshold values for mean grid size and maximum surface distance were modified, set at 15 mm and 30 mm, respectively.

Since the church modeled in this case study consists of a wide variety of elements with both regular and irregular geometries, different representative elements were selected for analysis. The chosen elements were the exterior entrance wall, a corridor wall, a truss, a column from the main nave, and a crypt column. These elements were selected to help visualize and assess the model's accuracy, as well as to evaluate the modeling decisions made.

The results showed that no element is entirely accurate, as all analyses revealed areas where portions of the elements were either above or below the actual surface. A clear explanation for these deviations is the irregularity of the surfaces analyzed, which is common in historical constructions. This is particularly evident in the entrance wall of the church (image 57) and the column in the central nave (right side of image 59), where the surfaces are notably rough due to the construction methods used.

In the case of the corridor wall (image 58), the color map presents semi-horizontal bands along the surface, caused by the lack of verticality in the real object on which the model is based. This highlights the challenges involved in accurately reproducing historical buildings. Conversely, the element with the least offset areas was the wooden truss (image 60) supporting the main church roof. As mentioned earlier, this is due to its regular shape and smooth surface, typical of elements made from this material.

While the model does exhibit some offset in its elements, these deviations fall within the expected tolerance of +/- 3 cm, a typical value for architectural surveys of this nature.

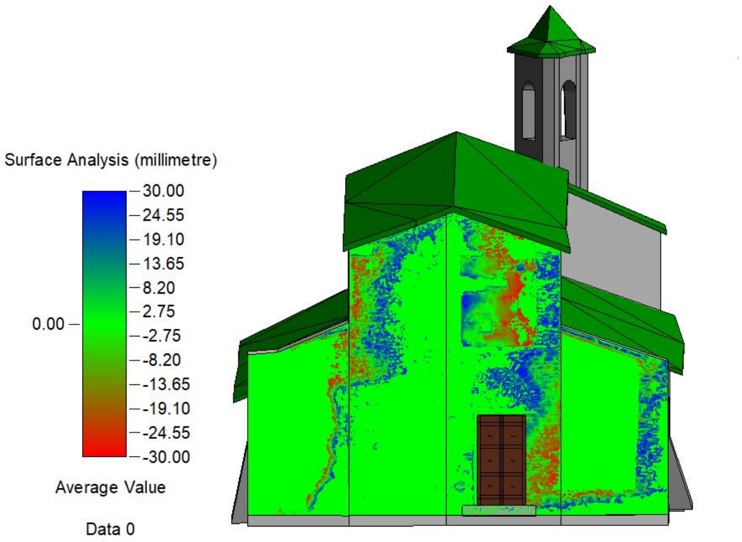

Image 57 - Color map of surface deviation for exterior entrance wall – Point cloud analysis.

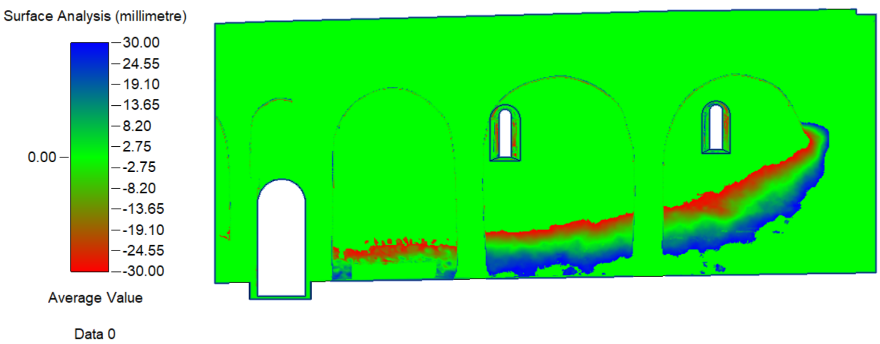

Image 58 - Color map of surface deviation for corridor wall – Point cloud analysis.

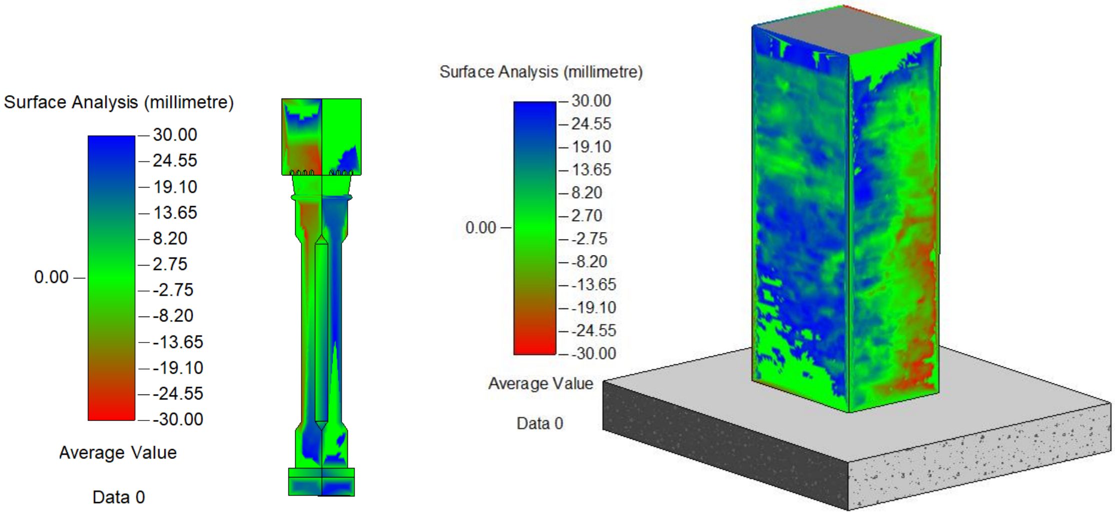

Image 59 - Color map of surface deviation for crypt column (left) and main nave column (right) – Point cloud analysis.

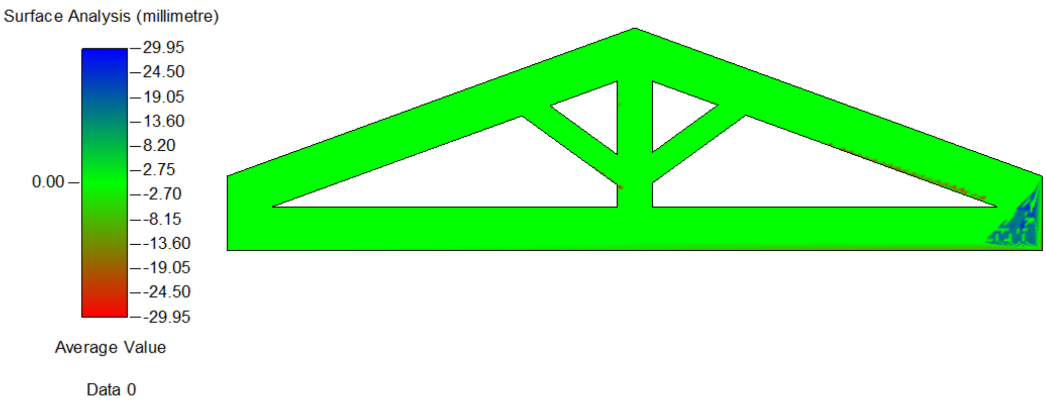

Image 60 - Color map of surface deviation for truss – Point cloud analysis.

7. Interoperability

The interoperability allows various systems, software, and datasets to work together effectively, making it possible to share, access, and utilize data seamlessly across platforms. In this project, interoperability is crucial as it enables different technologies and data sources to come together, creating a cohesive and accessible digital information model of the case study. This approach not only facilitates efficient information sharing but also supports ongoing collaboration among the different professionals involved in its further development.

Up to this point, the thesis has focused on constructing a precise, three-dimensional model of the church, developed through a combination of traditional and advanced tools. Each one contributed to enhancing the model's accuracy and extent. The result is a comprehensive digital representation of the church that integrates various formats and data into a unified structure.

The scope of this thesis pretends to extend the utility of this model beyond its original software environment by exporting it to a web-based platform, specifically 4main10ance. By hosting the model online, 4main10ance broadens its reach and functionality, providing a centralized space where the model can be accessed and utilized for ongoing preservation efforts. This platform not only makes the model available to multiple users but also offers the capability to establish a dedicated maintenance program, which is critical for managing the long-term care of the church.

7.1. The 4main10ance Platform

The main10ance project was originally conceived from the INTERREG Italia-Svizzera 2014-2020 program, which consists of a collaborative initiative between these two European countries, aimed primarily at enhancing the value of resources within the border areas. This program was structured around different themes or axes[20]. The Main10ance project was part of the second axis, which focused on the enhancement of natural and cultural heritage. Its objective was to develop a working methodology and operational tools that will guide its

[20] Interreg Italia-Svizzera. (n.d.). *Documento di sintesi - Programma di cooperazione Interreg V-A Italia-Svizzera 2014-2020.* Retrieved from https://www.interreg-italiasvizzera.eu/wps/portal/site/interreg-italia-svizzera/archivio-programma-2014-2020

various users in the creation of a planned conservation strategy for cultural heritage[21]. This strategy is based on the principles of sustainability, emphasizes a long-term vision for the planned interventions and seeks to optimize the use of available resources. The cultural subject chosen at the time of its development was the sacri monti.

This methodology used the construction of an information platform, supported by a database and a three-dimensional visualization tool, which were linked to allow the model to be queried or consulted.

As of today, the 4main10ance platform is a web-based tool, with a distinctive and innovative scope which is that of "a digital platform integrating BIM and GIS[22], with a common database structure behind it, has been developed starting from an accurate integrated 3D metric survey"[23] Matrone et al. (2023). The platform with its database serves as a central repository that stores detailed information about architectural elements, environmental conditions, and past interventions, making it accessible and updatable to all those involved in conservation efforts, thus creating a comprehensive, multiscale database that enables effective and long-term management of heritage assets such as the case study.

As mentioned earlier, the platform provides access to different types of users, each of whom is assigned specific roles and tasks. Upon login, the site customizes its interface based on the user's role, ensuring that each user sees only the tools and information relevant to their responsibilities. The platform accommodates three main user roles, each with different levels of access and functionality.

- The Tourist: requires no registration and provides limited access, allowing users to explore the BIM viewer while restricting access to sensitive conservation data.
- The Operator: requires registration and is typically assigned to professionals directly involved in conservation tasks. This role allows enhanced permissions meaning they can use the BIM viewer, review activities, and modify tasks related to the assets they oversee.

[21] Regione Piemonte. (n.d.). *Main10ance: I Sacri Monti, patrimonio comune di valori e laboratorio per la conservazione sostenibile.* Retrieved from https://www.regione.piemonte.it/web/temi/fondi-progetti-europei/programmi-progetti-europei/cooperazione-territoriale-europea-piemonte/main10ance-sacri-monti-patrimonio-comune-valori-laboratorio-per-conservazione-sostenibile-una

[22] GIS stands for: Geographic Information System.

[23] Matrone, F., Colucci, E., Iacono, E., & Ventura, G. M. (2023). *The HBIM-GIS Main10ance Platform to Enhance the Maintenance and Conservation of Historical Built Heritage.* Sensors, 23(19), 1-28. https://doi.org/10.3390/s23198112

- The Manager: is the highest level of access and is responsible for managing and controlling all data within the platform.

With the roles[24] clarified, it is important to explain the platform's tools and their functions, which support users in the asset management process. The platform offers three main viewers, the GIS viewer, the BIM viewer, and the artifact viewer as well as a planner and a dashboard.

The GIS viewer provides access to geographic data, giving users an overview of the environmental context surrounding the heritage asset, essential for environmental assessments. The BIM viewer provides a detailed 3D model of the architectural structure, allowing in-depth exploration of the building's physical characteristics and structural components. Meanwhile, the Artifact viewer focuses on interior features such as statues, frescoes, paintings, and decorative elements, helping to track the condition of these intricate details. In addition to these viewers, the Planner (available only to operators and managers) facilitates the planning and scheduling of maintenance activities, ensuring that tasks are organized efficiently. This tool will be discussed in more detail later. Finally, the Dashboard, available only to the manager, provides an overview of the health of the assets under management and general trends in maintenance activities, enabling effective monitoring and strategic planning.[25] For the fulfillment of to the scope of this thesis work the operator role was employed.

[24] Colucci, E., Iacono, E., Matrone, F., & Ventura, G. M. (2023). *The development of a 2D/3D BIM-GIS web platform for planned maintenance of built and cultural heritage: The Main10ance project.* The International Archives of the Photogrammetry, Remote Sensing and Spatial Information Sciences, XLVIII-M-2, 433-439. https://doi.org/10.5194/isprs-archives-XLVIII-M-2-2023-433-2023

[25] Ibidem.

Image 61 - Breakdown of the different users of the platform and the tools available to them.
Source: Fasana, S., & Zerbinatti, M. (2022). *Dal rilevo al progetto di conservazione programmata sostenibile: Materiali, tecniche, strumenti.* Politecnico di Torino. Retrieved from https://iris.polito.it/handle/11583/2973459

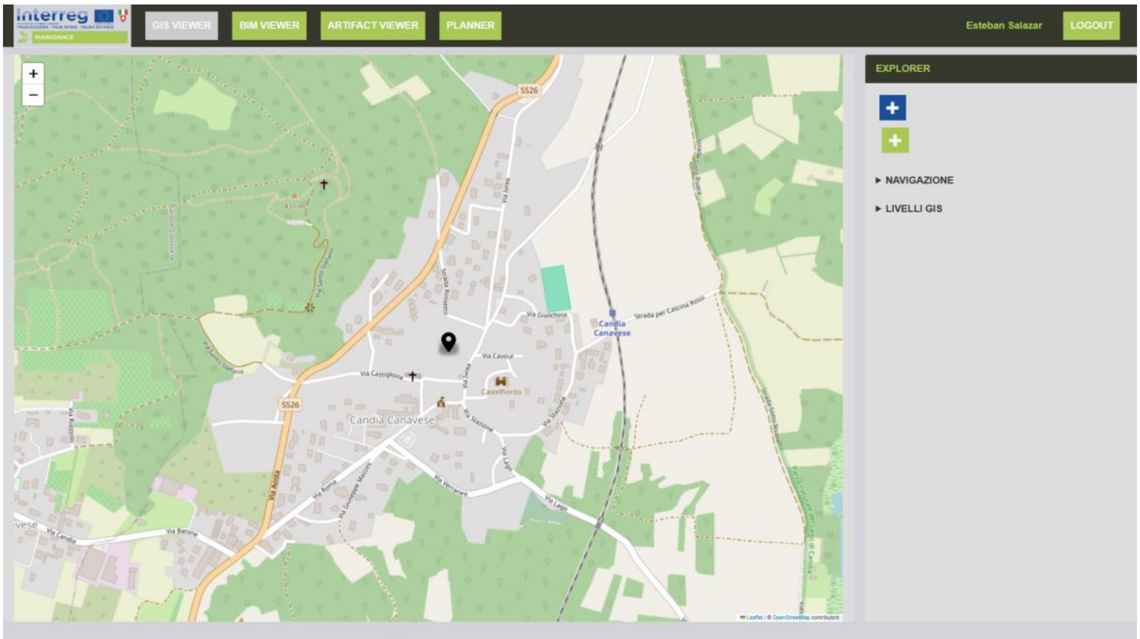

Image 62 – 4main10ance GIS Viewer showing location of Santo Stefano church in Candia Canavese.

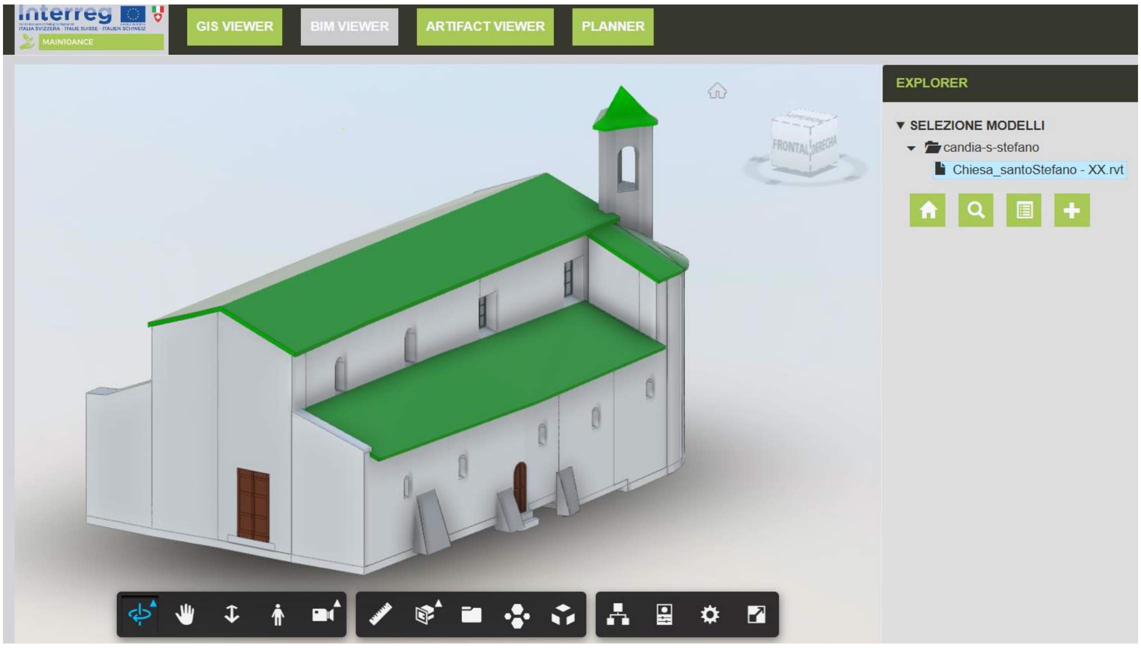

Image 63 - Exterior 3D Model of the Church of Santo Stefano in the BIM Viewer.

Image 64 - Interior 3D Model View of the Church of Santo Stefano in the BIM Viewer.

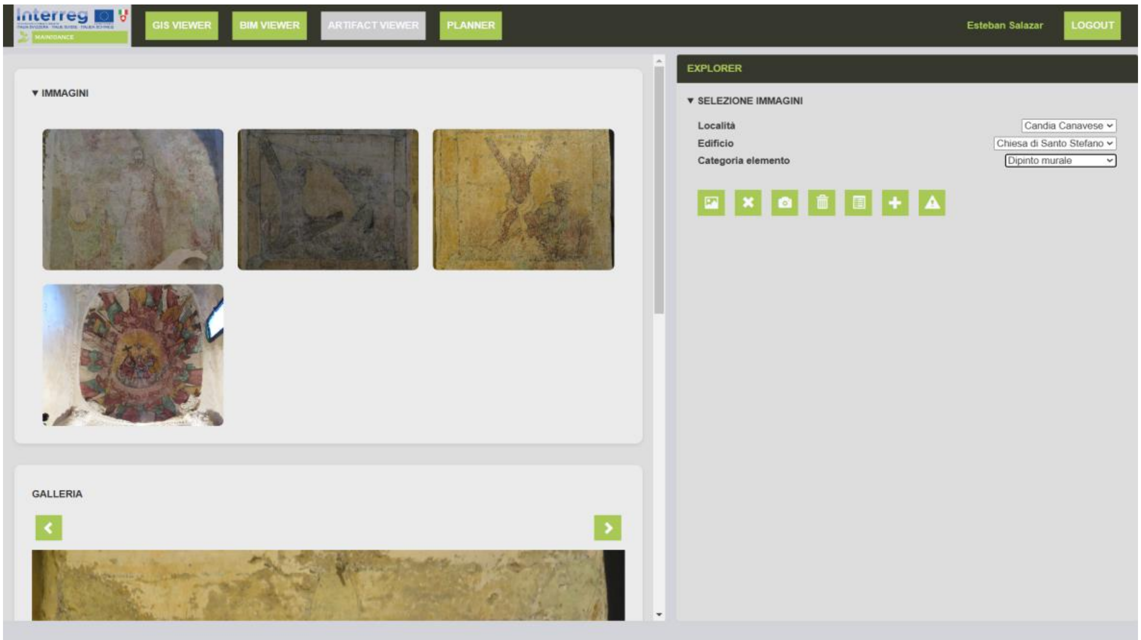

Image 65 – 4main10ance Artifact Viewer showing images of mural paintings at Santo Stefano church in Candia Canavese.

7.2. Model Parameterization

To fulfill the platform goal of developing a scheduled maintenance plan, the uploaded model must include additional information in the form of an alphanumeric identifier code or ID that differs from the numeric one assigned by the modelling program automatically when inserting an architectural or structural element that composes the digital twin. This allows the 4main10ance algorithm to properly recognize, assign, and manage the various elements within a specific model without the possibility of mixing elements from two different models, that may have a similar numeric identifier and thus compromising the correct function of the platform. Although assigning these codes manually is a simple task, it is also tedious and prone to errors. Therefore, automation tools are employed to streamline this process, making it faster and more reliable.

7.2.1. The Visual Programming Software Dynamo

Dynamo is an integrated tool within Revit that uses the concept of visual programming. This approach allows the creation of complex algorithms using pre-compiled nodes, each of which represents a predefined action or parameter. These nodes can be connected to form relationships that facilitate the execution of specific tasks. This method allows for more intuitive and direct programming, making it accessible to users without extensive programming knowledge.

Through these scripts, Dynamo enables the creation of complex parametric models and the automatic generation and manipulation of information within the model. To create a document or script, simply open Revit, go to the Manage tab, and select Visual Programming to launch Dynamo. This opens Dynamo's home page, as shown in image 66, where users can create a new script, modify an existing node, or open a saved script.

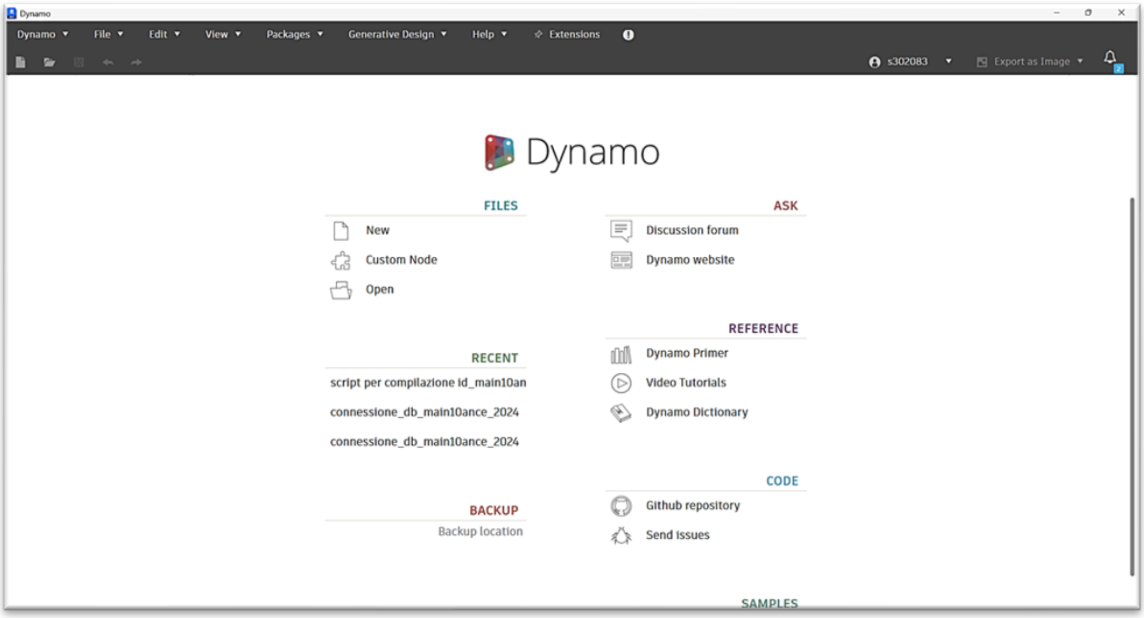

Image 66 - Dynamo Interface - Start Page Overview.

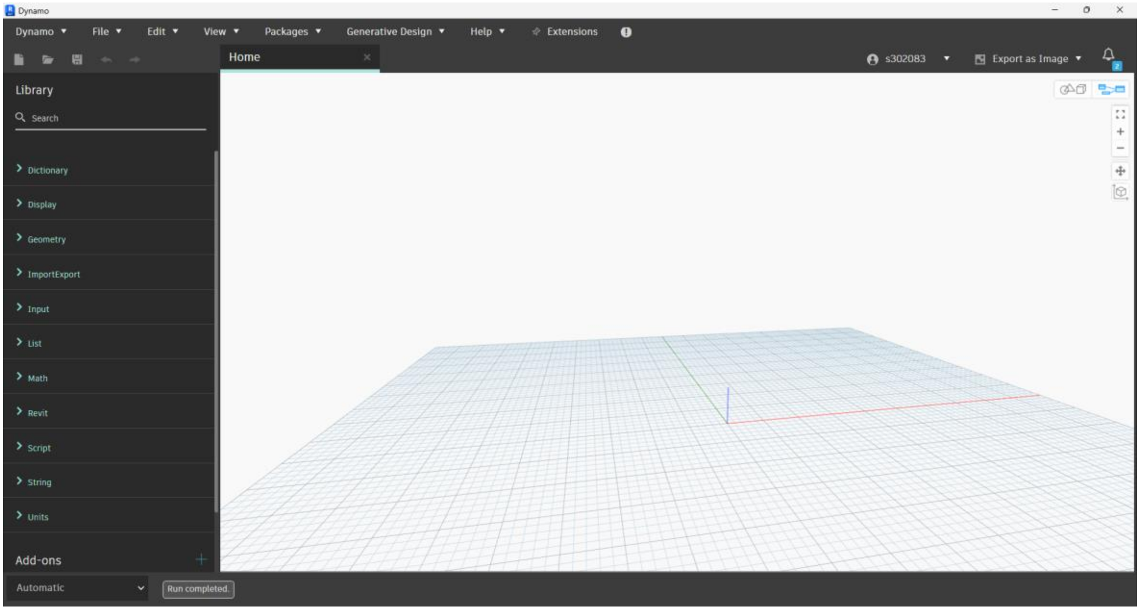

Image 67 - Dynamo Workspace for a new script.

7.2.2. Creation and Compilation of the Id_Main10ance

This alphanumeric identifier, known as “id_main10ance”, is constructed by combining four components. The first is a code representing the location of the case study; in this case, “CND” is used because the church is located in Candia Canavese. The second component is a code to identify the modeled building, here called ‘’s_stef’’ to represent the church. The third component is a parameter called “Entità” (Entity), which categorizes the type of element being compiled. The last component is the native numeric ID generated by Revit.

Each component within the id_main10ance parameter is separated by a vertical bar (“|’’), resulting in the following structure: ‘’Location|Building|Entity|Revit ID’’. The following table shows the data for a particular model element, such as a column.

Component	Example	Value
Location	Candia Canavese	CND
Building	Church of Santo Stefano	s_stef
Entità	Column	pilastro
Revit ID	525222	525222

Table 5 – Example data for id_main10ance compilation.

The id_main10ance and Entità parameters must be created in Revit to be compiled as described. By navigating to the Manage tab and opening the Project Parameter Settings, users can view, create, edit or delete parameters specific to the project. The process for creating both parameters is the same: clicking the “New Parameter” button opens a settings window where users can assign the parameter name, discipline, data type, category, select if it’s a type or instance parameter and other options to define its role within the project.

Once both have been created, the next step is to fill in the “Entitá” parameter, which serves as an information connector between the model and the platform's database. This parameter categorizes model elements using a set of predefined values (pavimento, pilastro, porta, scala, tetto, trave, volta, etc.) that are recognized by the database. These categories allow the database to classify and group similar elements in a systematic manner.

Finally, the id_main10ance parameter is compiled using the Dynamo plugin. A custom script is developed within Dynamo using nodes to automate this process. The script takes the various components of the identifier as input, organizes them and concatenates them with a vertical bar separator. As a result, all the id_main10ance for the model elements are generated almost instantly.

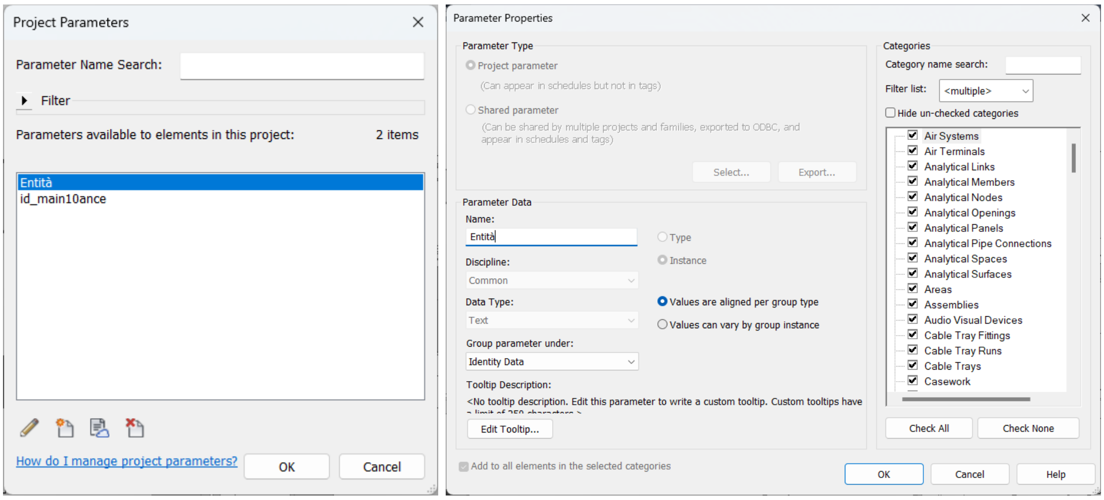

Image 68 - Creation of a project parameter (left) and assignment of its properties (right).

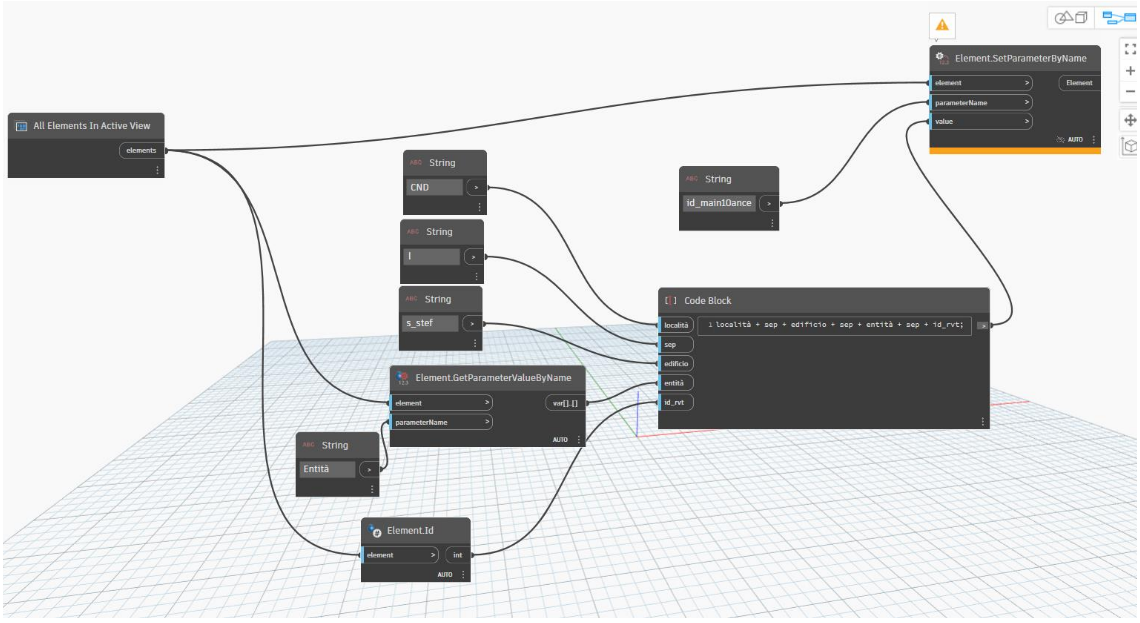

Image 69 - Dynamo script for the automatic compilation of the id_main10ance.

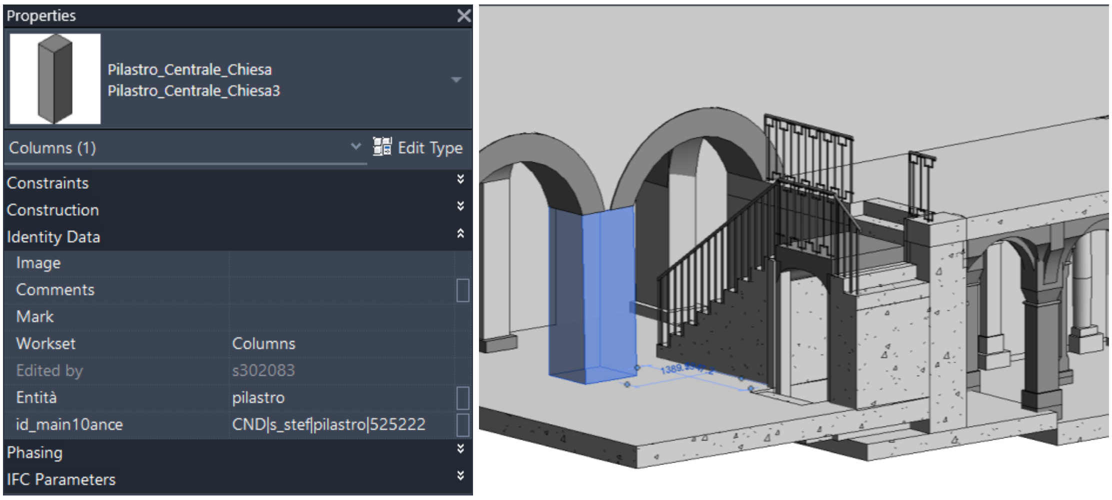

Image 70 - Example of a church’s column with its Entitá and id_main10ance parameters compiled.

7.3. Export of the Tridimensional Model and Its Data

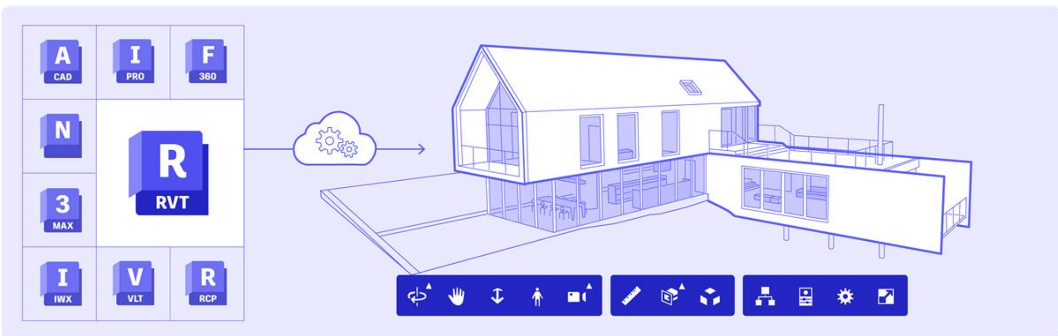

Image 71 - BIM model upload to the web browser viewer.
source: www.aps.autodesk.com

Once the id_main10ance parameter is compiled, the model information can be uploaded to the platform. This process is again facilitated by a Dynamo script that is more extensive and contains complex nodes that establish a connection between the model and the database. Through this connection, geometric information such as areas, volumes, dimensions, names, and identifiers of the model components can be exported.

In order to upload the model to the platform, first a "bucket" must be created. This bucket acts as a container or designated space on the platform for the model. Typically, the bucket is named after the location of the asset, so in this case it is named "candia-s-stefano".

With this designated space in place, the Revit model can then be uploaded to the platform, where it becomes accessible in the platform's BIM viewer. This web-based viewer, part of Autodesk Platform Services, allows for easy and direct import of the model. It also provides visualization tools that allow users to manipulate the model such as: control, section, measure, or even explode the view, as to better analyze its elements.

Finally, data validation is performed. This step is automated by the platform through a dedicated button. An algorithm checks that the id_main10ance identifier is correctly assigned to all elements, ensuring that each component follows the appropriate format for consistent identification throughout the model.

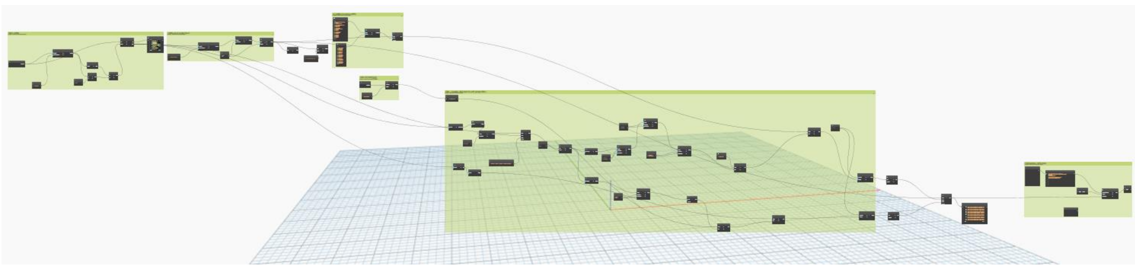

Image 72 - Dynamo script for the linkage to the database and data export.

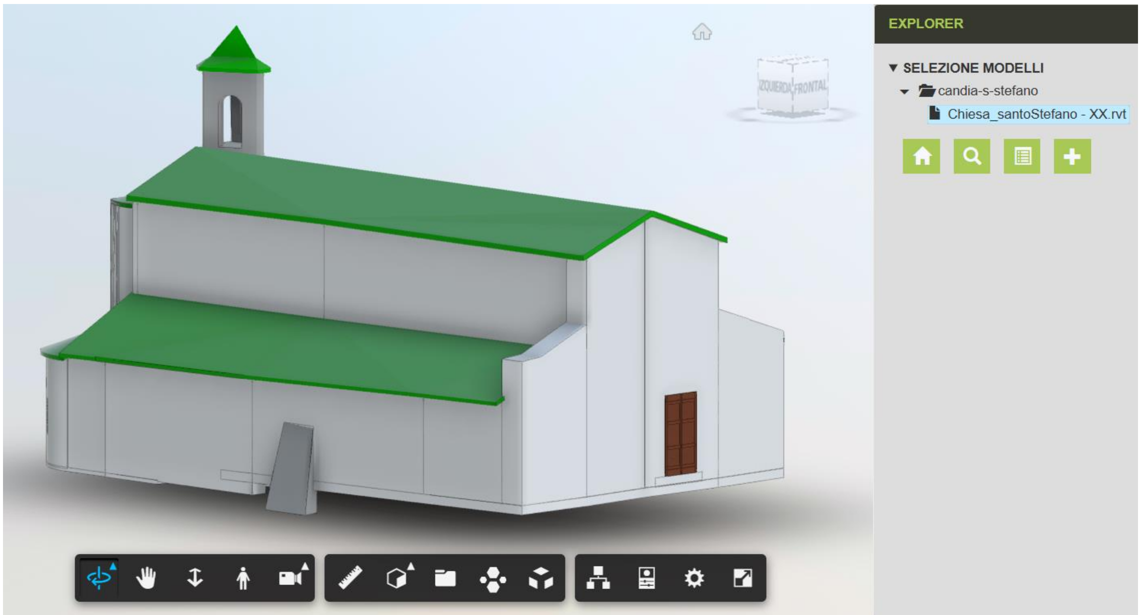

Image 73 - Final model uploaded to the main10ance platform.

7.4. Maintenance Plan Creation and Programming

To create a maintenance plan, the planner tab of the platform is used. This interface is divided into two main sections: one for creating and assigning tasks, where the person in charge defines the activities to be carried out with specific dates and details, and the other as a calendar explorer. The calendar displays scheduled activities based on the selected date, facilitating a clear and structured visualization of the activity schedule.

The platform's planner is divided into several modules: Work Summary, Planning, Scheduling, Overdue Scheduling, Previous Activities, Execution, and History.

In the Santo Stefano Church case study, the process begins with creating a new maintenance plan. This starts in the Planning module, where the location of the building is specified, the specific building within that location is selected, and finally an object class is selected. Each object class is assigned a set of cyclical activities that are applied to the elements included in that classification.

These activities are referred to as cyclical because they have a predictable impact on the elements being maintained. Each activity consists of the following components:

- Risk Statement: Identifies the situation or factor that causes a negative impact on the element.
- Control: Describes the action required to verify and assess the identified situation.
- Routine Maintenance: Defines the maintenance actions to be performed periodically.
- Frequency: Specifies the interval in months at which the activity should be performed.
- Start Date: Indicates the beginning of the maintenance cycle.

Once the activities in the Planning module are complete, they can be scheduled. When scheduling, additional information is added, such as the entity responsible for the execution, the tools required, the estimated cost, the estimated hours, the actual start date, and any additional notes, if necessary.

Finally, the scheduled activities are displayed in the Execution module, where all the previously entered information is consolidated. In addition, it is possible to see which specific model elements each maintenance activity applies to. These elements are highlighted in the BIM viewer when the control activity title is clicked, making it easier to identify and manage them correctly. This functionality ensures more efficient and accurate execution of scheduled tasks.

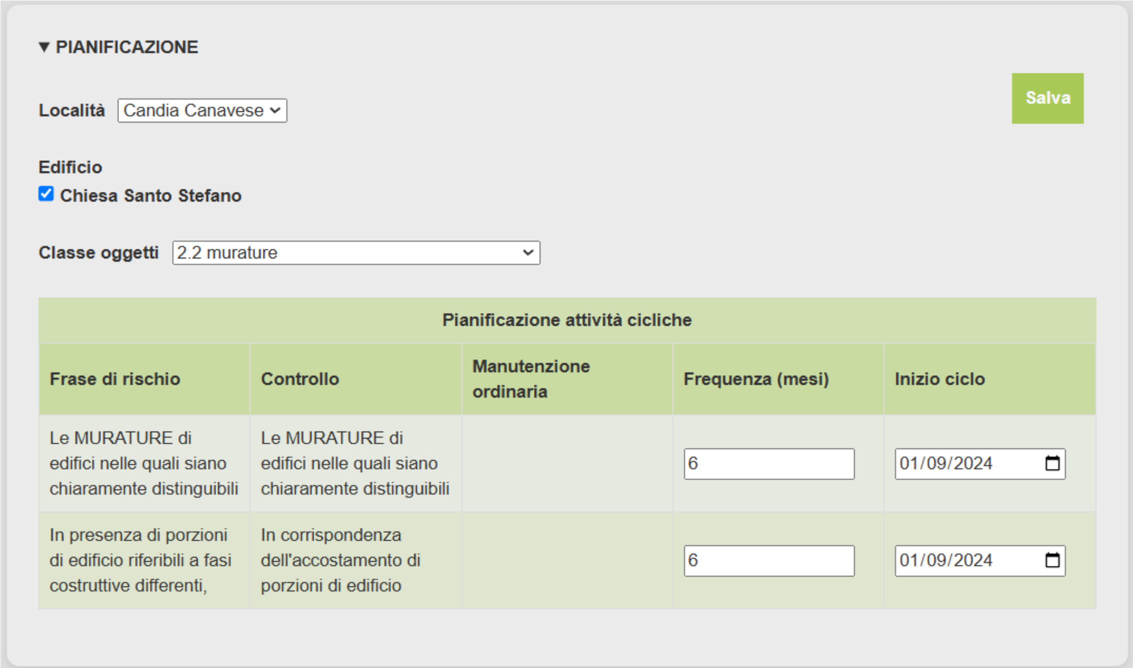

Image 74 - Planning module in the planner tab of the 4main10ance web platform.

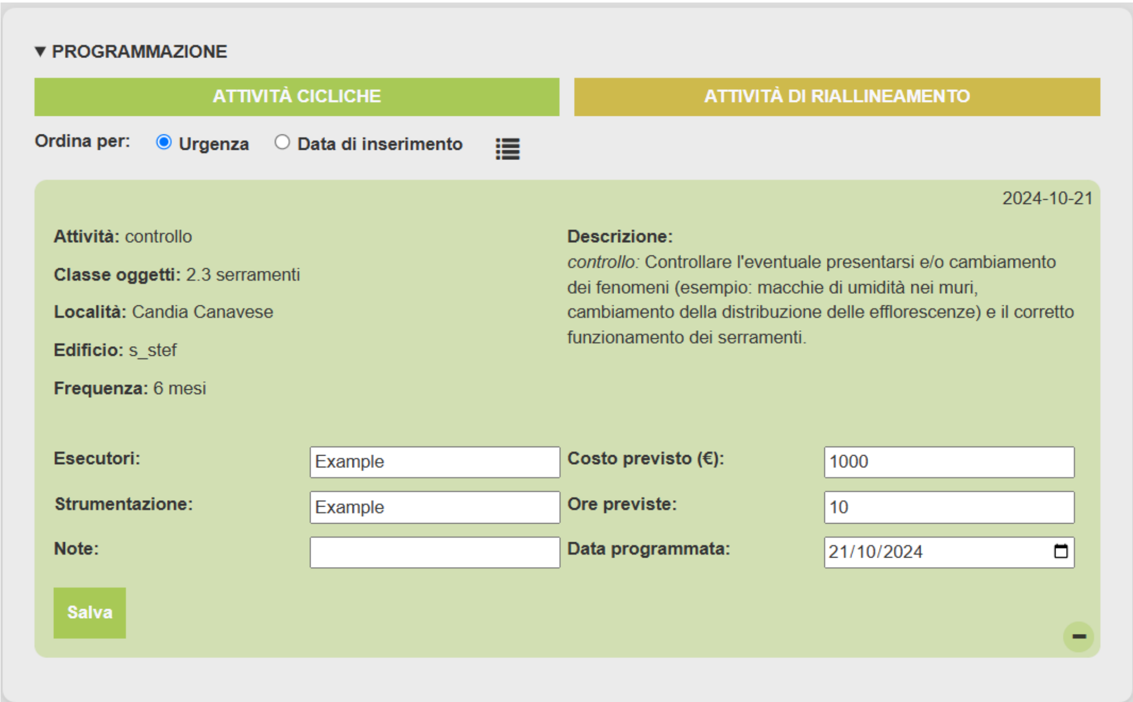

Image 75 - Scheduling module in the planner tab of the 4main10ance web platform

Attività di controllo n. 241116233914674

Località	Candia Canavese
Edificio	s_stef
Classe oggetti	2.3 serramenti
Tipo di controllo	Controllare l'eventuale presentarsi e/o cambiamento dei fenomeni (esempio: macchie di umidità nei muri, cambiamento della distribuzione delle efflorescenze) e il corretto funzionamento dei serramenti.
Strumentazione	Example
Costo previsto (€)	1000
Durata prevista (ore)	10
Data controllo	2024-10-21
Data programmazione attività	2024-11-16
Operatore	Example
Documenti	*Nessun valore*
Note	*Nessun valore*
Codice scheda controllo	241116233914674
Elementi da controllare	▼ **Vedi elementi** CND|s_stef|finestra|801847, CND|s_stef|finestra|809499, CND|s_stef|finestra|812408, CND|s_stef|finestra|812531, CND|s_stef|finestra|813440, CND|s_stef|finestra|813869, CND|s_stef|finestra|814115, CND|s_stef|finestra|814760, CND|s_stef|finestra|815254, CND|s_stef|finestra|815794, CND|s_stef|finestra|816890, CND|s_stef|finestra|817621, CND|s_stef|finestra|818678, CND|s_stef|finestra|819570, CND|s_stef|finestra|821586, CND|s_stef|porta|784034, CND|s_stef|porta|825567, CND|s_stef|porta|833415

Image 76 - Control activity details in the execution module in the planner tab of the 4main10ance Web Platform.

7.5. Insights for the Development and Implementation of Risk Phrases in the Creation of the Maintenance Plan

During the creation of a maintenance plan for the Church of Santo Stefano, the use of the risk phrases already existing in the 4main10ance platform's database, originally developed for the sacri monti project, revealed significant insights and challenges. While some of these phrases were well suited to the context of the church and were seamlessly adopted, others were not fully compatible due to the unique conditions and characteristics of the building. This led to the need to create new risk phrases specifically tailored to the church's context. These new phrases were developed using the same logic and methodology used for the sacri monti, ensuring consistency in structure while addressing the specifics of the case study.

The following sentences will be used as examples to illustrate these considerations and their usefulness in the further development of the platform:

1. "*A causa di fenomeni di DISSESTO/ASSESTAMENTO o di EROSIONE del TERRENO possono manifestarsi fenomeni di DISSESTO/DANNO delle strutture della COPERTURA/TETTO.*"
2. "Le MURATURE di edifici nelle quali siano chiaramente distinguibili fasi costruttive differenti, le aree di innesto tra porzioni ascrivibili a tali fasi possono essere soggette a fenomeni di FESSURAZIONE e/o DISTACCO di INTONACO e/o di strati di finitura sovrammessi, con conseguenti fenomeni di INFILTRAZIONE"
3. "Il VENTO forte può provocare la DISLOCAZIONE degli ELEMENTi DEL MANTO, con conseguente possibilità di INFILTRAZIONE"

From the phrases developed, the first and second are closely aligned with the specific context of the case study. For instance, considering the second phrase and the various construction phases the Church of Santo Stefano has undergone, it is crucial to highlight the implications and challenges these historical construction joints present for heritage conservation. This demonstrates that the process resulted in highly relevant and customized phrases that better reflect the actual conditions and risks associated with the building.

Despite the successful creation and adaptation of these phrases, certain limitations were identified in their application. In particular, the platform showed constraints in handling maintenance activities that do not align with predictable, cyclical scenarios, as observed in the third phrase. These unpredictable situations require immediate attention and cannot be pre-scheduled in the same way as routine maintenance. This limitation highlights a valuable opportunity for further platform development, such as integrating tools for real-time control and monitoring to address unforeseen issues more effectively. These insights enhance the platform's functionality by enabling it to not only manage planned activities but also dynamically respond to emerging maintenance needs. This approach of identifying risks and planning for their resolution enhances the overall preservation of the structure and contributes to its long-term conservation.

Conclusion

The methodology used in this study has made it possible to deepen and extend the knowledge and information already acquired about the Church of Santo Stefano. It facilitated the implementation of both traditional and modern architectural surveying tools, which were crucial for the construction of a detailed three-dimensional model. It’s integration into the 4main10ance platform allowed the development of a planned maintenance program for the conservation of the architectural heritage, becoming a reference case for future similar scenarios.

The primary objective of this thesis is to create the above-mentioned planned maintenance program. In doing so, the study aims to demonstrate the usefulness of such a tool, while providing an example of a representative case that can be replicated in different contexts of heritage diffused throughout the country.

The work began with an architectural surveying campaign, during which a network of points was constructed and subsequently integrated with point clouds obtained through terrestrial laser scanning and aerial photogrammetry. This georeferenced three-dimensional representation of the internal surfaces of the case study complemented previous work carried out on the same site, extending the existing knowledge and enabling a more comprehensive representation of the church in a BIM environment in this case, Revit. A specific HBIM framework was used due to the historic nature of the building.

Once the BIM model was complete, it was exported to the 4main10ance platform using visual programming tools to compile parameters and export the information contained in the model. These tools proved invaluable in facilitating the transition between Revit and the platform, streamlining a critical step in the development of the maintenance plan. With the data prepared, the portal's visualization and operational tools were used to create the maintenance plan for the case study.

Throughout the process, several limitations and opportunities were identified at various stages of development:

- Architectural survey:
  The main limitation was that the data collected focused only on the visible surfaces of the building, excluding information about the stratigraphy or composition of its

elements. However, the use of modern instruments, such as the terrestrial laser scanner, significantly reduced the time needed to link and prepare the point clouds, resulting in a highly accurate and georeferenced geometric representation.

- Creation of the three-dimensional model:
  Limitations included the lack of native tools in the modeling software to represent complex historical elements, such as the church's vaults, since the program is primarily intended for designing contemporary buildings with regular shapes. Another limitation was the lack of backward compatibility with the software, which prevented files from being opened in earlier versions of the program. Despite these challenges, the software provided considerable flexibility for modeling complex shapes that could be parameterized and adjusted within the model. In addition, as a BIM environment, the software ensured interoperability between programs and interdisciplinary collaboration on the same document.

- Construction of the maintenance plan:
  4main10ance, as a platform still under development, has limitations such as the lack of preconfigured data for newly uploaded models. However, its potential lies in its ability to serve as a unique repository for culturally significant buildings, enabling the development of planned maintenance programs. This facilitates the efficient management of cultural assets by governmental or private entities.

In conclusion, the methodology and workflow used in this study have not only contributed to a new case in the 4main10ance platform but have also highlighted the need for its continued development and refinement. The platform has demonstrated its potential effectiveness as a tool for architectural heritage conservation, while adapting to contemporary conservation and cultural management needs. Its application in different case studies continues to drive its development, ensuring that it becomes increasingly adaptable and effective in a wide range of contexts.

References

- Barnes, P. (2019). *BIM in principle and in practice (3rd ed.).* ICE Publishing. Retrieved September 18, 2024, from https://www.benardmakaa.com/wp-content/uploads/2021/11/P.T-Barnes-and-N.-Davies-BIM-in-Principle-and-In-Practice-ICE-Publishing-2014.pdf
- BOBBIO C. (1910). *Le Chiese del Canavese.* Tipografia Ditta F.
- Cavallari Murat, A. (1976). *Tra Serra d'Ivrea Orco e Po.* Torino: Istituto Bancario San Paolo.
- Colucci, E., Iacono, E., Matrone, F., & Ventura, G. M. (2023). *The development of a 2D/3D BIM-GIS web platform for planned maintenance of built and cultural heritage: The Main10ance project.* The International Archives of the Photogrammetry, Remote Sensing and Spatial Information Sciences, XLVIII-M-2, 433-439. https://doi.org/10.5194/isprs-archives-XLVIII-M-2-2023-433-2023
- Coursera. (2024, March 20). *What is photogrammetry?* Coursera. Retrieved September 18, 2024, from https://www.coursera.org/articles/what-is-photogrammetry
- Datumate. (n.d.). *Topographic Survey.* Retrieved July 13, 2024, from www.datumate.com/glossary/topographic-survey/
- Forneris, G. (1999). *Candia Canavese: Due passi e cento ricordi.* Comune Candia Canavese.
- Gasparovic, M., Gajski, D. (2016, May). *Unmanned Aerial Photogrammetric Systems in the Service of Engineering Geodesy [Paper presentation].* SIG 2016 – International Symposium on Engineering Geodesy. Conference 2026, Varaždin, Croatia. https://www.researchgate.net/publication/303458608_Unmanned_Aerial_Photogrammetric_Systems_in_the_Service_of_Engineering_Geodesy
- Ghilani, Charles D., Wolf, Paul R. (2002). *Elementary surveying: an introduction to geomatics.* Retrieved September 18, 2024, from https://www.academia.edu/44698915/Charles_D_Ghilani_Paul_R_Wolf_Elementary_Surv_BookFi_org_pdf
- Interreg Italia-Svizzera. (n.d.). Documento di sintesi - Programma di cooperazione Interreg V-A Italia-Svizzera 2014-2020. Retrieved November 10, 2024, from

https://www.interreg-italiasvizzera.eu/wps/portal/site/interreg-italia-svizzera/archivio-programma-2014-2020

- *MAIN10ANCE - I Sacri Monti: patrimonio comune di valori, laboratorio per la conservazione sostenibile ed una migliore fruibilità turistica dei beni culturali*. (s. f.). Regione Piemonte. https://www.regione.piemonte.it/web/temi/fondi-progetti-europei/programmi-progetti-europei/cooperazione-territoriale-europea-piemonte/main10ance-sacri-monti-patrimonio-comune-valori-laboratorio-per-conservazione-sostenibile-una
- Matrone, F., Colucci, E., Iacono, E., & Ventura, G. M. (2023). *The HBIM-GIS Main10ance Platform to Enhance the Maintenance and Conservation of Historical Built Heritage.* Sensors, 23(19), 1-28. https://doi.org/10.3390/s23198112
- McManamon, P. F. (2019). *LiDAR technologies and systems. Society of Photo-Optical Instrumentation Engineers.* Retrieved September 18, 2024, from https://www.spiedigitallibrary.org/samples/PM300.pdf#_=_
- Murphy, M., McGovern, E. (2012). *Historic building information modelling (HBIM).* Retrieved September 18, 2024, from https://www.researchgate.net/publication/241582141_Historic_building_information_modelling_HBIM
- Ramella, P. (2006). *Canavese: 100 secoli: Archeologia, insediamenti, chiese, castelli, statuti, storia, personalità.* Ivrea: Associazione Amici Museo del Canavese.
- 3DSourced. (2023, November 22). *Photogrammetry Guide 2023 – Definition, Advantages and Uses Explained - 3DSourced.* 3DSourced. Retrieved September 18, 2024, from https://www.3dsourced.com/guides/photogrammetry-guide/
- UNESCO World Heritage Centre. (n.d.). *World Heritage List.* UNESCO. Retrieved September 18, 2024, from https://whc.unesco.org/en/list/
- What is a laser? | NIST. (2022, March 17). NIST. Retrieved September 18, 2024, from https://www.nist.gov/director/pao/nists-role-laser-measurements-and-applications/what-laser

Graduation thesis

- Palazzo, I. (2020). *HBIM e GIS 3D per la gestione del patrimonio architettonico: il caso del Sacro Monte di Varallo (Master's thesis, Politecnico di Torino).* Politecnico di Torino.
- Dalpiaz, L. M. (2019). *HBIM e rilevamento metrico 3D per i beni architettonici: il caso studio del Sacro Monte di Ghiffa (Master's thesis, Politecnico di Torino).* Politecnico di Torino.
- Muscarà, M. (2017). *Rilievo metrico e metodologie H-BIM per il patrimonio storico. Applicazioni alla Chiesa di S. Stefano al Monte di Candia Canavese (Master's thesis, Politecnico di Torino).* Politecnico di Torino.

Webography

- http://www.chiesasantostefano.it/vicende_2.htm
- https://www.faro.com/
- https://www.agisoft.com/
- https://www.autodesk.com/
- https://www.dji.com/global/camera-drones?site=brandsite&from=nav
- https://leica-geosystems.com/
- https://www.comune.candia.to.it/
- https://www.chieseromaniche.it/schede/359-Candia-Canavese-Santo-Stefano-al-Monte.htm
- https://main10ance.eu/
- https://dynamobim.org/

Manuals

- Agisoft Metashape Manual
- Leica Cyclone Register 360 Quick Start Guide
- CloudCompare Manual
- FARO As-Built for Autodesk Revit Manual
- Agisoft Metashape Manual
- CloudCompare Manual
- Dynamo Language Manual

Acknowledgements

I would like to express my gratitude to Professor Marco Zerbinatti and Professor Sara Fasana for their guidance and support throughout the development of this fascinating thesis.

I also extend my thanks to Architect Francesca Matrone, Professor Andrea Lingua and Emmanuele Iacono, who assisted me in completing this work, from data collection to its subsequent development.

My heartfelt appreciation goes to Amici della Chiesa di Santo Stefano for their encouragement and support during this project, as well as for offering me a warm meal on a day I collected data for this thesis.

I am deeply grateful to everyone who was present, listened, and offered their help in completing this work.

Agradezco a la vida y a mi familia por permitirme estar donde estoy, todos mis logros y aciertos en la vida se los debo a ellos y por eso les estaré eternamente agradecido.

Appendices

Geomatic surveys

Place: Candia Canavese chiessa di Santo Stefano, 6 of June 2023

Politecnico di Torino

Operators: Andrea Lingua, Francesca Matrone, Esteban Salazar, Marco Zerbinatti

MONOGRAPHY

VERTEX 1000

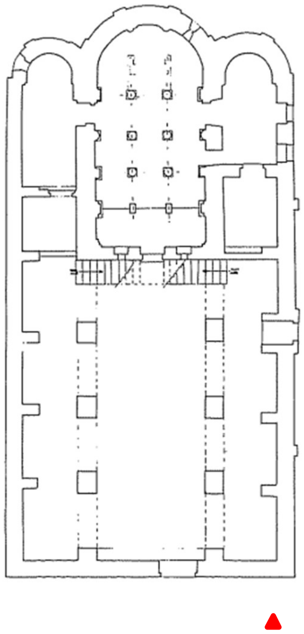

Out of scale plant view of Santo Stefano's church

Instrument reference point

Marking method: Painted on the floor
Photo caption: Smartphone Redmi Note 11 Esteban Salazar
Survey Instrument: Total Station
Instrument Height: 1.335 m
Measurement Instrument: Laser with prism
Date: 6 of June 2023

Coordinate [m]
X= 412455,338; y= 5020514,471;
z(ellissoidica)= 419,6418

Sistema: UTM WGS84

Geomatic surveys

Place: Candia Canavese chiessa di Santo Stefano, 6 of June 2023

Politecnico di Torino

Operators: Andrea Lingua, Francesca Matrone, Esteban Salazar, Marco Zerbinatti

MONOGRAPHY

VERTEX 11000

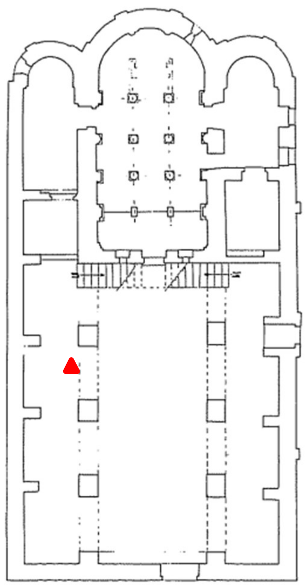

Out of scale plant view of Santo Stefano's church

Instrument reference point

Detail of the reference point

Marking method: Painted on the floor
Photo caption: Smartphone Redmi Note 11 Esteban Salazar
Survey Instrument: Total Station
Instrument Height: 1.585 m
Measurement Instrument: Laser with prism
Date: 6 of June 2023

Coordinate [m]
X= 412476,881; y= 5020530,802;
z(ellissoidica)= 420,19477

Sistema: UTM WGS84

Geomatic surveys

Place: Candia Canavese chiessa di Santo Stefano, 6 of June 2023

Politecnico di Torino

Operators: Andrea Lingua, Francesca Matrone, Esteban Salazar, Marco Zerbinatti

MONOGRAPHY

VERTEX 12000

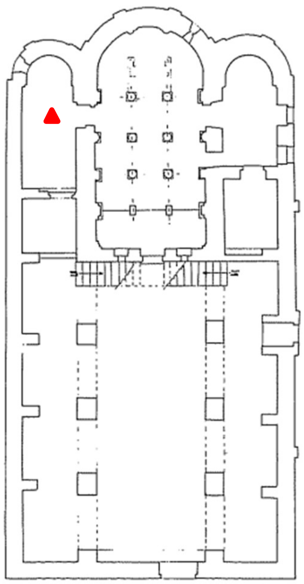

Out of scale plant view of Santo Stefano's church

Instrument reference point

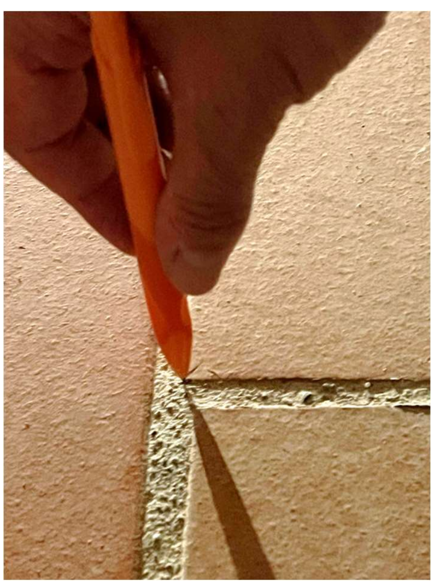

Detail of the reference point

Marking method: Painted on the floor
Photo caption: Smartphone Redmi Note 11 Esteban Salazar
Survey Instrument: Total Station
Instrument Height: 1.655 m
Measurement Instrument: Laser with prism
Date: 6 of June 2023

Coordinate [m]
X= 412486,455; y= 5020533,365;
z(ellissoidica)= 419,49214

Sistema: UTM WGS84

Geomatic surveys

Place: Candia Canavese chiessa di Santo Stefano, 6 of June 2023

Politecnico di Torino

Operators: Andrea Lingua, Francesca Matrone, Esteban Salazar, Marco Zerbinatti

MONOGRAPHY

VERTEX 13000

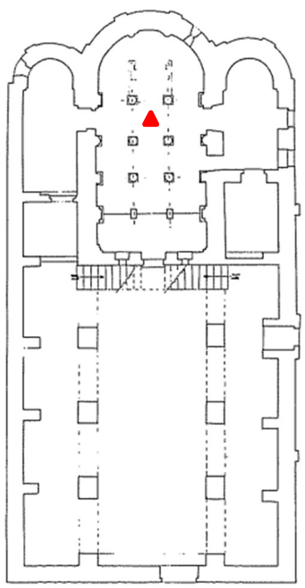

Out of scale plant view of Santo Stefano's church

Instrument reference point

Detail of the reference point

Marking method: Painted on the floor
Photo caption: Smartphone Redmi Note 11 Esteban Salazar
Survey Instrument: Total Station
Instrument Height: 1.525 m
Measurement Instrument: Laser with prism
Date: 6 of June 2023

Coordinate [m]
X= 412487,4175; y= 5020529,502;
z(ellissoidica)= 419,343

Sistema: UTM WGS84

Geomatic surveys

Place: Candia Canavese chiessa di Santo Stefano, 6 of June 2023

Politecnico di Torino

Operators: Andrea Lingua, Francesca Matrone, Esteban Salazar, Marco Zerbinatti

MONOGRAPHY

VERTEX 14000

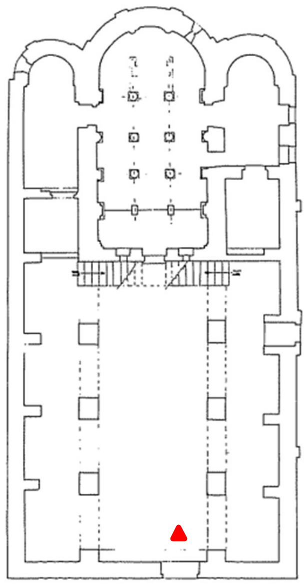

Out of scale plant view of Santo Stefano's church

Instrument reference point

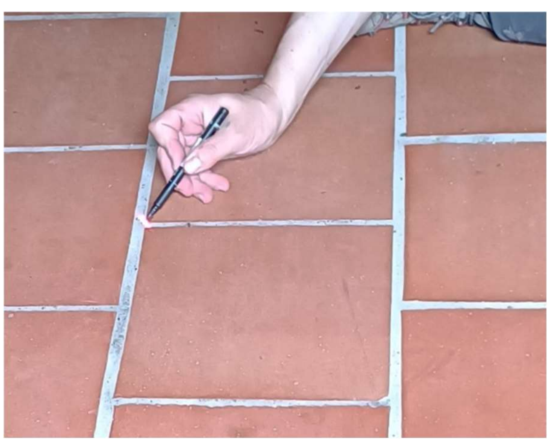

Detail of the reference point

Marking method: Painted on the floor
Photo caption: Smartphone Redmi Note 11 Esteban Salazar
Survey Instrument: Total Station
Instrument Height: 1.460 m
Measurement Instrument: Laser with prism
Date: 6 of June 2023

Coordinate [m]
X= 412470,8557; y= 5020526,061;
z(ellissoidica)= 420,31805

Sistema: UTM WGS84

Geomatic surveys

Place: Candia Canavese chiessa di Santo Stefano, 6 of June 2023

Politecnico di Torino

Operators: Andrea Lingua, Francesca Matrone, Esteban Salazar, Marco Zerbinatti

MONOGRAPHY

VERTEX 15000

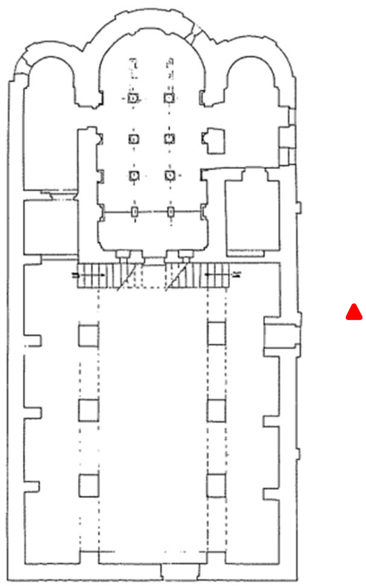

Out of scale plant view of Santo Stefano’s church

Instrument reference point

Marking method: Painted on the floor
Photo caption: Smartphone Redmi Note 11 Esteban Salazar
Survey Instrument: Total Station

Measurement Instrument: Laser with prism
Date: 6 of June 2023

Coordinate [m]
X= 412479,2739; y= 5020520,497;
z(ellissoidica)= 420,8134

Sistema: UTM WGS84

Cyclone REGISTER 360 PLUS
Informe de registro

oct. 27, 2023

Certificado por:

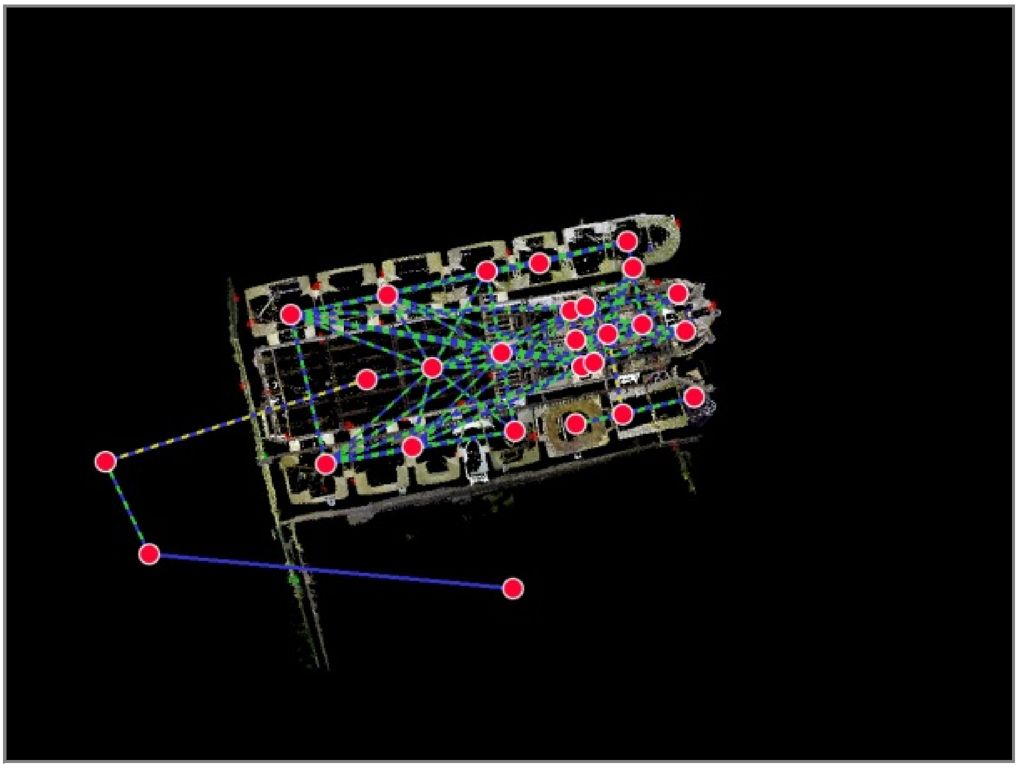

Candia

Calidad general

Resultados de error para Conjunto 1

Número de escaneos: 27
Número de enlaces: 66

Fuerza: 84 %
Solape: 55 %

Error de conjunto
0.002 m ✓

Solape
55 % ✓

Fuerza
84 % ✓

Nube a nube
0.003 m ✓

Error de diana
0.002 m ✓

Error máximo de 0.015 m. Error máximo de 0.020 m. Error mayor de 0.020 m.

Matriz de calidad de enlaces #1 -

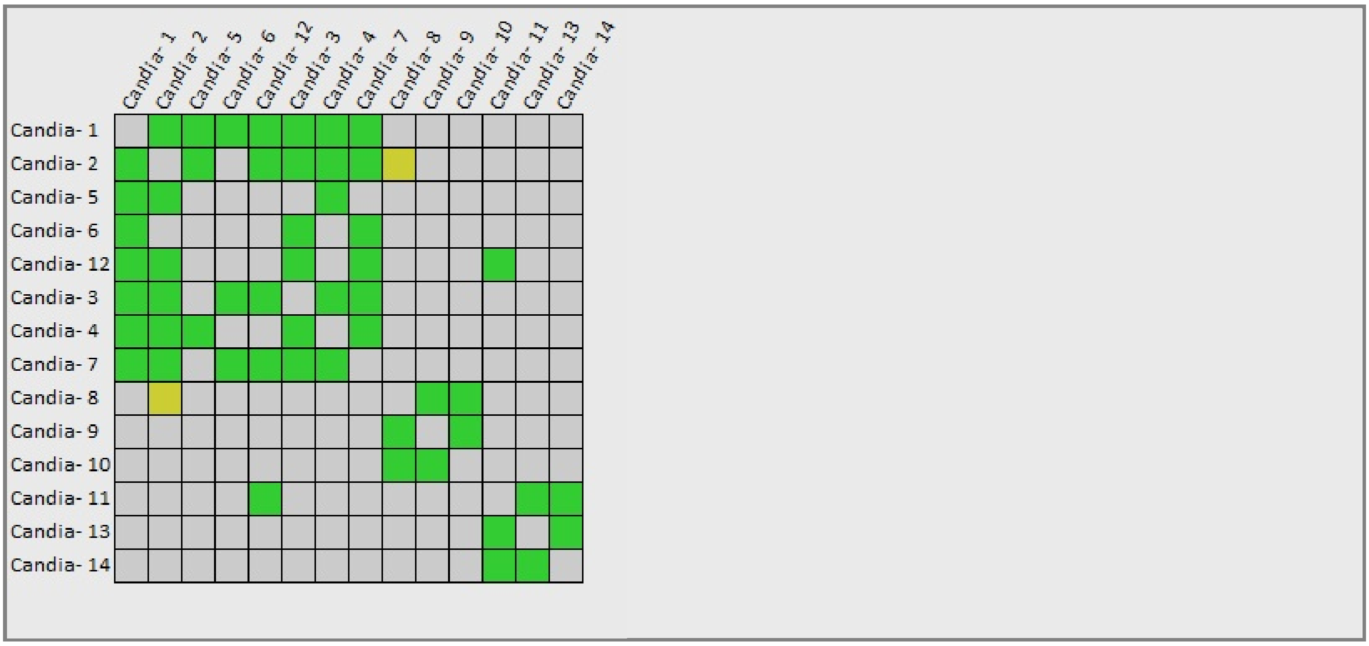

Matriz de calidad de enlaces #2 -

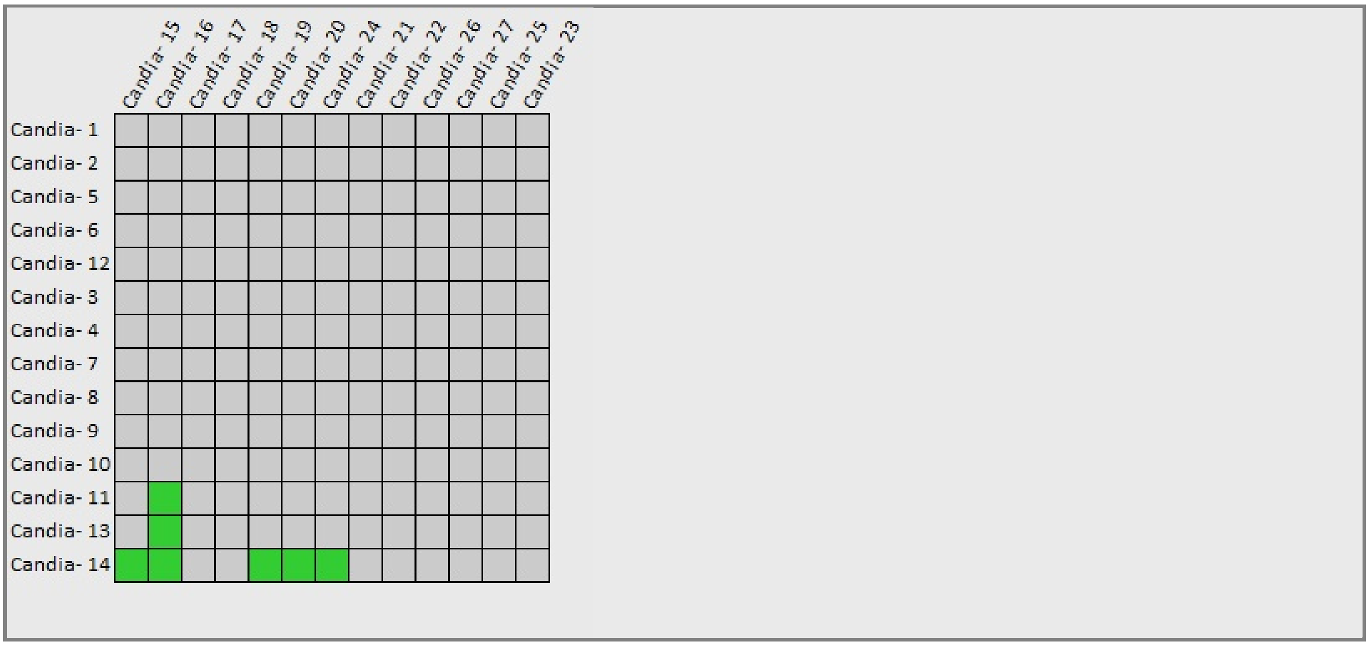

Matriz de calidad de enlaces #3 -

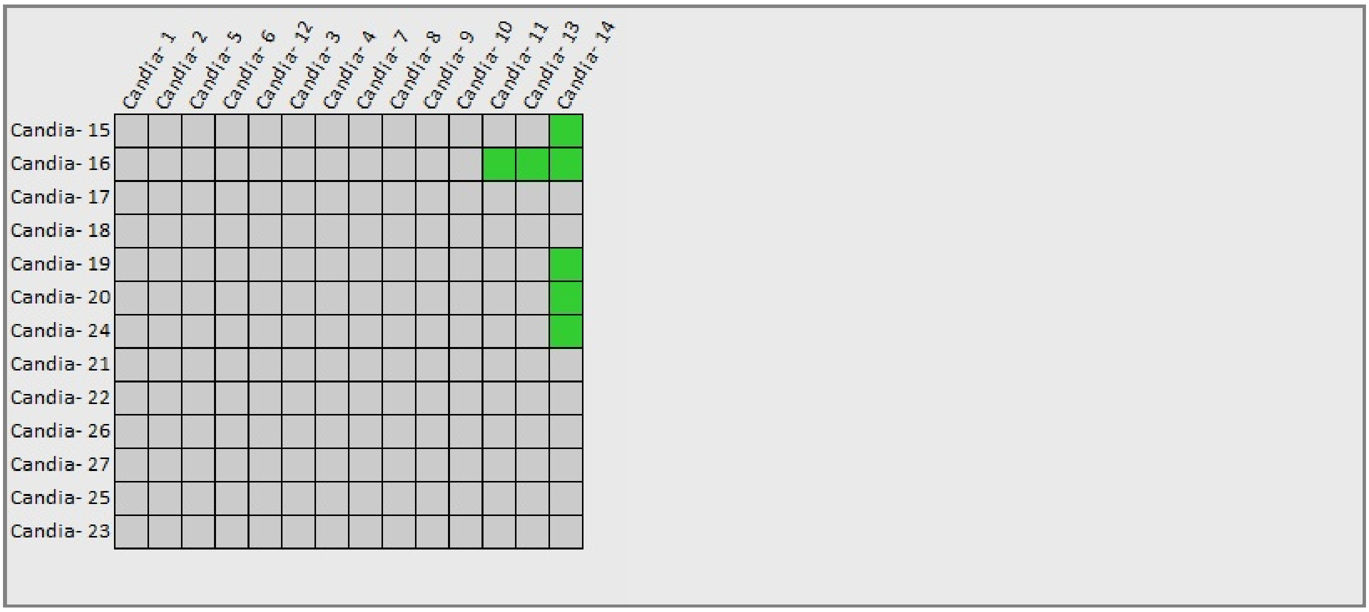

Matriz de calidad de enlaces #4 -

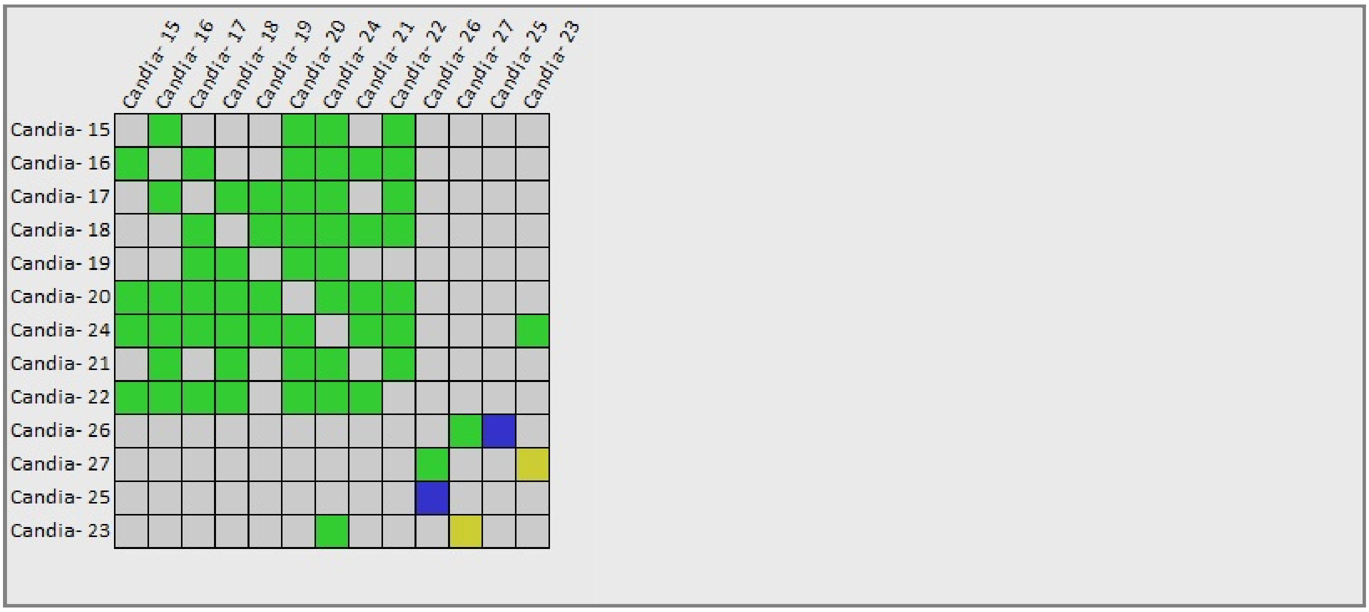

Informe de medición

Error medio Abs. de control a 'Conjunto 1': **0.005 m**

Nombre de conjunto	Escaneo	Etiqueta	Error
Conjunto 1	Candia- 1	13105	0.002 m
	Candia- 2	13105	0.002 m
	Candia- 7	12108	0.007 m
	Candia- 13	11025	0.008 m
	Candia- 11	11025	0.008 m
	Candia- 12	11025	0.005 m
	Candia- 11	12106	0.003 m
	Candia- 12	12106	0.001 m
	Candia- 13	11018	0.004 m
	Candia- 14	11018	0.005 m
	Candia- 20	11018	0.003 m
	Candia- 4	13105	0.003 m
	Candia- 24	11018	0.008 m
	Candia- 15	11018	0.004 m
	Candia- 14	11022	0.004 m
	Candia- 13	11022	0.003 m
	Candia- 14	11014	0.004 m
	Candia- 23	11014	0.006 m
	Candia- 24	11014	0.007 m
	Candia- 1	13101	0.003 m
	Candia- 2	13101	0.002 m
	Candia- 4	13101	0.006 m
	Candia- 1	13104	0.000 m
	Candia- 7	13101	0.009 m
	Candia- 3	13101	0.004 m
	Candia- 15	11024	0.004 m
	Candia- 14	11024	0.004 m
	Candia- 20	14110	0.006 m
	Candia- 16	11017	0.007 m
	Candia- 23	14101	0.006 m
	Candia- 17	14101	0.008 m
	Candia- 19	11011	0.004 m
	Candia- 2	13104	0.001 m
	Candia- 18	11011	0.004 m

	Candia- 1	13100	0.002 m
	Candia- 11	13100	0.005 m
	Candia- 12	13100	0.002 m
	Candia- 18	11015	0.006 m
	Candia- 20	14104	0.007 m
	Candia- 22	14109	0.008 m
	Candia- 1	13106	0.003 m
	Candia- 7	13106	0.003 m
	Candia- 5	13106	0.003 m
	Candia- 6	13104	0.000 m
	Candia- 6	13106	0.004 m
	Candia- 23	13102	0.001 m
	Candia- 1	13107	0.004 m
	Candia- 5	13107	0.005 m
	Candia- 6	13107	0.003 m
	Candia- 2	13107	0.004 m
	Candia- 7	13103	0.003 m
	Candia- 2	13103	0.006 m
	Candia- 2	14105	0.006 m
	Candia- 4	14105	0.006 m
	Candia- 4	13104	0.006 m
	Candia- 7	14105	0.007 m
	Candia- 24	11013A	0.005 m
	Candia- 13	11021	0.004 m
	Candia- 14	11021	0.005 m
	Candia- 15	11021	0.005 m
	Candia- 14	11023	0.002 m
	Candia- 14	11012	0.003 m
	Candia- 15	11012	0.006 m
	Candia- 7	13104	0.007 m
	Candia- 23	11019	0.008 m
	Candia- 16	11019	0.005 m
	Candia- 16	14102	0.007 m
	Candia- 23	11016	0.008 m
	Candia- 16	11016	0.007 m
	Candia- 12	12108	0.004 m
	Candia- 23	11020	0.009 m
	Candia- 24	11020	0.006 m
	Candia- 24	11010	0.004 m

	Candia- 23	11010	0.009 m
	Candia- 1	14106	0.007 m
	Candia- 2	14106	0.006 m
	Candia- 4	14106	0.007 m
	Candia- 7	14106	0.006 m
	Candia- 2	12108	0.006 m
	Candia- 26	e03	0.009 m
	Candia- 27	e03	0.010 m
	Candia- 26	e02	0.009 m
	Candia- 27	e02	0.008 m
	Candia- 26	e04	0.007 m
	Candia- 27	e04	0.008 m
	Candia- 27	e01	0.007 m
	Candia- 26	e01	0.009 m

Resultados de error de enlace

1 Vista general

Nombre de enlace	Escaneo 1	Escaneo 2	Solape	Error medio Abs.
Enlace 1	Candia- 1	Candia- 2	81 %	**0.002 m**
Enlace 2	Candia- 1	Candia- 5	81 %	**0.005 m**
Enlace 3	Candia- 1	Candia- 6	81 %	**0.004 m**
Enlace 5	Candia- 1	Candia- 12	35 %	**0.004 m**
Enlace 6	Candia- 2	Candia- 3	73 %	**0.003 m**
Enlace 7	Candia- 2	Candia- 4	71 %	**0.003 m**
Enlace 8	Candia- 2	Candia- 7	75 %	**0.003 m**
Enlace 10	Candia- 8	Candia- 9	63 %	**0.002 m**
Enlace 11	Candia- 8	Candia- 10	66 %	**0.001 m**
Enlace 12	Candia- 11	Candia- 13	77 %	**0.003 m**
Enlace 13	Candia- 13	Candia- 14	73 %	**0.002 m**
Enlace 14	Candia- 14	Candia- 15	62 %	**0.002 m**
Enlace 15	Candia- 15	Candia- 16	55 %	**0.002 m**
Enlace 16	Candia- 16	Candia- 17	45 %	**0.002 m**
Enlace 17	Candia- 17	Candia- 18	66 %	**0.001 m**
Enlace 18	Candia- 18	Candia- 19	56 %	**0.002 m**
Enlace 19	Candia- 19	Candia- 20	51 %	**0.002 m**
Enlace 20	Candia- 19	Candia- 24	59 %	**0.002 m**
Enlace 21	Candia- 20	Candia- 21	90 %	**0.001 m**
Enlace 23	Candia- 21	Candia- 22	92 %	**0.001 m**
Enlace 25	Candia- 26	Candia- 27	49 %	**0.003 m**
Enlace 26	Candia- 26	Candia- 25	6 %	**0.000 m**
Enlace 27	Candia- 27	Candia- 23	16 %	**0.006 m**
Enlace 30	Candia- 23	Candia- 24	90 %	**0.002 m**
Enlace 33	Candia- 14	Candia- 24	46 %	**0.003 m**
Enlace 34	Candia- 15	Candia- 24	52 %	**0.003 m**
Enlace 35	Candia- 16	Candia- 24	54 %	**0.003 m**
Enlace 36	Candia- 17	Candia- 24	61 %	**0.003 m**
Enlace 37	Candia- 18	Candia- 24	68 %	**0.002 m**
Enlace 38	Candia- 20	Candia- 24	82 %	**0.001 m**
Enlace 39	Candia- 21	Candia- 24	80 %	**0.002 m**
Enlace 40	Candia- 22	Candia- 24	81 %	**0.002 m**
Enlace 41	Candia- 14	Candia- 20	38 %	**0.002 m**
Enlace 42	Candia- 15	Candia- 20	39 %	**0.002 m**
Enlace 43	Candia- 16	Candia- 20	43 %	**0.002 m**
Enlace 44	Candia- 17	Candia- 20	49 %	**0.002 m**
Enlace 45	Candia- 18	Candia- 20	51 %	**0.002 m**
Enlace 46	Candia- 20	Candia- 22	90 %	**0.001 m**
Enlace 47	Candia- 17	Candia- 19	34 %	**0.003 m**

Enlace 48	Candia- 17	Candia- 22	35 %	**0.002 m**
Enlace 49	Candia- 15	Candia- 22	22 %	**0.003 m**
Enlace 50	Candia- 11	Candia- 14	64 %	**0.002 m**
Enlace 52	Candia- 14	Candia- 16	35 %	**0.002 m**
Enlace 53	Candia- 1	Candia- 3	68 %	**0.003 m**
Enlace 54	Candia- 1	Candia- 4	69 %	**0.003 m**
Enlace 55	Candia- 1	Candia- 7	75 %	**0.003 m**
Enlace 56	Candia- 2	Candia- 5	76 %	**0.005 m**
Enlace 57	Candia- 2	Candia- 12	30 %	**0.004 m**
Enlace 58	Candia- 3	Candia- 6	58 %	**0.004 m**
Enlace 59	Candia- 6	Candia- 7	64 %	**0.003 m**
Enlace 60	Candia- 4	Candia- 5	57 %	**0.004 m**
Enlace 61	Candia- 3	Candia- 7	68 %	**0.003 m**
Enlace 62	Candia- 4	Candia- 7	67 %	**0.003 m**
Enlace 63	Candia- 7	Candia- 12	23 %	**0.004 m**
Enlace 64	Candia- 16	Candia- 21	29 %	**0.002 m**
Enlace 65	Candia- 18	Candia- 21	34 %	**0.002 m**
Enlace 66	Candia- 3	Candia- 4	64 %	**0.003 m**
Enlace 67	Candia- 3	Candia- 12	22 %	**0.004 m**
Enlace 68	Candia- 16	Candia- 22	29 %	**0.003 m**
Enlace 69	Candia- 18	Candia- 22	31 %	**0.002 m**
Enlace 70	Candia- 9	Candia- 10	36 %	**0.002 m**
Enlace 71	Candia- 14	Candia- 19	26 %	**0.002 m**
Enlace 73	Candia- 11	Candia- 16	38 %	**0.003 m**
Enlace 75	Candia- 13	Candia- 16	50 %	**0.002 m**
Enlace 76	Candia- 2	Candia- 8	16 %	**0.003 m**
Enlace 77	Candia- 11	Candia- 12	76 %	**0.002 m**

2 Detalles

Nombre de enlace	Escaneo 1	Escaneo 2	Solape	Error medio Abs.
Enlace 1	Candia- 1	Candia- 2	81 %	**0.002 m**
		Nube a nube		**0.002 m**
		Diana	Error medio de diana:	**0.002 m**

Diana (Escaneo 1)	Diana (Escaneo 2)	Error
13105	13105	**0.004 m**
13104	13104	**0.001 m**
13101	13101	**0.001 m**

Nombre de enlace	Escaneo 1	Escaneo 2	Solape	Error medio Abs.
Enlace 2	Candia- 1	Candia- 5	81 %	**0.005 m**
		Nube a nube		**0.005 m**
		Diana	Error medio de diana:	--

Nombre de enlace	Escaneo 1	Escaneo 2	Solape	Error medio Abs.
Enlace 3	Candia- 1	Candia- 6	81 %	**0.004 m**
		Nube a nube		**0.004 m**
		Diana	Error medio de diana:	--

Nombre de enlace	Escaneo 1	Escaneo 2	Solape	Error medio Abs.
Enlace 5	Candia- 1	Candia- 12	35 %	**0.004 m**
		Nube a nube		**0.004 m**
		Diana	Error medio de diana:	--

Nombre de enlace	Escaneo 1	Escaneo 2	Solape	Error medio Abs.
Enlace 6	Candia- 2	Candia- 3	73 %	**0.003 m**
		Nube a nube		**0.003 m**
		Diana	Error medio de diana:	--

Nombre de enlace	Escaneo 1	Escaneo 2	Solape	Error medio Abs.
Enlace 7	Candia- 2	Candia- 4	71 %	**0.003 m**
		Nube a nube		**0.003 m**
		Diana	Error medio de diana:	--

Nombre de enlace	Escaneo 1	Escaneo 2	Solape	Error medio Abs.
Enlace 8	Candia- 2	Candia- 7	75 %	**0.003 m**
		Nube a nube		**0.003 m**
		Diana	Error medio de diana:	--

Nombre de enlace	Escaneo 1	Escaneo 2	Solape	Error medio Abs.
Enlace 10	Candia- 8	Candia- 9	63 %	**0.002 m**
		Nube a nube		**0.002 m**
		Diana	Error medio de diana:	--

Nombre de enlace	Escaneo 1	Escaneo 2	Solape	Error medio Abs.
Enlace 11	Candia- 8	Candia- 10	66 %	**0.001 m**
		Nube a nube		**0.001 m**
		Diana	Error medio de diana:	--

Nombre de enlace	Escaneo 1	Escaneo 2	Solape	Error medio Abs.
Enlace 12	Candia- 11	Candia- 13	77 %	**0.003 m**
		Nube a nube		**0.003 m**
		Diana	Error medio de diana:	--

Nombre de enlace	Escaneo 1	Escaneo 2	Solape	Error medio Abs.
Enlace 13	Candia- 13	Candia- 14	73 %	**0.002 m**
		Nube a nube		**0.001 m**
		Diana	Error medio de diana:	**0.003 m**

Diana (Escaneo 1)	Diana (Escaneo 2)	Error
11021	11021	**0.004 m**
11018	11018	**0.001 m**

Nombre de enlace	Escaneo 1	Escaneo 2	Solape	Error medio Abs.
Enlace 14	Candia- 14	Candia- 15	62 %	**0.002 m**
		Nube a nube		**0.002 m**
		Diana	Error medio de diana:	--

Nombre de enlace	Escaneo 1	Escaneo 2	Solape	Error medio Abs.
Enlace 15	Candia- 15	Candia- 16	55 %	**0.002 m**
		Nube a nube		**0.002 m**
		Diana	Error medio de diana:	--

Nombre de enlace	Escaneo 1	Escaneo 2	Solape	Error medio Abs.
Enlace 16	Candia- 16	Candia- 17	45 %	**0.002 m**
		Nube a nube		**0.002 m**
		Diana	Error medio de diana:	--

Nombre de enlace	Escaneo 1	Escaneo 2	Solape	Error medio Abs.
Enlace 17	Candia- 17	Candia- 18	66 %	**0.001 m**
		Nube a nube		**0.001 m**
		Diana	Error medio de diana:	--

Nombre de enlace	Escaneo 1	Escaneo 2	Solape	Error medio Abs.
Enlace 18	Candia- 18	Candia- 19	56 %	**0.002 m**
		Nube a nube		**0.002 m**
		Diana	Error medio de diana:	--

Nombre de enlace	Escaneo 1	Escaneo 2	Solape	Error medio Abs.
Enlace 19	Candia- 19	Candia- 20	51 %	**0.002 m**
		Nube a nube		**0.002 m**
		Diana	Error medio de diana:	--

Nombre de enlace	Escaneo 1	Escaneo 2	Solape	Error medio Abs.
Enlace 20	Candia- 19	Candia- 24	59 %	**0.002 m**
		Nube a nube		**0.002 m**
		Diana	Error medio de diana:	--

Nombre de enlace	Escaneo 1	Escaneo 2	Solape	Error medio Abs.
Enlace 21	Candia- 20	Candia- 21	90 %	**0.001 m**
		Nube a nube		**0.001 m**
		Diana	Error medio de diana:	--

Nombre de enlace	Escaneo 1	Escaneo 2	Solape	Error medio Abs.
Enlace 23	Candia- 21	Candia- 22	92 %	**0.001 m**
		Nube a nube		**0.001 m**
		Diana	Error medio de diana:	--

Nombre de enlace	Escaneo 1	Escaneo 2	Solape	Error medio Abs.
Enlace 25	Candia- 26	Candia- 27	49 %	**0.003 m**
		Nube a nube		**0.003 m**
		Diana	Error medio de diana:	**0.002 m**

Diana (Escaneo 1)	Diana (Escaneo 2)	Error
e04	e04	**0.003 m**
e03	e03	**0.001 m**

Nombre de enlace	Escaneo 1	Escaneo 2	Solape	Error medio Abs.
Enlace 26	Candia- 26	Candia- 25	6 %	**0.000 m**
		Nube a nube		**0.000 m**
		Diana	Error medio de diana:	--

Nombre de enlace	Escaneo 1	Escaneo 2	Solape	Error medio Abs.
Enlace 27	Candia- 27	Candia- 23	16 %	**0.006 m**
		Nube a nube		**0.006 m**
		Diana	Error medio de diana:	--

Nombre de enlace	Escaneo 1	Escaneo 2	Solape	Error medio Abs.
Enlace 30	Candia- 23	Candia- 24	90 %	**0.002 m**
		Nube a nube		**0.002 m**
		Diana	Error medio de diana:	--

Nombre de enlace	Escaneo 1	Escaneo 2	Solape	Error medio Abs.
Enlace 33	Candia- 14	Candia- 24	46 %	**0.003 m**
		Nube a nube		**0.003 m**
		Diana	Error medio de diana:	--

Nombre de enlace	Escaneo 1	Escaneo 2	Solape	Error medio Abs.
Enlace 34	Candia- 15	Candia- 24	52 %	**0.003 m**
		Nube a nube		**0.003 m**
		Diana	Error medio de diana:	--

Nombre de enlace	Escaneo 1	Escaneo 2	Solape	Error medio Abs.
Enlace 35	Candia- 16	Candia- 24	54 %	**0.003 m**
		Nube a nube		**0.003 m**
		Diana	Error medio de diana:	--

Nombre de enlace	Escaneo 1	Escaneo 2	Solape	Error medio Abs.
Enlace 36	Candia- 17	Candia- 24	61 %	**0.003 m**
		Nube a nube		**0.003 m**
		Diana	Error medio de diana:	--

Nombre de enlace	Escaneo 1	Escaneo 2	Solape	Error medio Abs.
Enlace 37	Candia- 18	Candia- 24	68 %	**0.002 m**
		Nube a nube		**0.002 m**
		Diana	Error medio de diana:	--

Nombre de enlace	Escaneo 1	Escaneo 2	Solape	Error medio Abs.
Enlace 38	Candia- 20	Candia- 24	82 %	**0.001 m**
		Nube a nube		**0.001 m**
		Diana	Error medio de diana:	--

Nombre de enlace	Escaneo 1	Escaneo 2	Solape	Error medio Abs.
Enlace 39	Candia- 21	Candia- 24	80 %	**0.002 m**
		Nube a nube		**0.002 m**
		Diana	Error medio de diana:	--

Nombre de enlace	Escaneo 1	Escaneo 2	Solape	Error medio Abs.
Enlace 40	Candia- 22	Candia- 24	81 %	**0.002 m**
		Nube a nube		**0.002 m**
		Diana	Error medio de diana:	--

Nombre de enlace	Escaneo 1	Escaneo 2	Solape	Error medio Abs.
Enlace 41	Candia- 14	Candia- 20	38 %	**0.002 m**
		Nube a nube		**0.002 m**
		Diana	Error medio de diana:	--

Nombre de enlace	Escaneo 1	Escaneo 2	Solape	Error medio Abs.
Enlace 42	Candia- 15	Candia- 20	39 %	**0.002 m**
		Nube a nube		**0.002 m**
		Diana	Error medio de diana:	--

Nombre de enlace	Escaneo 1	Escaneo 2	Solape	Error medio Abs.
Enlace 43	Candia- 16	Candia- 20	43 %	**0.002 m**
		Nube a nube		**0.002 m**
		Diana	Error medio de diana:	--

Nombre de enlace	Escaneo 1	Escaneo 2	Solape	Error medio Abs.
Enlace 44	Candia- 17	Candia- 20	49 %	**0.002 m**
		Nube a nube		**0.002 m**
		Diana	Error medio de diana:	--

Nombre de enlace	Escaneo 1	Escaneo 2	Solape	Error medio Abs.
Enlace 45	Candia- 18	Candia- 20	51 %	**0.002 m**
		Nube a nube		**0.002 m**
		Diana	Error medio de diana:	--

Nombre de enlace	Escaneo 1	Escaneo 2	Solape	Error medio Abs.
Enlace 46	Candia- 20	Candia- 22	90 %	**0.001 m**
		Nube a nube		**0.001 m**
		Diana	Error medio de diana:	--

Nombre de enlace	Escaneo 1	Escaneo 2	Solape	Error medio Abs.
Enlace 47	Candia- 17	Candia- 19	34 %	**0.003 m**
		Nube a nube		**0.003 m**
		Diana	Error medio de diana:	--

Nombre de enlace	Escaneo 1	Escaneo 2	Solape	Error medio Abs.
Enlace 48	Candia- 17	Candia- 22	35 %	**0.002 m**
		Nube a nube		**0.002 m**
		Diana	Error medio de diana:	--

Nombre de enlace	Escaneo 1	Escaneo 2	Solape	Error medio Abs.
Enlace 49	Candia- 15	Candia- 22	22 %	**0.003 m**
		Nube a nube		**0.003 m**
		Diana	Error medio de diana:	--

Nombre de enlace	Escaneo 1	Escaneo 2	Solape	Error medio Abs.
Enlace 50	Candia- 11	Candia- 14	64 %	**0.002 m**
		Nube a nube		**0.002 m**
		Diana	Error medio de diana:	--

Nombre de enlace	Escaneo 1	Escaneo 2	Solape	Error medio Abs.
Enlace 52	Candia- 14	Candia- 16	35 %	**0.002 m**
		Nube a nube		**0.002 m**
		Diana	Error medio de diana:	--

Nombre de enlace	Escaneo 1	Escaneo 2	Solape	Error medio Abs.
Enlace 53	Candia- 1	Candia- 3	68 %	**0.003 m**
		Nube a nube		**0.003 m**
		Diana	Error medio de diana:	--

Nombre de enlace	Escaneo 1	Escaneo 2	Solape	Error medio Abs.
Enlace 54	Candia- 1	Candia- 4	69 %	**0.003 m**
		Nube a nube		**0.003 m**
		Diana	Error medio de diana:	--

Nombre de enlace	Escaneo 1	Escaneo 2	Solape	Error medio Abs.
Enlace 55	Candia- 1	Candia- 7	75 %	**0.003 m**
		Nube a nube		**0.003 m**
		Diana	Error medio de diana:	--

Nombre de enlace	Escaneo 1	Escaneo 2	Solape	Error medio Abs.
Enlace 56	Candia- 2	Candia- 5	76 %	**0.005 m**
		Nube a nube		**0.005 m**
		Diana	Error medio de diana:	--

Nombre de enlace	Escaneo 1	Escaneo 2	Solape	Error medio Abs.
Enlace 57	Candia- 2	Candia- 12	30 %	**0.004 m**
		Nube a nube		**0.004 m**
		Diana	Error medio de diana:	--

Nombre de enlace	Escaneo 1	Escaneo 2	Solape	Error medio Abs.
Enlace 58	Candia- 3	Candia- 6	58 %	**0.004 m**
		Nube a nube		**0.004 m**
		Diana	Error medio de diana:	--

Nombre de enlace	Escaneo 1	Escaneo 2	Solape	Error medio Abs.
Enlace 59	Candia- 6	Candia- 7	64 %	**0.003 m**
		Nube a nube		**0.003 m**
		Diana	Error medio de diana:	--

Nombre de enlace	Escaneo 1	Escaneo 2	Solape	Error medio Abs.
Enlace 60	Candia- 4	Candia- 5	57 %	**0.004 m**
		Nube a nube		**0.004 m**
		Diana	Error medio de diana:	--

Nombre de enlace	Escaneo 1	Escaneo 2	Solape	Error medio Abs.
Enlace 61	Candia- 3	Candia- 7	68 %	**0.003 m**
		Nube a nube		**0.003 m**
		Diana	Error medio de diana:	--

Nombre de enlace	Escaneo 1	Escaneo 2	Solape	Error medio Abs.
Enlace 62	Candia- 4	Candia- 7	67 %	**0.003 m**
		Nube a nube		**0.003 m**
		Diana	Error medio de diana:	--

Nombre de enlace	Escaneo 1	Escaneo 2	Solape	Error medio Abs.
Enlace 63	Candia- 7	Candia- 12	23 %	**0.004 m**
		Nube a nube		**0.004 m**
		Diana	Error medio de diana:	--

Nombre de enlace	Escaneo 1	Escaneo 2	Solape	Error medio Abs.
Enlace 64	Candia- 16	Candia- 21	29 %	**0.002 m**
		Nube a nube		**0.002 m**
		Diana	Error medio de diana:	--

Nombre de enlace	Escaneo 1	Escaneo 2	Solape	Error medio Abs.
Enlace 65	Candia- 18	Candia- 21	34 %	**0.002 m**
		Nube a nube		**0.002 m**
		Diana	Error medio de diana:	--

Nombre de enlace	Escaneo 1	Escaneo 2	Solape	Error medio Abs.
Enlace 66	Candia- 3	Candia- 4	64 %	**0.003 m**
		Nube a nube		**0.003 m**
		Diana	Error medio de diana:	--

Nombre de enlace	Escaneo 1	Escaneo 2	Solape	Error medio Abs.
Enlace 67	Candia- 3	Candia- 12	22 %	**0.004 m**
		Nube a nube		**0.004 m**
		Diana	Error medio de diana:	--

Nombre de enlace	Escaneo 1	Escaneo 2	Solape	Error medio Abs.
Enlace 68	Candia- 16	Candia- 22	29 %	**0.003 m**
		Nube a nube		**0.003 m**
		Diana	Error medio de diana:	--

Nombre de enlace	Escaneo 1	Escaneo 2	Solape	Error medio Abs.
Enlace 69	Candia- 18	Candia- 22	31 %	**0.002 m**
		Nube a nube		**0.002 m**
		Diana	Error medio de diana:	--

Nombre de enlace	Escaneo 1	Escaneo 2	Solape	Error medio Abs.
Enlace 70	Candia- 9	Candia- 10	36 %	**0.002 m**
		Nube a nube		**0.002 m**
		Diana	Error medio de diana:	--

Nombre de enlace	Escaneo 1	Escaneo 2	Solape	Error medio Abs.
Enlace 71	Candia- 14	Candia- 19	26 %	**0.002 m**
		Nube a nube		**0.002 m**
		Diana	Error medio de diana:	--

Nombre de enlace	Escaneo 1	Escaneo 2	Solape	Error medio Abs.
Enlace 73	Candia- 11	Candia- 16	38 %	**0.003 m**
		Nube a nube		**0.003 m**
		Diana	Error medio de diana:	--

Nombre de enlace	Escaneo 1	Escaneo 2	Solape	Error medio Abs.
Enlace 75	Candia- 13	Candia- 16	50 %	**0.002 m**
		Nube a nube		**0.002 m**
		Diana	Error medio de diana:	--

Nombre de enlace	Escaneo 1	Escaneo 2	Solape	Error medio Abs.
Enlace 76	Candia- 2	Candia- 8	16 %	**0.003 m**
		Nube a nube		**0.003 m**
		Diana	Error medio de diana:	--

Nombre de enlace	Escaneo 1	Escaneo 2	Solape	Error medio Abs.
Enlace 77	Candia- 11	Candia- 12	76 %	**0.002 m**
		Nube a nube		**0.002 m**
		Diana	Error medio de diana:	--

Gráficos

Candia-1

ProjectIcon

Agisoft Metashape

Processing Report

20 October 2023

Survey Data

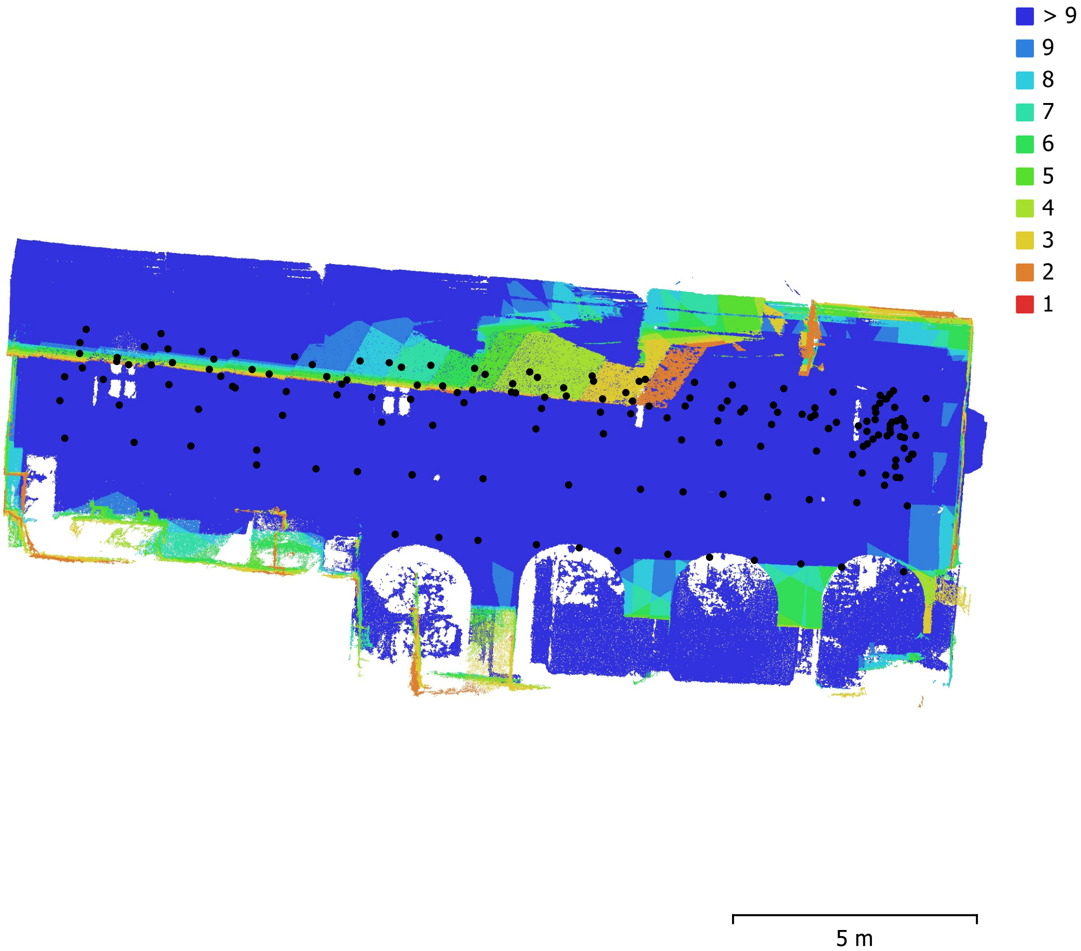

Fig. 1. Camera locations and image overlap.

Number of images:	170	Camera stations:	170
Flying altitude:	3.11 m	Tie points:	168,495
Ground resolution:	1.04 mm/pix	Projections:	654,428
Coverage area:	132 m²	Reprojection error:	0.988 pix

Camera Model	Resolution	Focal Length	Pixel Size	Precalibrated
FC3582 (6.72mm)	4032 x 3024	6.72 mm	2.4 x 2.4 µm	No
FC3582 (6.72mm)	4032 x 3024	6.72 mm	2.25 x 2.25 µm	No

Table 1. Cameras.

Camera Calibration

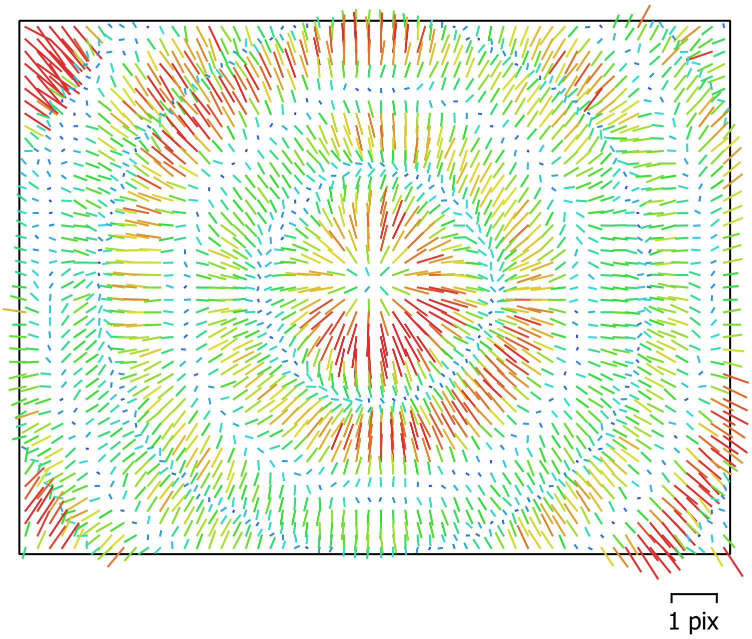

Fig. 2. Image residuals for FC3582 (6.72mm).

FC3582 (6.72mm)

155 images

Type	Resolution	Focal Length	Pixel Size
Frame	**4032 x 3024**	**6.72 mm**	**2.4 x 2.4 µm**

	Value	Error	F	Cx	Cy	B1	B2	K1	K2	K3	K4	P1	P2
F	**2833.24**	0.063	1.00	-0.07	0.01	-0.58	0.08	-0.27	0.27	-0.26	0.24	-0.06	-0.19
Cx	**2.04024**	0.11		1.00	-0.07	0.23	-0.12	-0.01	0.01	-0.01	0.01	0.96	-0.02
Cy	**-12.4045**	0.077			1.00	-0.08	0.09	0.00	-0.00	-0.00	0.01	-0.07	0.91
B1	**-0.937485**	0.056				1.00	-0.04	-0.00	-0.00	0.00	-0.00	0.21	0.12
B2	**0.977116**	0.052					1.00	0.00	-0.00	0.00	-0.00	-0.19	0.08
K1	**0.096533**	0.00012						1.00	-0.97	0.93	-0.88	-0.01	-0.00
K2	**-0.176412**	0.00066							1.00	-0.99	0.96	0.01	0.00
K3	**0.130936**	0.0014								1.00	-0.99	-0.01	-0.00
K4	**-0.00949445**	0.00099									1.00	0.01	0.01
P1	**-0.000871227**	1e-05										1.00	-0.03
P2	**-0.000118056**	7.1e-06											1.00

Table 2. Calibration coefficients and correlation matrix.

Camera Calibration

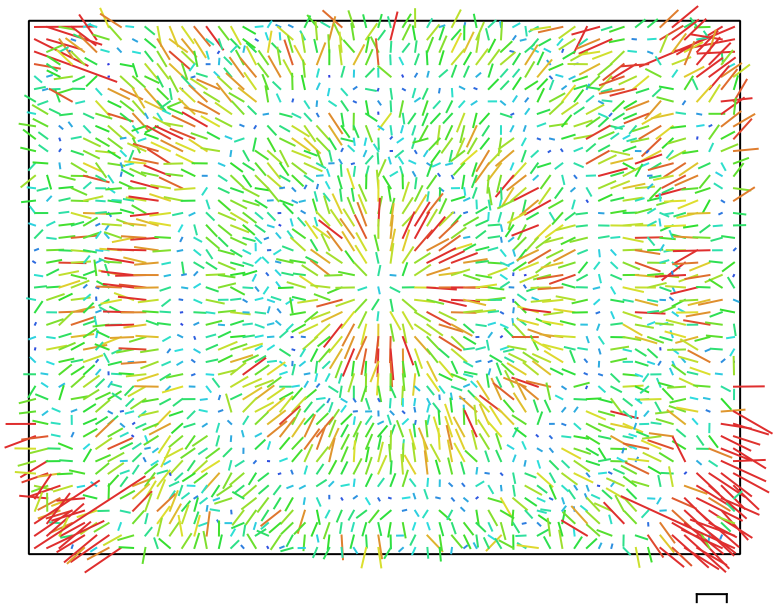

Fig. 3. Image residuals for FC3582 (6.72mm).

FC3582 (6.72mm)

15 images

Type	Resolution	Focal Length	Pixel Size
Frame	**4032 x 3024**	**6.72 mm**	**2.25 x 2.25 µm**

	Value	Error	F	Cx	Cy	B1	B2	K1	K2	K3	K4	P1	P2
F	**3034.45**	0.19	1.00	-0.01	0.08	-0.30	0.02	-0.41	0.40	-0.37	0.34	0.00	0.02
Cx	**1.61303**	0.21		1.00	0.06	0.09	-0.09	0.01	-0.00	0.00	-0.00	0.92	0.05
Cy	**-15.1764**	0.2			1.00	0.10	0.04	0.01	-0.01	0.01	-0.01	0.06	0.86
B1	**-3.38658**	0.079				1.00	-0.01	-0.00	-0.01	0.01	-0.00	0.07	0.08
B2	**0.867433**	0.072					1.00	-0.00	-0.00	0.00	-0.00	-0.07	0.05
K1	**0.105017**	0.00062						1.00	-0.97	0.93	-0.88	0.01	0.01
K2	**-0.270303**	0.0038							1.00	-0.99	0.96	-0.01	-0.01
K3	**0.406164**	0.0091								1.00	-0.99	0.01	0.01
K4	**-0.25971**	0.0074									1.00	-0.01	-0.01
P1	**-0.000952929**	2.3e-05										1.00	0.06
P2	**-0.000361172**	2.1e-05											1.00

Table 3. Calibration coefficients and correlation matrix.

Camera Locations

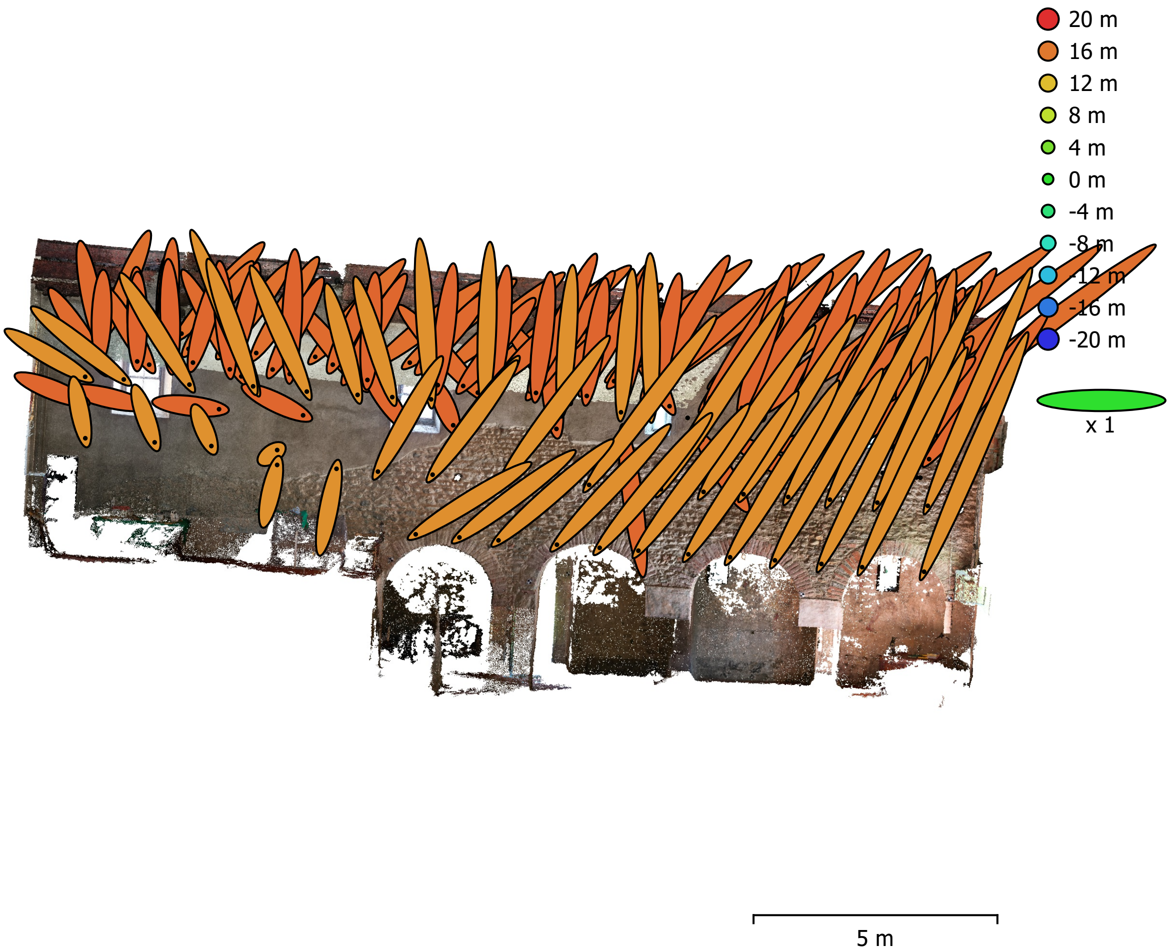

Fig. 4. Camera locations and error estimates.
Z error is represented by ellipse color. X,Y errors are represented by ellipse shape.
Estimated camera locations are marked with a black dot.

X error (m)	Y error (m)	Z error (m)	XY error (m)	Total error (m)
1.52386	2.30628	16.1929	2.76425	16.4271

Table 4. Average camera location error.
X - Easting, Y - Northing, Z - Altitude.

Ground Control Points

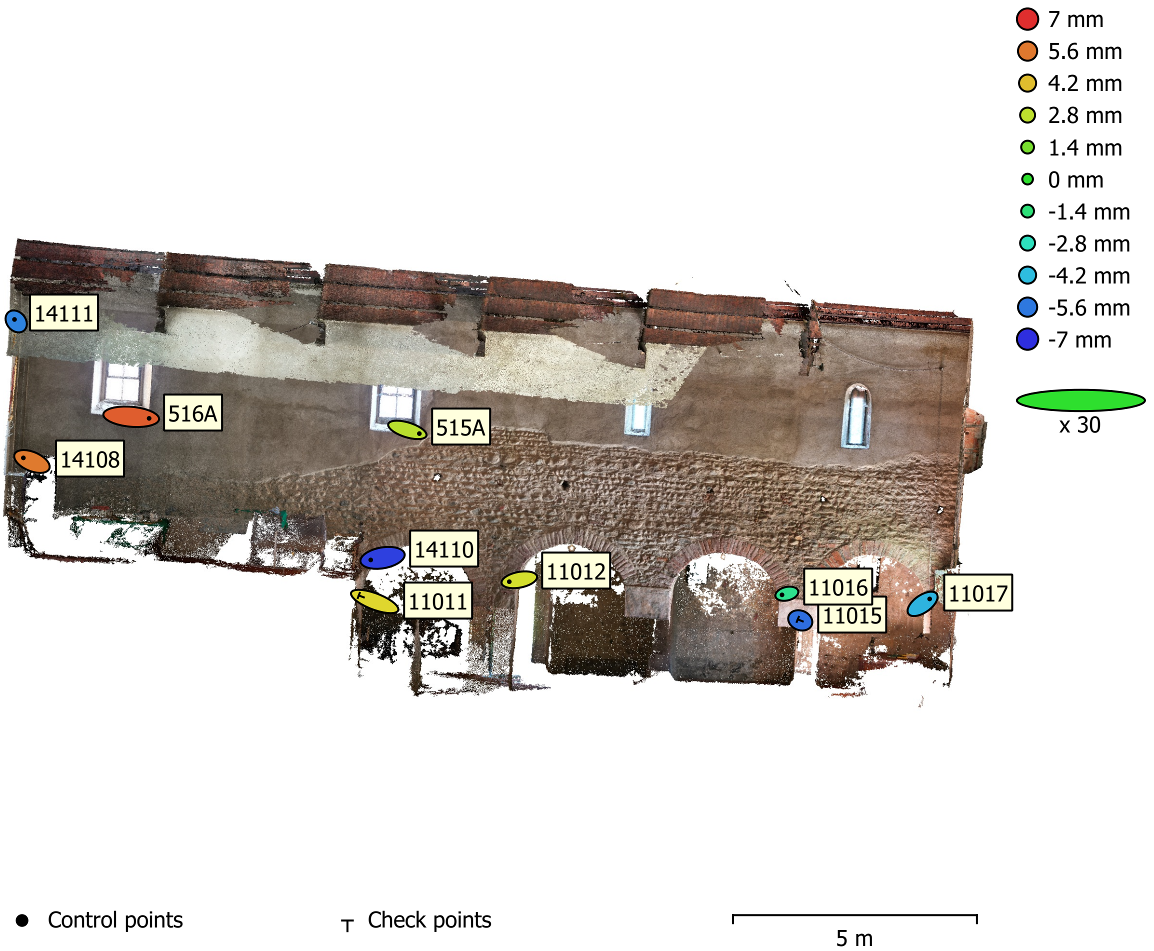

Fig. 5. GCP locations and error estimates.
Z error is represented by ellipse color. X,Y errors are represented by ellipse shape.
Estimated GCP locations are marked with a dot or crossing.

Count	X error (cm)	Y error (cm)	Z error (cm)	XY error (cm)	Total (cm)
8	1.41163	0.395373	0.477276	1.46596	1.54169

Table 5. Control points RMSE.
X - Easting, Y - Northing, Z - Altitude.

Count	X error (cm)	Y error (cm)	Z error (cm)	XY error (cm)	Total (cm)
2	1.55492	0.589128	0.484017	1.66278	1.73179

Table 6. Check points RMSE.
X - Easting, Y - Northing, Z - Altitude.

Label	X error (cm)	Y error (cm)	Z error (cm)	Total (cm)	Image (pix)
11012	-1.37025	-0.263193	0.329004	1.43356	1.145 (9)
11016	-0.659912	-0.157117	-0.183593	0.702763	1.403 (4)
11017	0.965896	0.676588	-0.438634	1.25822	1.330 (4)
14108	-1.16977	0.491591	0.553093	1.38417	2.299 (7)
14110	-1.61347	-0.284003	-0.667747	1.76913	0.718 (9)
14111	-0.233996	0.268541	-0.537582	0.644875	0.314 (6)
515A	1.63964	-0.507038	0.271858	1.73765	2.210 (20)
516A	2.44557	-0.217504	0.610974	2.53011	1.493 (19)
Total	**1.41163**	**0.395373**	**0.477276**	**1.54169**	**1.637**

Table 7. Control points.
X - Easting, Y - Northing, Z - Altitude.

Label	X error (cm)	Y error (cm)	Z error (cm)	Total (cm)	Image (pix)
11011	-2.17287	0.821739	0.367112	2.35189	0.936 (4)
11015	-0.337871	0.137438	-0.577731	0.683242	0.583 (3)
Total	**1.55492**	**0.589128**	**0.484017**	**1.73179**	**0.804**

Table 8. Check points.
X - Easting, Y - Northing, Z - Altitude.

Digital Elevation Model

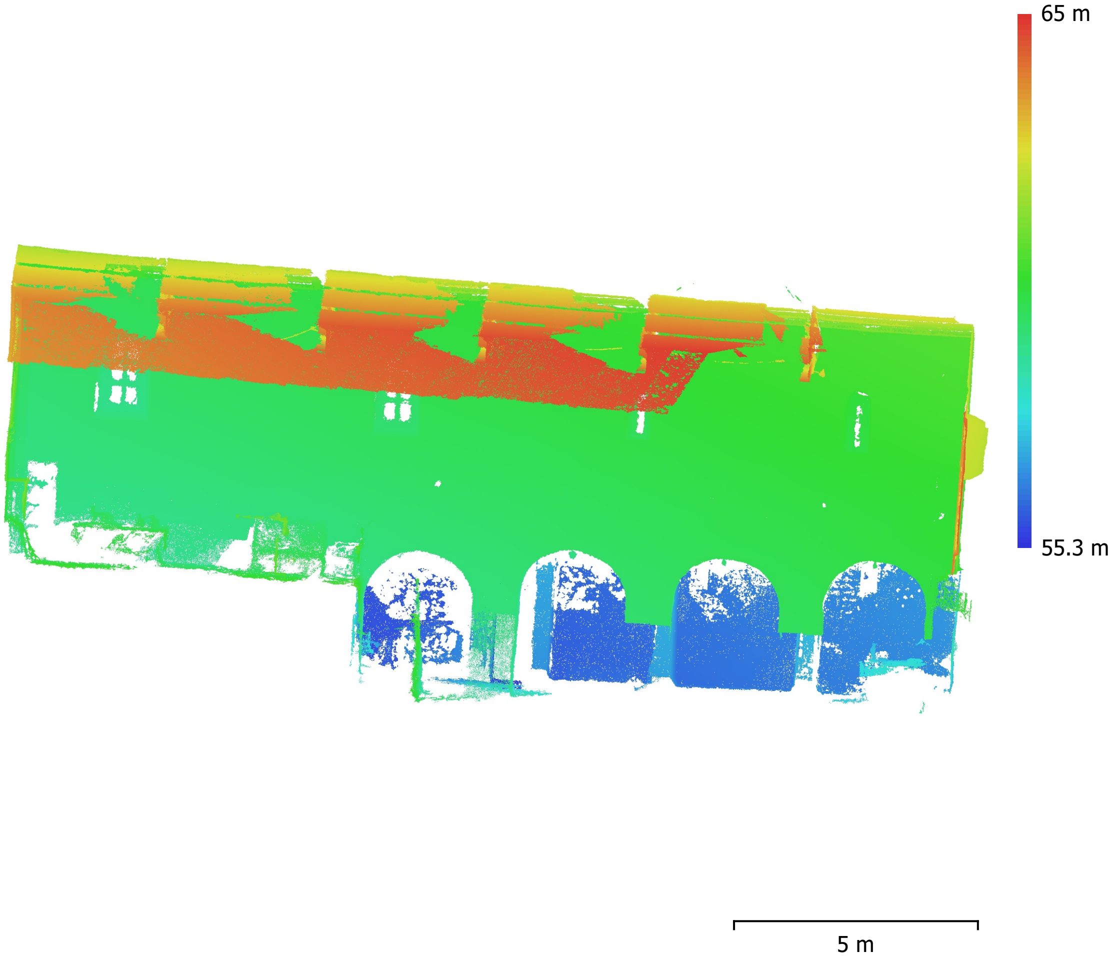

Fig. 6. Reconstructed digital elevation model.

Resolution:	unknown
Point density:	unknown

Processing Parameters

General	
Cameras	170
Aligned cameras	170
Markers	10
Coordinate system	WGS 84 / UTM zone 32N (EPSG::32632)
Rotation angles	Omega, Phi, Kappa
Tie Points	
Points	168,495 of 183,840
RMS reprojection error	0.394885 (0.98775 pix)
Max reprojection error	2.7354 (48.7398 pix)
Mean key point size	2.88207 pix
Point colors	3 bands, uint8
Key points	No
Average tie point multiplicity	3.97523
Alignment parameters	
Accuracy	Highest
Generic preselection	Yes
Reference preselection	Source
Key point limit	40,000
Key point limit per Mpx	1,000
Tie point limit	4,000
Exclude stationary tie points	Yes
Guided image matching	No
Adaptive camera model fitting	No
Matching time	1 minutes 52 seconds
Matching memory usage	2.45 GB
Alignment time	54 seconds
Alignment memory usage	237.41 MB
Optimization parameters	
Parameters	f, b1, b2, cx, cy, k1-k4, p1, p2
Adaptive camera model fitting	No
Optimization time	1 seconds
Date created	2023:10:14 16:10:11
Software version	2.0.3.16960
File size	15.56 MB
Depth Maps	
Count	170
Depth maps generation parameters	
Quality	Medium
Filtering mode	Moderate
Max neighbors	16
Processing time	1 minutes 51 seconds
Memory usage	2.09 GB
Date created	2023:10:20 15:17:09
Software version	2.0.2.16404
File size	183.39 MB
Point Cloud	
Points	18,304,480
Point attributes	
Color	3 bands, uint8

Normal	
Confidence	1 - 31
Point classes	
Created (never classified)	18,304,480
Depth maps generation parameters	
Quality	Medium
Filtering mode	Moderate
Max neighbors	16
Processing time	1 minutes 51 seconds
Memory usage	2.09 GB
Point cloud generation parameters	
Processing time	1 minutes 47 seconds
Memory usage	4.96 GB
Date created	2023:10:20 15:19:00
Software version	2.0.2.16404
File size	261.62 MB
System	
Software name	Agisoft Metashape Professional
Software version	2.0.3 build 16960
OS	Windows 64 bit
RAM	15.65 GB
CPU	11th Gen Intel(R) Core(TM) i7-11800H @ 2.30GHz
GPU(s)	Intel(R) UHD Graphics
	NVIDIA GeForce RTX 3050 Laptop GPU